

1990

# Actin In Silk Gland Nuclear Development

Scott C. Henderson

Follow this and additional works at: <https://ir.lib.uwo.ca/digitizedtheses>

---

## Recommended Citation

Henderson, Scott C., "Actin In Silk Gland Nuclear Development" (1990). *Digitized Theses*. 2003.  
<https://ir.lib.uwo.ca/digitizedtheses/2003>

This Dissertation is brought to you for free and open access by the Digitized Special Collections at Scholarship@Western. It has been accepted for inclusion in Digitized Theses by an authorized administrator of Scholarship@Western. For more information, please contact [tadam@uwo.ca](mailto:tadam@uwo.ca), [wlsadmin@uwo.ca](mailto:wlsadmin@uwo.ca).

## LIST OF FIGURES

Plates	Description	Page
1	Silk gland nuclei form complex 3-dimensional shapes (stereo pair of P1-labelled silk gland nuclear lobes).....	4
2,3	Silk gland nuclei have highly irregular profiles and multiple lamellar nucleoli.....	6
4	The silk gland of <i>Calpodes</i> is divided into 5 morphological regions.....	9
5	Silk gland cells have 2 separate cytoskeletal networks.....	11
6-11	Silk gland nuclei from early larval stadia are smooth and ovoid.....	31
12,13	The first signs of nuclear branching appear during the third larval stadium.....	31
14-18	Regionally characteristic nuclear shapes are most elaborate by the middle of the fifth stadium.....	33
19-22	Feulgen-negative patches which form in the anterior region nuclei during the 4 <sup>th</sup> moult are caused by nuclear compression.....	36
23	The nuclear skeleton of silk gland cells conforms to the elaborate shape of the nucleus.....	38
24	Intranuclear filaments of the silk gland nuclear matrix are arranged parallel to each other.....	38



National Library  
of Canada

Bibliothèque nationale  
du Canada

Canadian Theses Service    Service des thèses canadiennes

Ottawa Canada  
K1A 0N4

The author has granted an irrevocable non-exclusive licence allowing the National Library of Canada to reproduce, loan, distribute or sell copies of his/her thesis by any means and in any form or format, making this thesis available to interested persons.

The author retains ownership of the copyright in his/her thesis. Neither the thesis nor substantial extracts from it may be printed or otherwise reproduced without his/her permission.

L'auteur a accordé une licence irrévocable et non exclusive permettant à la Bibliothèque nationale du Canada de reproduire, prêter, distribuer ou vendre des copies de sa thèse de quelque manière et sous quelque forme que ce soit pour mettre des exemplaires de cette thèse à la disposition des personnes intéressées.

L'auteur conserve la propriété du droit d'auteur qui protège sa thèse. Ni la thèse ni des extraits substantiels de celle-ci ne doivent être imprimés ou autrement reproduits sans son autorisation.

ISBN 0-315-59118-8

## ABSTRACT

Nuclei in the giant silk gland cells of *Calpodes ethlius* grow continuously to form highly branched, regionally characteristic shapes. These cells were studied in an attempt to correlate the arrangement of nuclear and cytoskeletons with nuclear shape.

Nuclear matrices, examined *in situ* by SEM, have filament meshworks with shapes similar to those of Feulgen stained nuclei. Isolated nuclear matrices, examined by TEM, have parallel filaments within the nuclear branches. H $\ddot{o}$ chst stained DNA has a similar alignment. Immunofluorescence microscopy indicated that, although extraordinary in shape, these nuclei have some of the same matrix antigens found in smaller, spherical nuclei. SDS-PAGE of the nuclear-associated (nuclear matrix) fraction revealed few polypeptides, including a nuclear isoform of actin (43 kD, pI 6.45). Nuclear branches label at their periphery with antibodies to actin and myosin and with rhodaminyl-phalloin which is specific for f-actin. The nuclear-associated fraction contains a lamina-like structure that binds heavy meromyosin and antibodies to actin and myosin. This suggests that actin and myosin are components of a layer at the nucleocytoplasmic boundary called the nuclear shell which may correspond to a cytoplasmic zone containing filaments associated with the nuclear envelope.

During larval moults, globules, which label with antibodies to actin, form in the cytoplasm. Similar globules co-isolate with the nuclear matrix fractions from moulting larvae and label with antibodies to actin, but not to nuclear matrix antigens. The globules may be reserves of g-actin for growth of the perinuclear actin shell.

Labelling of silk glands with rhodaminyl-phalloin shows cytoskeletal f-actin in parallel bundles around the lumen. The bundles dissociate when larval feeding stops during the moults, and the f-actin forms coats around vacuoles. After the moult, f-actin reforms in periluminal bundles. Regional differences exist in the density of these bundles. The greatest density occurs in the narrower anterior regions of the gland and may be correlated with the increased hoop stress resulting from the reduced luminal diameter. F-actin coated vacuole formation during larval moults occurs in all but the duct and green regions.

As the formation of cytoplasmic actin-coated vacuoles occurs, the f-actin in the nuclear shell maintains its location. Thus, two kinds of f-actin deployment take place concurrently within these cells.

**key words:** nuclear shape, nuclear morphology, nuclear matrix, silk gland, nuclear actin, perinuclear actin, nuclear myosin, nuclear shell, actin bodies, f-actin, phalloin, periluminal circumferential actin bundles, actin-coated vacuoles

## ACKNOWLEDGMENTS

I thank my thesis supervisor, Prof. Michael Locke, for his guidance, support and patience throughout the course of this work. It has been a privilege to have such a distinguished scientist as a mentor. He has graciously shared his knowledge with me both in and out of the lab.

I also wish to thank the members of my advisory committee, Dr. G. Kidder and Dr. R. Shivers, for their help during the period of this study.

Antibodies to nuclear matrix antigens were donated by Dr. David L. Brown (University of Ottawa). Rhodaminyl-phalloin was donated by Th. Wieland (Max-Planck Institut für Medizinische Forschung, Heidelberg, West Germany). Antibody to sea urchin  $\beta$ -tubulin (from the lab of Dr. J. Richard McIntosh, University of Colorado) was donated by Dr. G. Kidder (U.W.O.).

Technical assistance was provided by Harry Leung, Jackie Sparks, Lora Wilkie, and Rick Harris. I am especially grateful to Harry for his advice on immunogold labelling and to Harry and Rick for their assistance in confocal microscopy. Photographic assistance was provided by Ian Craig.

I also wish to thank my colleagues (both past and present) in the lab: Dr. Patric Delhanty, Harold Fife, Andrew Jackson, Dr. Cheryl Ketola, Helen Kirk, Dr. Subba Reddy Palli, and J.T. Reddy for their discussion, advice and encouragement.

I wish to thank Betty Singh (Agriculture Canada) who provided my initial opportunity to work with electron microscopy.

Finally, I would like to thank my family for their love and emotional support. My Mom and Dad are the two greatest people I know. I am truly blessed to have such wonderful parents.

My wife Margaret deserves special mention. She has gone beyond the call of duty as the spouse of a graduate student. Not only has Margaret endured late nights in the lab and my continual depression when experiments failed, she has, as an expert reference librarian, provided several on-line searches for my research. Additionally, she collected *Pieris* larvae, provided a constant supply of nylon mesh for filtration of tissue homogenates, and helped raise some hawk-moth larvae. Many parts of this manuscript were typed by her. She is my dearest friend and companion. It is to her credit that this thesis was finally written.

## DEDICATION

I dedicate this thesis to  
my Mom & Dad  
and to Margaret

---

In loving memory of  
Dr. Gordon L. Henderson  
Dec. 23, 1927 - Aug. 7, 1990

## TABLE OF CONTENTS

CERTIFICATE OF EXAMINATION .....	ii
ABSTRACT .....	iii
ACKNOWLEDGEMENTS .....	v
DEDICATION .....	vi
TABLE OF CONTENTS .....	vii
LIST OF FIGURES .....	x
LIST OF APPENDICES .....	xv
ABBREVIATIONS .....	xvi
<b>CHAPTER 1    General Review.....</b>	<b>1</b>
1.1    Nuclear shape.....	1
1.2    Silk glands.....	2
1.3    Silk gland cytoskeleton.....	7
1.4    Nuclear matrix.....	12
1.5    Objectives.....	15
<b>CHAPTER 2    Materials and Methods.....</b>	<b>16</b>
2.1    Experimental animals.....	16
2.2    Chemicals.....	16
2.3    Feulgen staining of silk glands.....	16
2.4    Immunofluorescent labelling of silk glands.....	17
2.5    Labelling of silk glands with rhodaminyl-phalloin and Hoechst.....	18
2.6    Fluorescence microscopy.....	18
2.7    Transmission electron microscopy of unextracted silk glands.....	19
2.8 <sup>35</sup> S-Methionine labelling of silk gland polypeptides...	19
2.9.    Nuclear matrix isolation .....	20
2.10    Preparation of fractions for electrophoresis.....	22
2.11    Polyacrylamide gel electrophoresis.....	22
2.12    Immunoblotting.....	23
2.13    Preparation of silk gland nuclear matrices for scanning electron microscopy.....	24



2.14	Preparation of fractions for transmission electron microscopy.....	25
2.15	Immunogold labelling of sections.....	25
2.16	Heavy meromyosin labelling of silk gland nuclear-associated (nuclear matrix) fractions.....	26
<b>CHAPTER 3</b>	<b>The development of branched silk gland nuclei: the silk gland nuclear matrix.....</b>	<b>28</b>
3.1	Introduction.....	28
3.2	Results.....	29
3.2.1	<i>The regional development of branched nuclear patterns during larval life.....</i>	<i>29</i>
3.2.2	<i>The 3-dimensional arrangement of the nuclear matrix resembles the shape of intact nuclei.....</i>	<i>34</i>
3.2.3	<i>The polypeptides forming the nuclear matrix.....</i>	<i>39</i>
3.2.4	<i>Antigens found in other eukaryote nuclei also occur in silk gland nuclei.....</i>	<i>44</i>
3.3	Discussion.....	44
<b>CHAPTER 4</b>	<b>A shell of f-actin surrounds the branched nuclei of silk gland cells.....</b>	<b>49</b>
4.1	Introduction.....	49
4.2	Results.....	50
4.2.1	<i>Silk gland nuclear-associated fraction has an isoform of actin .....</i>	<i>50</i>
4.2.2	<i>Silk gland nuclei label with antibodies to actin and myosin.....</i>	<i>55</i>
4.2.3	<i>The silk gland nuclear-associated fraction contains the nuclear shell which labels with antibodies to actin and myosin.....</i>	<i>55</i>
4.2.4	<i>Silk gland nuclear branches label for f-actin.....</i>	<i>68</i>
4.2.5	<i>Nuclear shells contain f-actin.....</i>	<i>68</i>
4.2.6	<i>The location of the nuclear shell.....</i>	<i>75</i>
4.3	Discussion.....	80

<b>CHAPTER 5</b>	<b>Cytoplasmic actin storage bodies in silk gland cells.....</b>	<b>83</b>
5.1	Introduction.....	83
5.2	Results.....	83
5.2.1	<i>Actin storage bodies appear in the silk gland cytoplasm during the larval moults.....</i>	83
5.2.2	<i>Spheres resembling the actin storage bodies co-isolate with the nuclear matrix.....</i>	88
5.2.3	<i>Nuclear matrix-associated bodies label for actin.....</i>	88
5.3	Discussion.....	88
<b>CHAPTER 6</b>	<b>The redeployment of f-actin in silk glands during moulting.....</b>	<b>94</b>
6.1	Introduction.....	94
6.2	Results.....	95
6.2.1	<i>Periluminal circumferential f-actin bundles.....</i>	95
6.2.2	<i>F-actin coated vacuoles form during the larval moults.....</i>	95
6.3	Discussion.....	106
<b>CHAPTER 7</b>	<b>Regional differences in the apical f-actin cytoskeleton.....</b>	<b>113</b>
7.1	Introduction.....	113
7.2	Results.....	113
7.2.1	<i>Regional differences in the density of actin bundles along the length of the gland.....</i>	113
7.2.2	<i>Regional differences in f-actin coated vacuole formation during moulting.....</i>	116
7.3	Discussion.....	116
<b>SUMMARY AND CONCLUSIONS</b>	<b>.....</b>	<b>123</b>
<b>REFERENCES</b>	<b>.....</b>	<b>142</b>
<b>VITA</b>	<b>.....</b>	<b>161</b>

## LIST OF FIGURES

Plates	Description	Page
1	Silk gland nuclei form complex 3-dimensional shapes (stereo pair of P1-labelled silk gland nuclear lobes).....	4
2,3	Silk gland nuclei have highly irregular profiles and multiple lamellar nucleoli.....	6
4	The silk gland of <i>Calpodes</i> is divided into 5 morphological regions.....	9
5	Silk gland cells have 2 separate cytoskeletal networks.....	11
6-11	Silk gland nuclei from early larval stadia are smooth and ovoid.....	31
12,13	The first signs of nuclear branching appear during the third larval stadium.....	31
14-18	Regionally characteristic nuclear shapes are most elaborate by the middle of the fifth stadium.....	33
19-22	Feulgen-negative patches which form in the anterior region nuclei during the 4 <sup>th</sup> moult are caused by nuclear compression.....	36
23	The nuclear skeleton of silk gland cells conforms to the elaborate shape of the nucleus.....	38
24	Intranuclear filaments of the silk gland nuclear matrix are arranged parallel to each other.....	38

25	The spatial arrangement of DNA within the silk gland nuclei reflects the arrangement of the nuclear matrix.....	38
26-28	Sheets of nuclear laminae label with P1.....	41
29-32	The silk gland nuclear matrix fraction is characterized by an abundance of a very few polypeptides.....	43
33-36	Silk gland nuclei label with monoclonal antibodies to nuclear matrix antigens found in more typical nuclei.....	46
37-42	The silk gland nuclear-associated fraction contains an isoform of a polypeptide, similar in molecular weight to actin.....	52
43	Western blots of the silk gland nuclear-associated fraction bind antibodies to actin.....	54
44	Silk gland nuclei are highly branched and several hundred micrometres across by the time of the 4 <sup>th</sup> larval moult.....	57
45	Silk gland nuclei label with antibodies to actin.....	57
46-49	Antibodies to actin and the nuclear matrix co-localize to the silk gland nuclear lobes early and late in development..	59
50-53	Antibodies to myosin and the nuclear matrix co-localize to the silk gland nuclear lobes early and late in development..	61
54,55	Antibodies to actin and myosin localize to the nuclear periphery.....	63

56,57	One of the lamina-like structures of the silk gland nuclear-associated fraction labels with a monoclonal antibody to the nuclear matrix antigen - peripherin (P1) but not with antibodies to actin.....	65
58,59	A less electron-dense lamina-like structure of the silk gland nuclear-associated fraction labels with antibodies to actin and myosin.....	67
60,61	Silk gland nuclear branches label specifically for f-actin.....	70
62,63	A shell of f-actin surrounds the nuclear periphery.....	72
64-67	A lamina-like structure of the silk gland nuclear-associated fraction labels with heavy meromyosin.....	74
68-71	Silk gland nuclei are surrounded by a zone of exclusion.....	77
72	The probable location of the nuclear shell.....	79
73-75	Electron-dense spherical bodies appear in the cytoplasm during the larval moults.....	85
76,77	Moult-associated cytoplasmic bodies label with antibodies to actin.....	87
78	Spherical protein bodies co-isolate with the nuclear matrix prepared from silk glands of moulting larvae.....	90
79,80	Moult associated protein bodies which co-isolate with the nuclear matrix fraction label with antibodies to actin.....	92
81-84	F-actin bundles surround the lumen of the silk gland during each larval intermoult stage.....	97

85	F-actin bundles overlap between opposing cells.....	99
86,87	Thick bundles of microfilaments which label for actin are found immediately beneath the plasma membrane in the apical cytoplasm of silk gland cells.....	101
88-90	F-actin-coated vacuoles form during each of the larval moults.....	103
91	F-actin-coated vacuoles form as the periluminal circumferential actin bundles dissociate.....	105
92	Occasionally the f-actin bundles redistribute throughout the cytoplasm.....	105
93	F-actin is at the periphery of the moult-associated vacuoles.....	105
94	F-actin-coated vacuoles in the silk glands of <i>Pieris rapae</i> appear to bud from the apical surface as oblong pockets.....	105
95,96	Large silk-containing spheres in the apical cytoplasm of silk gland cells from moulting larvae immunogold label at their periphery with antibodies to actin.....	108
97	Nuclear shell and periluminal actin display different behaviours with respect to the moult/intermoult cycle.....	112
98-102	Regional differences exist in the density of periluminal circumferential actin bundles in the silk gland.....	115
103-107	The formation of actin-coated vacuoles during the larval moults occurs only in certain regions of the gland.....	118

108-111	The regional differences in the density of the periluminal circumferential actin bundles are not as conspicuous in earlier larval intermolt stages.....	120
112-115	The regional patterns of f-actin-coated vacuole formation are similar during each of the larval moults.....	120
116-121	No autofluorescence occurs within the cells of the anterior, mid, and posterior regions of the silk glands.....	128
122-127	Fluorescent-tagged secondary antibodies do not bind to any sites within silk gland cells.....	130
128-131	Binding of primary antibodies is specific.....	133
132-133	Technique used to expose intracellular regions does not alter the distribution of microtubules in silk gland cells.....	136
134-136	Gold-tagged secondary antibodies, alone, do not bind to nuclear or cytoplasmic structures which label for actin or peripherin.....	139
137-138	Nuclear matrices prepared from mouse liver label with antibodies to peripherin but not with antibodies to actin.....	141

## LIST OF APPENDICES

Appendices	Description	Page
1	Controls for immunofluorescence microscopy.....	126
2	Controls for immunogold labelling.....	137



## ABBREVIATIONS

a	actin
ANA	anti-nuclear antibodies
BL	basal lamina
BSA	bovine serum albumin
Ci	Curies
CSK	cytoskeletal buffer
°C	degrees Celsius
DNA	deoxyribonucleic acid
DNase I	deoxyribonuclease I
DTT	dithiothreitol
Du	duct
EGTA	ethylene glycol-bis-(2-aminoethyl ether) N,N,N',N'-tetraacetic acid
f-actin	filamentous actin
FITC	fluorescein isothiocyanate
g	grams
× g	gravitational units
g-actin	globular actin
Gr	green region
hc	heterochromatin
HMM	heavy meromyosin
IEF	isoelectric focusing
IgG	immunoglobulin G
IgGAM	immunoglobins G, A, and M
INM	intranuclear matrix
kD	kilodalton
kV	kilovolts
l	lamin
L	litres
Lu	lumen
M	molar
MB	microfilament bundle
MF	microfilament
mg	milligram

mL	millilitre
mm	millimetre
mM	millimolar
MT	microtubule
MTM	Tris, low magnesium buffer
mv	microvilli
μCi	microCuries
μg	microgram
μL	microlitre
μm	micrometre
N	nucleus
NB	nuclear bodies
NE	nuclear envelope
NL	nuclear lamina
nm	nanometres
NM	nuclear matrix
NP	nuclear pore
NS	nuclease supernatant
NSh	nuclear shell
NTM	sodium, Tris, magnesium buffer
Nu	nucleolus
PAGE	polyacrylamide gel electrophoresis
PBS	phosphate buffered saline
pI	isoelectric point
PIPES	piperazine-N,N'-bis (2-ethanesulphonic acid)
PMSF	phenyl methyl sulfonyl fluoride
PNS	post nuclear supernatant
RhPhn	rhodaminyl-phalloin
RNA	ribonucleic acid
RNase A	ribonuclease A
SDS	sodium dodecyl sulfate
SEM	scanning electron microscope
SGNAF	silk gland nuclear-associated fraction
snRNP	small nuclear ribonucleoprotein
SS	salt wash supernatant
STM	sucrose, Tris, magnesium buffer

sv	secretory vesicles
TBS	Tris-buffered saline
TCA	trichloroacetic acid
TEM	transmission electron microscopy
TTBS	Tween in Tris-buffered saline
TTM	Triton X, Tris, magnesium buffer
Tr	tracheoles
TXS	Triton X-100 supernatant
v	vacuole
V	volts
vol.	volume
WS	wash supernatant
ZE	zone of exclusion
1°	primary
2°	secondary

The author of this thesis has granted The University of Western Ontario a non-exclusive license to reproduce and distribute copies of this thesis to users of Western Libraries. Copyright remains with the author.

Electronic theses and dissertations available in The University of Western Ontario's institutional repository (Scholarship@Western) are solely for the purpose of private study and research. They may not be copied or reproduced, except as permitted by copyright laws, without written authority of the copyright owner. Any commercial use or publication is strictly prohibited.

The original copyright license attesting to these terms and signed by the author of this thesis may be found in the original print version of the thesis, held by Western Libraries.

The thesis approval page signed by the examining committee may also be found in the original print version of the thesis held in Western Libraries.

Please contact Western Libraries for further information:

E-mail: [libadmin@uwo.ca](mailto:libadmin@uwo.ca)

Telephone: (519) 661-2111 Ext. 84796

Web site: <http://www.lib.uwo.ca/>

## CHAPTER 1

### GENERAL REVIEW

#### 1.1. Nuclear Shape

*"A striking feature of many neoplastic cells is their altered nuclear morphology. Tumor cell nuclei frequently acquire a variable and highly irregular shape; their chromatin becomes decondensed, and their nucleoli increase in number and size. Thus, the question of what determines nuclear shape and size is of interest to oncologists and cytopathologists as well as cell biologists."* (Kaufmann *et al.*, 1986)

In recent years, much attention has been devoted to cataloguing the information held within the nucleus and to understanding nuclear functions. Although the structure of the nucleus has received extensive study, how most nuclei form and maintain their shape remains unclear. One of the reasons for this is that most nuclei are spherical or oviform in shape. Even though the nucleus dissociates and reforms during each round of mitosis, the shape formed is always similar. The simple spherical shape of the nucleus represents the lowest energy state of a fluid object (Sears *et al.*, 1980). However, recent studies show that these apparently simple spheres of packaged DNA dissociate and reform in a highly co-ordinated fashion (Fisher, 1987; Newport, 1987; Newport & Spann, 1987) and that the internal organization of the interphase nucleus is not random as previously assumed (Gruenbaum *et al.*, 1984; Hochstrasser *et al.*, 1986; Locke & Leung, 1985; van Dekken *et al.*, 1989).

Some nuclei have non-spherical shapes. The nuclei of spermatids are usually fusiform and are thought to be shaped by a manchette of microtubules (Dustin, 1978; Kessel, 1966; Tokuyasu, 1974; Wilkinson *et al.*, 1974; Yasuzumi *et al.*, 1971). These nuclei, however, are inactive; their shape represents the need for compaction and streamlining for transport rather than specialized functional activities.

Many types of cancers are characterized by nuclei which form blebs, pockets, and projections (Achong & Epstein, 1966; Ahearn *et al.*, 1974; Aubock, 1976; Burns *et al.*, 1971; Conforti *et al.*, 1976; McDuffie, 1967; Popoff & Ellsworth, 1969; Vielkind & Vielkind, 1970). These nuclei are "active", yet

their shapes are not as easily predicted or characterized. The purpose of nuclear projections and how they are formed are unknown. Nuclear compression by cytoskeletal elements is not as apparent in cancer cells as in spermatids. However, cancer cells are often polyploid and have a thickened nuclear lamina, which suggests that the shape generating forces may occur within the nucleus (either from proteins and/or nucleic acids).

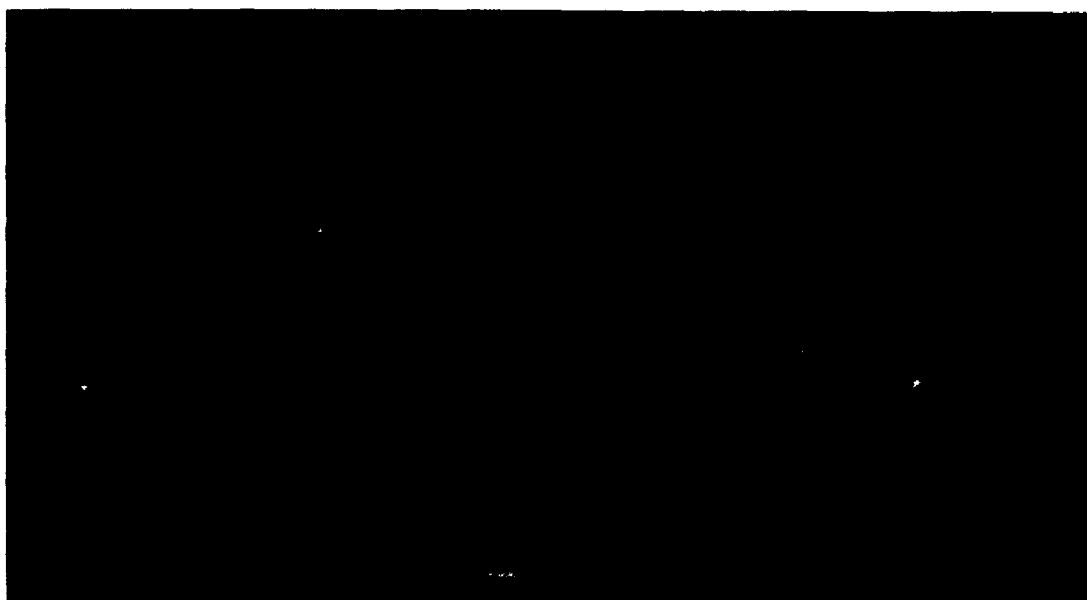
The giant nuclei in silk gland cells of many Lepidopteran larvae (figs. 1 & 2) are another example of atypically shaped nuclei (Akai, 1965; Sehnal & Akai, 1982; Tamura *et al.*, 1982; Tashiro *et al.*, 1968; Wiley & Lai-Fook, 1974). Although these cells are differentiated, the nuclei have all of the characteristics described by Kaufmann *et al.* (1986) in the quote above. The nuclei are highly polyploid and contain multiple nucleoli (fig. 3). In *Bombyx mori*, it has been estimated that, throughout larval life, the nuclei undergo up to 19 rounds of endomitosis (or endoreduplication) (Gage, 1974; Perdrix-Gillot, 1979). As these nuclei grow to sizes several hundred micrometres across, they form multiple branches. In some regions there may be several hundred branches. The nuclei in silk gland cells, unlike cancer cells, branch at a predictable rate over several days and form regionally characteristic shapes.

In this study, silk gland cells are used as a model system for the investigation of the control of nuclear shape.

## 1.2 Silk Glands

The silk glands are a pair of blind-ended simple epithelial tubes found within the abdomen of most Lepidopteran larvae (for reviews of silk gland structure and function, see: Akai (1983); Akai (1984)). The glands are 2 cells in diameter and several hundred cells in length. In the embryo, the cells divide normally and the nuclei are spherical (Tashiro *et al.*, 1976). However, by the end of embryogenesis, mitosis stops and throughout larval life, the DNA is replicated without cell division (Perdrix-Gillot, 1979). Early in the third stadium, the nuclei start to form branches (Matsuura & Tashiro, 1976). Nuclear branching is most extensive by the middle of the fifth stadium (Tashiro *et al.*, 1968). It is thought that endoreduplication and nuclear ramification are adaptations for the export of massive amounts of message for the silk proteins during larval life (Akai, 1983). The number of

**Fig. 1. Silk gland nuclei form complex 3-dimensional shapes. (Stereo pair of P1 labelled silk gland nucleus). Fractured silk glands were labelled with a monoclonal antibody (P1) (Chaly *et al.*, 1984) to a nuclear matrix antigen (peripherin) followed by an FITC-conjugated 2° antibody. Sixteen optical sections were taken by confocal microscopy (Leitz CSLM) through a depth of 46 µm. The sections were then "stacked" to give an extended focus image and processed by the confocal microscope's software to generate a second image with a 15° rotation. Scale bar = 10 µm**





**Fig. 2. Silk gland nuclei have a highly irregular shape. TEM of nuclei in the duct region of silk glands from the 4<sup>th</sup> moult reveals that the nuclear surface develops elaborate projections. (N = nucleus)**

Scale bar = 1  $\mu$ m

**Fig. 3. The nucleoplasm contains many irregularly shaped nucleoli. TEM of cells from the mid gland region in the fifth stadium shows that within each nucleus are multiple heterochromatin patches (hc) and nucleoli (Nu). The nucleoli are less electron dense and often form elaborate lamellar projections. Scale bar = 1  $\mu$ m**



silk genes is multiplied without nuclear shutdown for "open" mitosis (*i.e.* dissolution of the nuclear envelope) and the nuclear surface area is greatly increased to facilitate nucleocytoplasmic exchange (Akai, 1984). During the larval to pupal moult, the glands undergo histolysis (Matsuura *et al.*, 1968).

The secretory product of these cells, the silk, is synthesized as several layers by different regions of the gland (Akai, 1984). The posterior region of the gland secretes fibroin, the core silk protein. The mid gland region secretes sericin and acts as a reservoir for the silk. In the glands of *Bombyx*, the anterior region serves primarily as a conduit to the spinnerets. The gland regions also differ in the extent of nuclear branching. In *Bombyx*, the most ramified nuclei occur in the posterior and mid regions (Akai, 1984).

The silk glands of *Calpodes ethlius* used in this study are divided into 5 morphological (and presumably functional) regions (fig. 4) (Wiley & Lai-Fook, 1974). The posterior and mid regions are analogous to those in *Bombyx*. However, the anterior gland region appears to be secretory as well. Between the anterior gland and the duct is a short region of secretory cells called the green region because of its natural colour (Wiley & Lai-Fook, 1974). The function of this region is unknown.

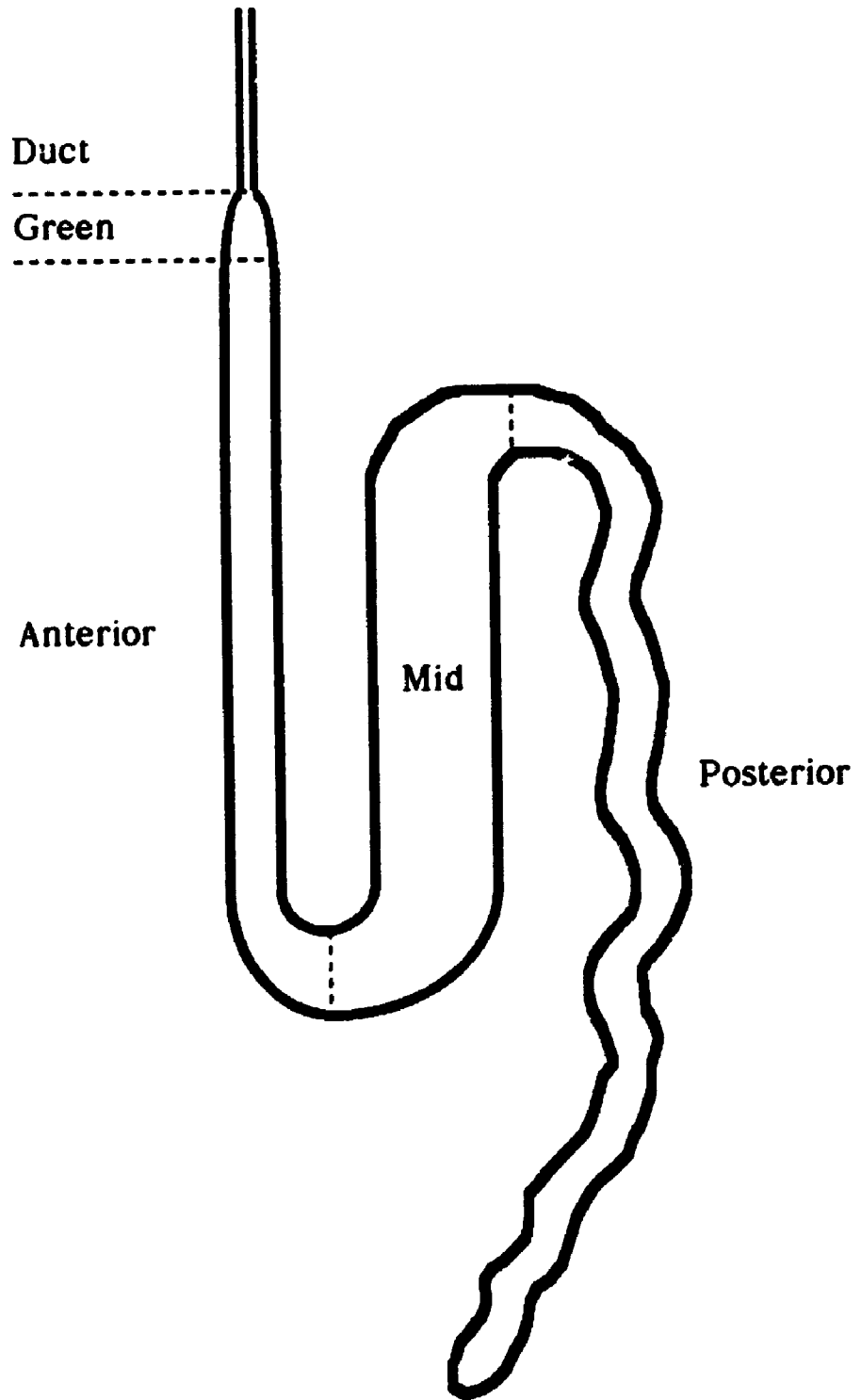
### 1.3 Silk Gland Cytoskeleton

One of the possible mechanisms for nuclear ramification in silk gland cells is compression by the cytoskeleton, in a manner similar to that which occurs in some types of spermatids (Dustin, 1978).

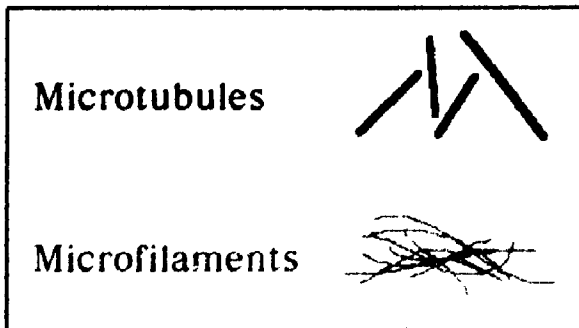
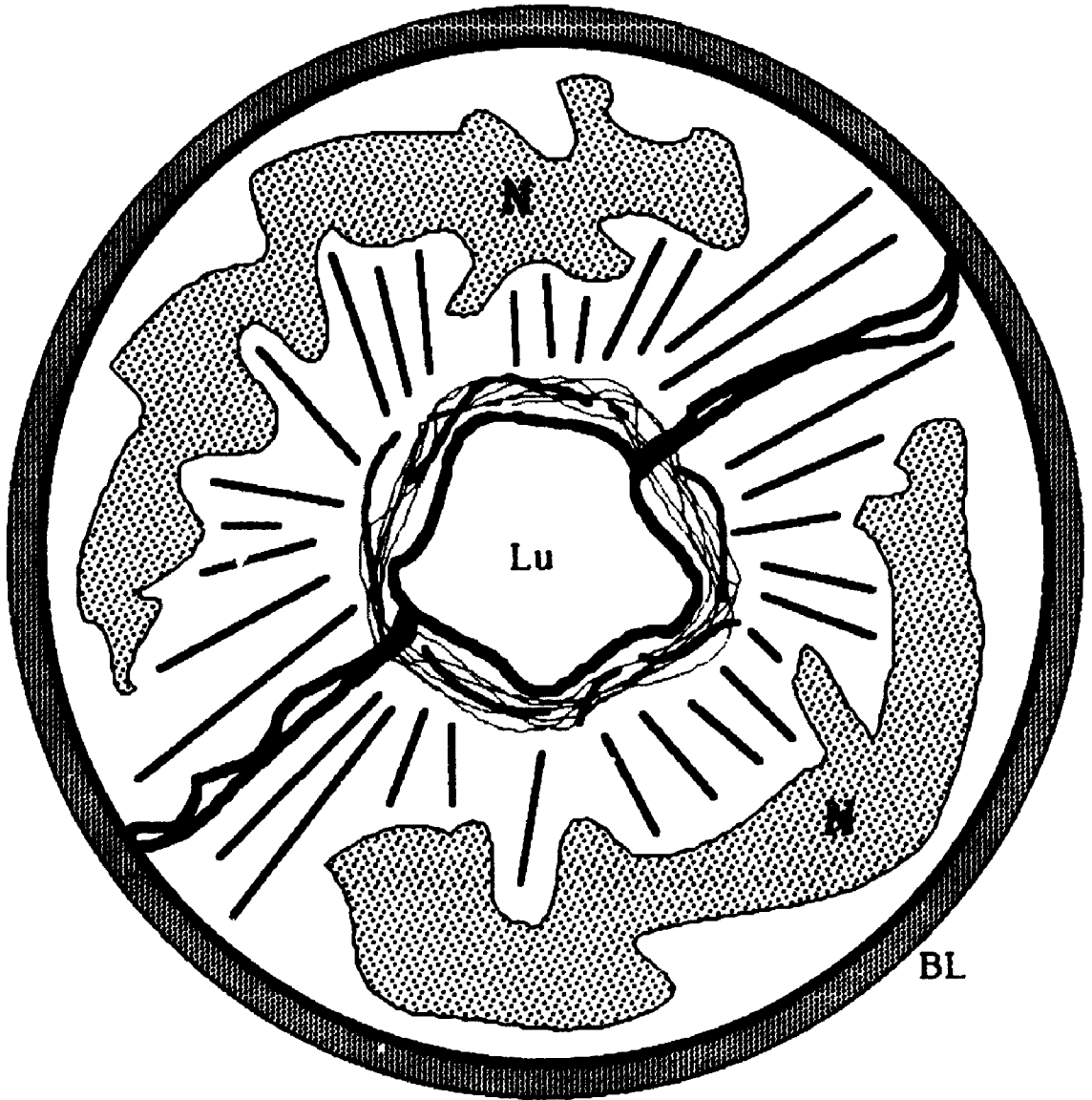
The cytoskeleton in silk gland cells is highly organized. Microtubules are arranged parallel to one another and run from the basal to apical end of the cell (figs. 5 & 133). This radial microtubule system is responsible for the transport of secretory vesicles to the apical (luminal) end of the cell (Sasaki, 1977; Sasaki *et al.*, 1981; Sasaki & Tashiro, 1976; Tashiro *et al.*, 1982). Treatment of silk glands with colchicine or vinblastin sulfate results in the accumulation of secretory vesicles around the Golgi complexes in the middle of the cell (Sasaki, 1977; Sasaki *et al.*, 1981).

The second cytoskeletal network is a system of microfilaments and microtubules at the apical end of the cell (figs. 5 & 98-102). This system surrounds the gland lumen and is oriented perpendicular to the long axis of the gland (Couple *et al.*, 1984; Sasaki *et al.*, 1981; Tashiro *et al.*, 1982). The

**Fig. 4.** The silk glands of *Calpodes ethlius* are divided into 5 morphological regions. *Calpodes* silk glands are simple blind-ended tubes, 2 cells in diameter and approximately 700-800 in length (Wiley & Lai-Fook, 1974). The anterior and posterior regions are comparable in length and form the greatest proportion of the length of the gland. The mid region is slightly shorter but is the greatest in diameter. The green region, given this name because of its natural colour (Wiley & Lai-Fook, 1974), is only about 20 to 30 cells in length. A short duct leads to the opening of the gland. (Diagram not drawn to scale).



**Fig. 5. Silk gland cells have 2 separate cytoskeletal networks. Most of the microtubules in silk gland cells are oriented towards the apical/luminal face of the cell. These microtubules form the radial microtubule system. This system is thought to assist in the transport of secretory vesicles to the apical end of the cell. A second cytoskeletal system of microtubules and microfilaments surrounds the lumen of the gland. This system may play a role in the secretion of silk and/or the peristalsis of silk along the length of the lumen of the gland. (N = nucleus; Lu = lumen; BL = basal lamina). (Diagram not drawn to scale).**



purpose of this system is not as clearly established. The microtubule component is thought to be a continuation of the radial microtubule system which integrates with the microfilaments. The radial microfilament system has been hypothesized to play a role in silk secretion (Couple *et al.*, 1984; Sasaki *et al.*, 1981; Tashiro *et al.*, 1982) and/or in the peristalsis of the luminal silk (Sasaki, 1977; Sasaki & Tashiro, 1976). Similar treatments of silk glands with cytochalasin give conflicting results; in one study cytochalasin enhanced the release of secretory vesicles (Sasaki *et al.*, 1981); in another study it prevented secretory vesicle release (Couple *et al.*, 1984).

#### 1.4 Nuclear Matrix

Another possible mechanism for nuclear ramification is by the generation of force from within the nucleus. The fact that not all polyploid cells have ramified nuclei and that isolated silk gland nuclei maintain their arborescent shapes even after the DNA has been removed (Ichimura *et al.*, 1985) suggests that a protein skeleton may at least be responsible for maintaining nuclear shape in silk gland cells.

The nuclear matrix \* is thought to be (in part) the nuclear equivalent of the cytoskeleton (for reviews on the nuclear matrix, see: Comerford *et al.* (1986); Kaufmann *et al.* (1986); Verheijen *et al.* (1988)). First characterized in mammalian liver cells by Berezney & Coffey (1974), the nuclear matrix has received considerable study because of its association with such cellular events as DNA replication (Berezney & Coffey, 1975; Jackson & Cook, 1986; Razin, 1987), RNA transcription and processing (Jackson & Cook, 1985;

---

\* *N.B.* In this study, the term "nuclear skeleton" refers to the protein skeleton of the nucleus, identified by electron microscopy. This skeleton forms part of the nuclear matrix, which by definition is the biochemical fraction that resists extraction with detergent, nucleases and high ionic strength solutions. In vertebrate cells, the nuclear matrix includes the lamina, which has a skeletal (supportive) function, and may include an amorphous intranuclear network of granules and filaments. Some researchers believe that the intranuclear components of the matrix have no skeletal function (*i.e.* provide no structural/supportive function) and are present due to oxidative cross-linking of loosely bound proteins during matrix preparation (Kaufmann *et al.*, 1986).



Jackson *et al.*, 1981), steroid hormone binding (Alexander *et al.*, 1987; Barrack, 1987; Barrack & Coffey, 1982), viral binding (Ciampor, 1988; Simard *et al.*, 1986) and organization of chromatin following mitosis (Benavente & Krohne, 1986). However, the role of some of its components remains controversial due to the variety of conditions under which nuclear matrices are prepared (Comerford *et al.*, 1986; Cook, 1988). The nuclear matrix is defined as the subnuclear pellet which resists extraction with a non-ionic detergent, nucleases, and high ionic strength solutions (Verheijen *et al.*, 1988). It has been shown that the composition and/or the morphology of the residual nuclear matrix is affected by the order of the extraction steps (Kaufmann *et al.*, 1981), the ionic strength of the salt solutions (Capco *et al.*, 1982), the presence of certain divalent cations (Dijkwel & Wenink, 1986; Lewis *et al.*, 1984), the presence of reducing agents (Kaufmann *et al.*, 1986) (fig. 137), and the presence of RNase during extraction (Bouvier *et al.*, 1985; Fey *et al.*, 1986a). To add further confusion, nuclear matrices have been prepared from isolated nuclei and *in situ* from cultured cells (Capco *et al.*, 1982; Staufenbiel & Deppert, 1984) or disembedded tissue (Capco *et al.*, 1987). While *in situ* extraction avoids possible artefacts from homogenization, many cytoskeletal elements remain by this procedure (Capco *et al.*, 1982; Fey *et al.*, 1984b).

The nuclear matrix consists of the peripheral nuclear lamina/pore complex fraction (fig. 137) and may or may not contain an intranuclear matrix and a nucleolar matrix.

The primary components of the lamina are the nuclear lamins (for reviews, see: Franke (1987); Gerace (1986); Krohne & Benavente (1986)). The lamins are related to the intermediate filaments (Fisher *et al.*, 1986; McKeon *et al.*, 1986) and are thought to be the ancestors of cytoskeletal intermediate filaments (Weber *et al.*, 1989). In mammals, there are 3 lamins (designated A,B,C) which range in molecular mass between 60,000 and 75,000 Da. Each of the lamins is expressed by a separate message (Laliberté *et al.*, 1984). Lamins A and C are homologous (except for their carboxy ends). Lamin B is the only lamin which binds to the nuclear envelope (Georgatos & Blobel, 1987; Gerace & Blobel, 1980; Lebel & Raymond, 1984). Together, these 3 lamins form a meshwork of filaments immediately beneath the nuclear envelope (Aebi *et al.*, 1986). It is thought that the lamins may serve to connect the nucleoskeleton with the cytoskeleton via interactions with the

intermediate filaments (Carmo-Fonseca *et al.*, 1987; Fey *et al.*, 1984b; French *et al.*, 1989; Georgatos & Blobel, 1987; Katsuma *et al.*, 1987). During mitosis, the lamins dissociate as they become hyperphosphorylated prior to the envelope breakdown. The lamins become dephosphorylated as the nucleus reforms following mitosis (Gerace & Blobel, 1980; Ottaviano & Gerace, 1985). In mammalian cells, the expression of one or all of the lamins is related to the state of differentiation of the cell (Collard & Raymond, 1990; Lebel *et al.*, 1987; Lourim & Lin, 1989; Paulin-Levasseur *et al.*, 1988; Stewart & Burke, 1987).

In other classes, the number of lamin proteins varies. Amphibians have at least 5 different lamins which are expressed in a tissue-specific or developmentally-dependent manner (Benavente & Franke, 1985; Benavente *et al.*, 1985; Krohne & Benavente, 1986; Stick & Hausen, 1985).

Insects appear to have only 1 lamin gene. In *Drosophila* embryos, 2 lamin proteins Dm<sub>1</sub> (74 kD) and Dm<sub>2</sub> (76 kD) are derived from a single gene. The product of the lamin gene, Dm<sub>0</sub> is enzymatically cleaved to produce Dm<sub>1</sub> before insertion into the nuclear envelope. Dm<sub>1</sub> is then phosphorylated which results in an increase in molecular mass to give Dm<sub>2</sub> (Fisher, 1988; Gruenbaum *et al.*, 1988; Smith & Fisher, 1989; Smith *et al.*, 1987). It is noteworthy that although most insect cells do not contain intermediate filaments (Bartnik & Weber, 1989) (an exception is in *Drosophila* Kc cells (Walter & Biessmann, 1984)), they still express the intermediate filament-related lamin.

The existence of an internal nuclear matrix remains controversial. The presence of an intranuclear network depends upon the extraction conditions used (Cook, 1988; Dijkwel & Wenink, 1986; Fields *et al.*, 1986; Kaufmann *et al.*, 1981; Kaufmann *et al.*, 1986). Evidence supporting the existence of an intranuclear matrix includes: TEM visualization of an internal matrix *in situ* (Brasch, 1982; Pouchelet *et al.*, 1986), immunofluorescent localization of nuclear matrix antigens during extraction (Chaly *et al.*, 1985; Lehner *et al.*, 1986; Staufienbiel & Deppert, 1984), similarities in patterns of extracted and unextracted nuclei (Herlan *et al.*, 1978), and generation of a nuclear matrix during reactivation of matrixless nuclei (LaFond *et al.*, 1983; Woodcock & Woodcock, 1986). An intranuclear matrix has been observed using a variety of techniques including: TEM of isolated matrices (Berezney & Coffey, 1977; Comings &

Harris, 1976; Fisher *et al.*, 1982), extracted whole mounts (Capco *et al.*, 1982), and resinless sections of extracted tissue (Capco *et al.*, 1987; Fey *et al.*, 1984a; Fey *et al.*, 1986a; Fey *et al.*, 1986b; Fey *et al.*, 1984b); and freeze fracture (Haggis *et al.*, 1982; Maraldi *et al.*, 1986). Studies have also demonstrated the presence of a nucleolar skeleton (Benavente *et al.*, 1984; Bourgeois *et al.*, 1987; Corben *et al.*, 1989; Fields *et al.*, 1986; Franke *et al.*, 1981; Krohne *et al.*, 1982).

Common proteins in different nuclear matrix studies include actin (Boyle & Baluda, 1987; Nakayasu & Ueda, 1983; Nakayasu & Ueda, 1985b; Valkov *et al.*, 1989), RNPs (Berezney, 1980; Fey *et al.*, 1986a; Yancheva *et al.*, 1986), and topoisomerase II (Berrios *et al.*, 1985) which is part of the chromosome scaffold (Earnshaw *et al.*, 1985; Earnshaw & Heck, 1985). Nuclear matrix actin may participate in DNA localization within the nucleus (Valkov *et al.*, 1989), transcription and/or RNA processing (Carmo-Fonseca *et al.*, 1989; Nakayasu & Ueda, 1984; Nakayasu & Ueda, 1985a; Scheer *et al.*, 1984; Schröder *et al.*, 1987), and nucleocytoplasmic transport (Schindler & Jiang, 1986).

## 1.5 Objectives

The giant arborescent nuclei of the silk gland cells of *Calpodes ethlius* were studied in an attempt to determine the mechanism of nuclear shape change and maintenance in cells. The hypothesis of this study is that the regionally-dependent nuclear shapes are generated by changes (either in distribution or state of polymerization) in the nuclear skeleton and/or the cytoskeleton. The aim of this thesis was to identify the nucleoskeletal and cytoskeletal elements, to determine if their arrangements are related to nuclear shape, and to establish if any changes occur in the distribution of the skeletal elements with respect to changes in nuclear shape.

## CHAPTER 2

### MATERIALS AND METHODS

#### 2.1 Experimental animals

*Calpodex ethlius* larvae were reared in a greenhouse on *Canna* plants as described previously (Locke, 1970). The 3<sup>rd</sup>, 4<sup>th</sup> and 5<sup>th</sup> stadia last for 3, 3.5 and 8 days respectively. Moulting events begin about 36 hours prior to the 4<sup>th</sup> to 5<sup>th</sup> ecdysis.

Larvae of *Pieris rapae* were collected in the wild.

Silk glands were dissected from the larva under artificial haemolymph: 25 mM KCl; 5 mM Na<sub>2</sub>HPO<sub>4</sub>; 1 mM MgCl<sub>2</sub>-6H<sub>2</sub>O; 4 mM CaCl<sub>2</sub>; 50 mM glucose; 5.6 mM alanine; 2.5 mM glutamic acid; 30.1 mM glycine; 13.1 mM histidine; 5.7 mM lysine; 18.1 mM serine; 2.2 mM threonine; 0.2 mM streptomycin sulphate; 84 µM penicillin; 17 µM phenol red; pH: 7.1 (Ryerse, 1978).

The liver from one female mouse was dissected under PBS (130.9 mM NaCl, 5.1 mM Na<sub>2</sub>HPO<sub>4</sub>, 1.6 mM KH<sub>2</sub>PO<sub>4</sub>, pH 7.0), and washed with PBS prior to preparation of nuclear matrices.

#### 2.2 Chemicals

All chemicals used in this study were purchased from the J.T. Baker Chemical Company (Phillipsburg, N.J.), Fisher Scientific (Toronto, Ontario), or the Sigma Chemical Company (St. Louis, MO.) unless otherwise noted in the text.

#### 2.3 Feulgen staining of silk glands (Galigher & Kozloff, 1971)

Silk glands were fixed in 5% paraformaldehyde in 0.1 M phosphate buffer (pH 7.4) containing 4% sucrose at 4° C for 1 hour to overnight. They were then washed in several changes of 0.1 M phosphate buffer (pH 7.4) containing 4% sucrose and hydrolyzed in 1 normal HCl at room temperature for 2 minutes and then at 60° C for 8 minutes. The glands were rinsed in distilled water and stained with basic fuchsin for 1 hour (in the dark), before being washed with distilled water and 3 changes of dilute

sulphurous acid (10 mL of 1 normal HCl, 200 mL distilled H<sub>2</sub>O, and 1 g sodium bisulfite). Finally, the glands were washed in several changes of water, dehydrated through a graded series of ethanol, cleared with xylene, and mounted in Permount.

#### 2.4 Immunofluorescent labelling of silk glands

A thick basal lamina which surrounds the silk gland prevents the penetration of antibodies into the cell (even after permeabilization with acetone or Triton X-100). Therefore, in order to make the intracellular antigens accessible to the antibodies, the glands were "fractured" open. Silk glands were compressed between glass microscope slides which had been pre-coated with 1% gelatin in PBS, pH 7.0. The "squashed" glands were placed on dry ice for 2 minutes. The slides were then pried apart and fixed for 5 minutes in formaldehyde freshly prepared from 3% to 5% paraformaldehyde in PBS, pH 7.0. The slides were washed in three 5 minute changes of PBS and then permeabilized with cold acetone for 10 minutes or with 0.2% Triton X-100 in PBS (pH 7.0) for 20 minutes. The slides were washed three times in PBS. The slides were then "blocked" in 0.1% gelatin in PBS for 5 minutes followed by a brief wash in PBS. Drops (50  $\mu$ L) containing 1<sup>o</sup> antibody in PBS (pH 7.4) with 0.1% gelatin were placed on each slide over which was placed a coverslip. The slides were placed in humidity chambers (*i.e.* sealed plastic boxes lined with wet paper towels) and left at room temperature for 3 hours (or at 4°C overnight). The following dilutions of antibodies were used: anti-actin (1:10) (Biomedical Technologies IgG (rabbit)); anti-myosin (1:10) (Biomedical Technologies IgG (rabbit)); anti-nuclear matrix monoclonal antibodies P1 (1:400) and P11 (1:400) (Chaly *et al.*, 1984; Chaly *et al.*, 1985); anti-sea urchin  $\beta$ -tubulin monoclonal antibody (1:10) (Leslie *et al.*, 1984; Scholey *et al.*, 1984); and anti-nuclear antibody (auto antibody control ANA positive, speckled pattern; Sigma diagnostics, Sigma Chemical Co., St. Louis, MO.) (1:4). The slides were washed three times (for 5 minutes each) in PBS. Following the washes, 50  $\mu$ L drops containing 2<sup>o</sup> antibody in PBS (pH 7.4) with 0.1% gelatin were placed on each slide over which was placed a coverslip. Slides labelled with anti-actin or anti-myosin were incubated with FITC-conjugated anti-rabbit IgG (ICN ImmunoBiologicals) (1:50) or rhodamine-conjugated anti-

rabbit IgG (Cooper Biomedical) (1:50); slides labelled with P1 or P11 were incubated with rhodamine-conjugated anti-mouse IgGAM (ICN ImmunoBiologicals) (1:50) or FITC-conjugated anti-mouse IgG (H+L) (Cooper Biomedical) (1:50); slides labelled with anti-tubulin were incubated with rhodamine-conjugated anti-mouse IgGAM (ICN ImmunoBiologicals) (1:50); slides labelled with anti-nuclear antibody were incubated with FITC-conjugated anti-human IgG containing an Evan's Blue counterstain (Sigma diagnostics, Sigma Chemical Co., St. Louis, MO.) (undiluted). A coverslip was placed on each slide and the slides were incubated in humidity chambers in the dark at room temperature for 2 hours or at 4°C overnight. For double-labelling studies, incubation with the second 1° antibody followed labelling with the first 2° antibody.

Control studies indicated that antibody labelling was specific (appendix 1; figs. 122-131).

## **2.5 Labelling silk glands with rhodaminy-phalloin and Hœchst**

Labelling of fractured preparations with rhodaminy-phalloin followed labelling with fluorescein-tagged antibodies. Slides were incubated (in the dark) with 50 µL drops of rhodamine-conjugated phalloin (0.5 µg/mL in PBS, pH 7.0) for 30 minutes at room temperature.

Labelling of fractured preparations with Hœchst for DNA followed labelling with rhodamine-tagged antibodies. Slides were incubated (in the dark) with 50 µL drops of Hœchst 33258 (Calbiochem, Behring Diagnostics, La Jolla, CA.) (10 µg/mL in PBS) for 30 minutes at room temperature.

Labelling of whole silk glands was by incubation (in the dark) with 100 µL of Hœchst (10 µg/mL in PBS) and/or rhodamine-conjugated phalloin (0.5 µg/mL in PBS, pH 7.0) in microfuge tubes for 30 minutes at room temperature.

## **2.6 Fluorescence microscopy**

Following labelling, the slides (or whole glands) were washed in 3 changes of PBS and mounted in a 9/1 mixture of glycerol/PBS and stored at -10° C. Bleaching of fluorescent label was not a problem; therefore, no anti-fading agents were included in the mounting medium. Slides were examined by epifluorescence microscopy with a Zeiss photomicroscope II

and photographed with Tri-X Pan film (Kodak, Rochester, N.Y.) at 400 ASA. Slides were also examined with the BioRad/MRC Lasersharp 500 confocal microscope (set up for simultaneous detection of fluorescein and rhodamine fluorescence) or the Leitz CSLM microscope. Confocal images were photographed directly from the monitor with Kodak Plus-X or T-Max film.

Control studies indicated that detection of each label was specific (appendix 1; figs. 122-131).

## **2.7 Transmission electron microscopy of unextracted silk glands**

Silk glands were fixed in 5% glutaraldehyde in 0.1 M phosphate buffer (pH 7.4) containing 4% sucrose at room temperature for 30 minutes. The glands were then cut into 2 mm lengths and fixed in the above fixative supplemented with 1% tannic acid for 3 hours at room temperature. Following fixation, the glands were washed three times (10 minutes each) in 0.1 M phosphate buffer (pH 7.4) containing 4% sucrose and then post-fixed in 1% OsO<sub>4</sub> in 0.1 M phosphate buffer (pH 7.4) containing 4% sucrose for 3 hours at room temperature. The glands were then washed twice in 0.1 M phosphate buffer (pH 7.4) containing 4% sucrose and four times in distilled H<sub>2</sub>O. The glands were stained *en bloc* in half-saturated aqueous uranyl acetate at 60°C overnight (Locke & Huie, 1980). Gland fragments were dehydrated through an ethanol series, taken through a transition step of propylene oxide and then a change of 1/1 propylene oxide/araldite before embedding in araldite. Silver sections were cut with either glass or diamond knives on a Reichart OMU 3 ultramicrotome, stained with lead citrate and uranyl acetate (Locke & Huie, 1980), and examined in a Philips 300 TEM at 80 kV.

## **2.8 <sup>35</sup>S-Methionine labelling of silk gland polypeptides**

To determine which newly synthesized proteins are incorporated into the nuclear matrix of branching nuclei, silk glands were dissected from 4<sup>th</sup> stadium larvae (*i.e.* at a stage when nuclei are still growing) (Morimoto *et al.*, 1968). Silk glands were dissected from 15 to 25 larvae. The glands were incubated in 20 to 40 µL of <sup>35</sup>S-methionine (1148 Ci/mmol., 10 µCi/µL; New England Nuclear) in 200 µL of artificial haemolymph for 3 hours.

Nuclear matrices were then prepared from the labelled glands as outlined below.

### 2.9.1 Nuclear matrix isolation (Fisher *et al.*, 1982)

Silk gland nuclear matrices were isolated from fourth stadium or fourth moult female larvae according to the method of Fisher *et al.* (1982) with slight modifications. Their nomenclature for the fractions is used throughout this study, except that the term "nuclear-associated fraction" is used instead of "subnuclear fraction", for reasons that will become apparent. Preparation of mouse liver nuclear matrices was by the same procedure. All steps were performed at 4°C unless otherwise noted.

For electron microscopic examination, nuclear matrices were prepared from silk glands from 20 to 40 fourth moult larvae. For electrophoretic analysis of silk gland subnuclear proteins, silk glands were labelled as outlined above.

The glands were homogenized in 10 mL of *Extraction buffer* (50 mM Tris-Cl (pH 7.5); 50 mM NaCl; 5 mM MgCl<sub>2</sub>; 250 mM sucrose; 1 mM PMSF; ±20 mM DTT) and filtered through 1 layer of nylon mesh. The material trapped by the nylon mesh was resuspended in extraction buffer and saved (fraction F). The filtered homogenate was centrifuged at 1,000 x g for 10 minutes. The post-nuclear supernatant (fraction PNS) was decanted and saved. The pellet was resuspended in 5 mL of extraction buffer and centrifuged at 1,000 x g for 10 minutes. The supernatant was decanted and the pellet was washed a second time with 5 mL of extraction buffer. Following centrifugation at 1,000 x g for 10 minutes, the "wash" supernatants (fraction WS) were pooled and saved. The pellet was resuspended in 10 mL of *DNase/RNase buffer* (20 mM Tris-Cl (pH 7.5); 5 mM MgCl<sub>2</sub>; ±20 mM DTT) containing 150 µg/mL DNase I (Cooper Biomedical 1958 units/mg) and 150 µg/mL RNase A (Cooper Biomedical 4790 units/mg) and incubated at 37°C for 20 to 60 minutes. The sample was centrifuged at 1,000 x g for 10 minutes at 4°C, and the nuclease supernatant (fraction NS) was then decanted and saved. The pellet was resuspended in 10 mL of buffer containing 2% Triton X-100 (*Detergent buffer* : (a) 290 mM sucrose; 10 mM Tris-Cl (pH 7.5); 0.1 mM MgCl<sub>2</sub>; ±29 mM DTT; (b) 20% Triton X-100; 0.9 vol. (a) + 0.1 vol. (b)) and incubated on ice for 10 minutes.



The suspension was centrifuged at 1,000 x g for 10 minutes, and the Triton-X soluble supernatant (fraction TXS) was decanted and saved. The pellet was resuspended in 5 mL of salt buffer containing 1 M NaCl (*Salt buffer* : (a) 290 mM sucrose; 100 mM Tris-Cl (pH 7.5); 0.1 mM MgCl<sub>2</sub>; ±20 mM DTT; (b) 2 M NaCl; 0.5 vol. (a) + 0.5 vol. (b)) and incubated on ice for 10 minutes. The suspension was centrifuged at 10,000 x g for 10 minutes. The supernatant was decanted and the salt wash described above was repeated. The "salt wash" supernatants (fraction SS) were pooled and saved. The pellet (silk gland nuclear-associated fraction, SGNAF) was resuspended in buffer (20 mM Tris-Cl (pH 7.5); 5 mM MgCl<sub>2</sub>) and saved.

There was little difference in the structure or arrangement of intranuclear filaments in fractions prepared in the presence or absence of DTT (*i.e.* intranuclear filaments persist in the presence of DTT) (see fig. 24).

### 2.9.2 Nuclear matrix isolation (Berezney & Coffey, 1974)

Silk glands were homogenized in 10 mL of 0.25 *STM buffer* (0.25 M sucrose; 50 mM Tris buffer (pH 7.4); 5 mM MgCl<sub>2</sub>; 1 mM PMSF). The homogenate was then filtered through 1 layer of nylon mesh. The material trapped by the nylon was saved (fraction F). The filtered homogenate was centrifuged at 780 x g for 10 minutes. The post nuclear supernatant (fraction PNS) was decanted and saved. The pellet was resuspended in 10 mL of 2.2 *STM buffer* (2.2 M sucrose; 50 mM Tris buffer (pH 7.4); 5 mM MgCl<sub>2</sub>; 1 mM PMSF) and centrifuged at 40,000 x g for 90 minutes (Beckman L2-65B; SW-40 rotor). The supernatant was decanted and saved (fraction 2.2 S). The pellet was then washed in 10 mL of 0.25 *STM buffer*, and centrifuged at 780 x g for 10 minutes. The first wash supernatant (fraction WS-1) was saved. The pellet was then resuspended in 10 mL of *MTM buffer* (0.2 mM MgCl<sub>2</sub>; 10 mM Tris buffer (pH 7.4); 1 mM PMSF) and incubated for 10 minutes. The sample was centrifuged at 780 x g for 20 minutes and the second wash supernatant (fraction WS-2) was saved. The pellet was resuspended in 10 mL of *NTM buffer* (2 M NaCl; 10 mM Tris buffer (pH 7.4); 0.2 mM MgCl<sub>2</sub>; 1 mM PMSF) and incubated for 10 minutes. The sample was then centrifuged at 780 x g for 40 minutes, after which the salt soluble supernatant (fraction SS) was decanted and saved. The pellet was resuspended in 10 mL of *TTM buffer* (1% Triton X-100; 10 mM Tris buffer (pH 7.4); 5 mM MgCl<sub>2</sub>; 1 mM

PMSF) and incubated for 10 minutes. The sample was centrifuged at 780 x g for 20 minutes and the Triton-X soluble supernatant (fraction TXS) was saved. The pellet was resuspended in 10 mL of *DNase/RNase buffer* (10 mM Tris buffer (pH 7.4); 5 mM MgCl<sub>2</sub>; 1 mM PMSF; DNase 1 (150 µg/mL); RNase A (150 µg/mL)) and incubated at room temperature for 1 to 2 hours. The sample was then centrifuged at 780 x g for 20 minutes, and the nuclease soluble supernatant (fraction NS) was decanted and saved. The pellet (SGNAF) was washed in 0.25 STM buffer and saved.

### 2.10 Preparation of fractions for electrophoresis

Fractions were precipitated with 15% TCA on ice for 30 minutes and then centrifuged at 5,000 x g for 10 minutes at 4°C. The supernatants were decanted and the pellets were overlaid with ether. The pellets were centrifuged at 5,000 x g, the ether was decanted, and the pellets were desiccated under vacuum overnight. The pellets were then homogenized in 8 or 9M urea, 5% β-mercaptoethanol, 1 mM PMSF (200 µL per fraction). The fractions were sonicated and then centrifuged for 2 minutes (Eppendorf 5414). Samples for electrophoresis were drawn from the supernatants. The amount of radioactive label incorporated into each of the fractions was quantified by adding 5 µL of sample to 10 mL of Aquasol (New England Nuclear), and then counting the samples in a liquid scintillation counter (Beckman LS-255).

### 2.11 Polyacrylamide gel electrophoresis

SDS-polyacrylamide gel electrophoresis was done according to the method of Laemmli (1970), with the exception that the separating gel consisted of a 7.5% to 17.5% gradient and was overlaid with a 3% stacking gel (Atkinson, 1981). The gels were calibrated by the co-electrophoresis of proteins of known molecular mass (*i.e.* low molecular weight standards: phosphorylase B (94,000), bovine serum albumin (67,000), ovalbumin (43,000), carbonic anhydrase (30,000), soybean trypsin inhibitor (20,100), and α-lactalbumin (14,400); Pharmacia Fine Chemicals, Piscataway, N.J.).

Two-dimensional electrophoresis was performed according to the method of O'Farrell (1975) with a 4/1 mixture of pH 3.5-10 and pH 4-6 ampholines (LKB Instruments Inc., Rockville, England). The pH gradients

established in IEF gels were determined by measuring the pH of slices of a blank gel equilibrated in boiled distilled H<sub>2</sub>O (Saleem & Atkinson, 1976). Approximately 100,000 counts per minute of each fraction were loaded onto tube gels. Following electrophoresis in the first dimension (BioRad Tube Cell, model 150A), prior to loading the IEF gels onto the second dimension, the gels were extruded and stained according to the method of Gower & Tytell (1985). Following electrophoresis in the second dimension, gels were stained with 0.5% Coomassie Blue R250 in 50% methanol and 10% acetic acid (Weber & Osborn, 1969). Gels to be processed for fluorography were first soaked in En<sup>3</sup>Hance (New England Nuclear) for 1 hour and then washed in running water for 30 minutes. The gels were dried onto a piece of Whatman 3MM filter paper with a BioRad 224 gel slab dryer and then placed with an opposing preflashed film (Kodak X-Omat AR-5) in a -70°C freezer (Laskey & Mills, 1975). The films were exposed for 2 to 3 weeks.

## 2.12 Immunoblotting

The silk gland nuclear-associated fraction prepared from 45 fourth moult larvae was separated by SDS-polyacrylamide gel electrophoresis in one dimension. The fraction (solubilized in 200 µL of 9M urea, 5% β-mercaptoethanol, 1 mM PMSF) was loaded into a single well which extended the entire width of a 12% minigel (BioRad Mini Protean II). Immediately following electrophoresis, the separated polypeptides were transferred to nitrocellulose for 3.5 hours at 70V (BioRad Transfer Cell) following the method of Towbin *et al.* (1979). After transfer, a 5 mm vertical strip was cut from the blot and stained in 0.1% amido black in 50% methanol and 10% acetic acid. The remainder of the blot was placed immediately in a blocking solution of 3% gelatin in TBS (20 mM Tris, pH 7.5, 500 mM NaCl) and incubated with gentle agitation for 1 hour at room temperature. The blot was then washed twice in TTBS (0.05% Tween-20 in TBS, pH 7.5) for 10 minutes. Vertical strips (5 mm in width) were cut from the blot for immunolabelling and the remainder of the blot was dried and stored. The strips were each placed in individual 15 mL culture tubes (with screw caps) which contained 5 mL of 1° antibody (anti-actin; IgG (rabbit) Biomedical Technologies, Stoughton, MA.) diluted (1:200) in buffer (1% gelatin in TTBS). The blots were incubated with gentle agitation at room

temperature overnight. Following two 5 minute washes in TTBS, the blots were placed in 5 mL of 2° antibody (alkaline phosphatase-conjugated goat anti-rabbit IgG (H+L), BioRad, Richmond, CA.) diluted (1:2000) in buffer. The blots were incubated with gentle agitation at room temperature for 1.5 hours. The blots were then washed twice (5 minutes each) in TTBS and once in TBS. Development of the blots was performed according to the method outlined in the BioRad Immunoblot Assay Kit.

### 2.13 Preparation of silk gland nuclear matrices for scanning electron microscopy

Silk gland nuclear matrices were prepared *in situ* for SEM by the method of Fey *et al.* (1984b) with slight modifications. Silk glands were dissected from mid fifth stadium *Calpodes* larvae under artificial hæmolymph. Extraction and examination of silk gland nuclei by SEM is prevented by the presence of a thick basal lamina which resists digestion with proteases and is difficult to remove mechanically. Occasional tears in the basal lamina (partially digested with trypsin) produce windows through which the extracted cells can be viewed. Prior to extracting the glands for nuclear matrices, the glands were placed in a 50/50 solution of glycerol/*Calpodes* ringers (25 mM KCl; 5 mM Na<sub>2</sub>HPO<sub>4</sub>; 1 mM MgCl<sub>2</sub>·6H<sub>2</sub>O; 4 mM CaCl<sub>2</sub>; pH 8.1 (Ryerse, 1978)) containing 0.5% trypsin and digested for 20 minutes at room temperature. Following trypsinization, the glands were placed in CSK buffer (100 mM NaCl, 300 mM sucrose, 10 mM PIPES, pH 6.8, 3 mM MgCl<sub>2</sub>, 1.2 mM PMSF) containing 1% Triton X-100 and extracted for 40 minutes at 4°C. The glands were then placed in extraction buffer (250 mM (NH<sub>4</sub>)<sub>2</sub>SO<sub>4</sub>, 300 mM sucrose, 10 mM PIPES, pH 6.8, 3 mM MgCl<sub>2</sub>, 1.2 mM PMSF, and 0.5% Triton X-100) and extracted for 20 minutes at 4°C. To remove nucleic acids from the nuclei, the glands were digested for 1 hour at room temperature in CSK buffer (with 50 mM NaCl) containing 200 µg/mL each of DNase 1 and RNase A. Following this digestion, an equal volume of 0.5 M (NH<sub>4</sub>)<sub>2</sub>SO<sub>4</sub> was added to the glands in suspension and incubated for 10 minutes at room temperature. The extracted glands were fixed in 2.5% glutaraldehyde in CSK buffer for 40 minutes followed by a wash i.. CSK buffer. The extracted tissue was dehydrated through acetone and critical point dried (Tousimis Samdri-PVT-3B critical point dryer). The dehydrated

tissue was then mounted on SEM stubs, coated with gold in a sputter coater (Hummer VI; Anatech, Ltd.), and viewed with an Hitachi S-570 SEM at 20 kV. As was found by Fey *et al.* (1984b), some cytoskeletal elements (*i.e.* extranuclear filaments) resist extraction with this protocol (fig. 23).

#### 2.14 Preparation of fractions for transmission electron microscopy

Glutaraldehyde (25%) was added to nuclear fractions (see section 2.9.1) in suspension to give a final concentration of 2.5%. The samples were vortexed and allowed to fix at 4°C for at least 1 hour (for immunogold labelling, a fixation time of only 1 hour was used). After fixation, the samples were centrifuged at 5,000 x g for 10 minutes. The supernatants were decanted and the pellets were washed three times in 0.1 M phosphate buffer (pH 7.4) containing 4% sucrose. Pellets to be prepared for conventional TEM were postfixed in 1% OsO<sub>4</sub> in 0.1 M phosphate buffer (pH 7.4) containing 4% sucrose. Pellets to be embedded in LR White and immunogold labelled were not postfixed in osmium in order to preserve actin filaments (Maupin-Szamier & Pollard, 1978) and to avoid excessive heating during polymerization (Newman, 1987). Following postfixation, the pellets were washed three times in 0.1 M phosphate buffer followed by three washes in distilled H<sub>2</sub>O. For conventional TEM, the pellets were stained *en bloc* with half-saturated aqueous uranyl acetate (Locke & Huie, 1980) and then dehydrated through an ethanol series. The pellets were then taken through a transition step of propylene oxide and then a change of 1/1 propylene oxide/araldite prior to embedding in araldite. Pellets to be immunogold labelled were either dehydrated to 70% ethanol and then passed through three changes of LR White before polymerization in LR White or dehydrated up to 100% ethanol and then passed through three changes of LR White prior to polymerization (*N.B.* ratio of accelerator to resin = 15µL to 10 mL) (Newman, 1987). Pellets in LR White were polymerized in sealed 1.5 mL microfuge tubes (Eppendorf) placed in ice.

#### 2.15 Immunogold labelling of sections (Leung *et al.*, 1989)

Silver sections, collected on 300 mesh nickel grids, were "blocked" by placing the grids section-side down on a drop of 3% BSA for 20 minutes. Without washing, the grids were transferred to drops containing 1° antibody

in PBS (pH 7.4) and left at room temperature for 3 hours (or at 4°C overnight) in humidity chambers (*i.e.* sealed plastic boxes lined with wet paper towels). The following dilutions of antibodies were used: anti-actin (1:25) (Biomedical Technologies IgG (rabbit)); anti-myosin (1:25) (Biomedical Technologies IgG (rabbit)); anti nuclear matrix monoclonal antibody P1 (1:400) (Chaly *et al.*, 1984; Chaly *et al.*, 1985). Following incubation in 1° antibody, the grids were washed three times (for 5 minutes each) by placing them section-side down on drops of PBS in a petri dish placed on a magnetic stirrer. Following the washes, the grids were placed section side down on drops of PBS containing a 1:100 dilution of 2° antibody. Sections labelled with anti-actin or anti-myosin were incubated in 5 nm gold-conjugated anti-rabbit IgG (Janssen Life Sciences, Olen, Belgium); sections labelled with P1 were incubated in 10 nm gold-conjugated anti-mouse IgG (Sigma Chemical Co., St. Louis, MO.). Sections were incubated at room temperature for 2 hours in humidity chambers. The grids were then washed three times in PBS (as described above) and rinsed in distilled water before staining with half-saturated aqueous uranyl acetate (10 minutes) and lead citrate (2 minutes) (Locke & Huie, 1980).

*N.B.:* sections which were double labelled with antibodies to actin and the nuclear matrix antigen P1 were labelled on the same side of the section since the antibody to actin was raised in rabbit and the antibody to P1 was raised in mouse.

Control studies indicated that antibody labelling was specific (see appendix 2).

### **2.16 Heavy meromyosin labelling of silk gland nuclear-associated (nuclear matrix) fractions**

Pellets of the silk gland nuclear-associated fraction from fourth moult larvae were incubated in *microfilament stabilization buffer* (70 mM KCl, 5 mM MgCl<sub>2</sub>, 1 mM EGTA, 1 mM PMSF, 20 mM Tris, pH 7.0) containing 2 mg/mL of heavy meromyosin (Sigma) for 1 hour at room temperature (Hirokawa *et al.*, 1983). The sample was briefly centrifuged (Eppendorf 5414). The supernatant was decanted and the pellet was washed in three changes of stabilization buffer. The pellet was then fixed in 2.5% glutaraldehyde in stabilization buffer containing 0.2% tannic acid at 4°C overnight. Following

fixation, the pellet was washed three times in stabilization buffer and then three times in distilled H<sub>2</sub>O. The pellet was stained *en bloc* with half-saturated aqueous uranyl acetate (Locke & Huie, 1980) for 3 hours at room temperature. The pellet was then washed, dehydrated through ethanol, passed through a transition step of propylene oxide and then a change of 1/1 propylene oxide/araldite prior to embedding in araldite.

## CHAPTER 3

### The Development of Branched Silk Gland Nuclei: the Silk Gland Nuclear Matrix

#### 3.1 Introduction

Although the cytoskeletal control of cell shape has received much attention, little is known about the way that the shape of nuclei is determined. The nuclear skeleton or nuclear matrix (Berezney & Coffey, 1974) (for reviews, see: Comerford *et al.* (1986); Kaufmann *et al.* (1986); Verheijen *et al.* (1988)) is thought to determine nuclear shape in much the same way that the cytoskeleton regulates cell shape (Clark & Spudich, 1977; Höner *et al.*, 1988). The nuclear matrix consists of a peripheral nuclear lamina (Franke, 1987; Gerace, 1986; Krohne & Benavente, 1986) and an internal network of filaments, granules and residual nucleoli, depending on the isolation conditions used (Fields *et al.*, 1986; Kaufmann *et al.*, 1981; Kaufmann *et al.*, 1986).

There have been many studies showing the non-random organization of nuclear contents (*e.g.* chromosomes (Gruenbaum *et al.*, 1984; Hochstrasser *et al.*, 1986; Hochstrasser & Sedat, 1987a; Hochstrasser & Sedat, 1987b; van Dekken *et al.*, 1989), nucleoli (Locke & Leung, 1985), RNPs (Fey *et al.*, 1986a; Smith *et al.*, 1986; Spector, 1989), mRNA tracks (Lawrence *et al.*, 1989)). One study has shown changes in the nuclear matrix with changes in nuclear size (Wunderlich & Herlan, 1977), yet no one has correlated the arrangement of the nuclear matrix with changes in nuclear shape. One reason for this is that most nuclei remain unchanging spheres or ovoids during development. Any subtle changes would be difficult, if not impossible, to detect. The branched nuclei of Lepidopteran silk gland cells are an exception.

During larval life, DNA is replicated without cell division in the silk glands. In *Bombyx mori* there are about 18, 19, and 13 rounds of endomitosis (or endoreduplication) in the posterior, mid, and anterior regions, respectively (Perdrix-Gillot, 1979). Fully formed nuclei may be several hundred micrometres across and visible to the naked eye when stained. As each nucleus grows, it can form hundreds of branches throughout the cell (Akai, 1984).



The arborescent nuclei of silk glands were studied in an attempt to find a correlation between nuclear shape and the arrangement of nuclear matrix components. It was expected that growth in these nuclei would involve an exaggeration of the elements that control nuclear shape in less elaborate nuclei, thus making the processes easier to observe. It was found that matrix elements are aligned parallel to the long axes of nuclear branches, as would be expected if shape depends upon the arrangement of the matrix.

## **3.2 Results**

### **3.2.1 The regional development of branched nuclear patterns during larval life**

Feulgen stained silk glands from 2<sup>nd</sup> instar *Calpodes* larvae had ovoid nuclei with little difference in shape between regions (figs. 6-9). Slight indentations or projections at the surfaces of nuclei in the mid region (fig. 10), and dumbbell-shaped nuclei in the posterior region (fig. 11) foreshadowed the future complex patterns.

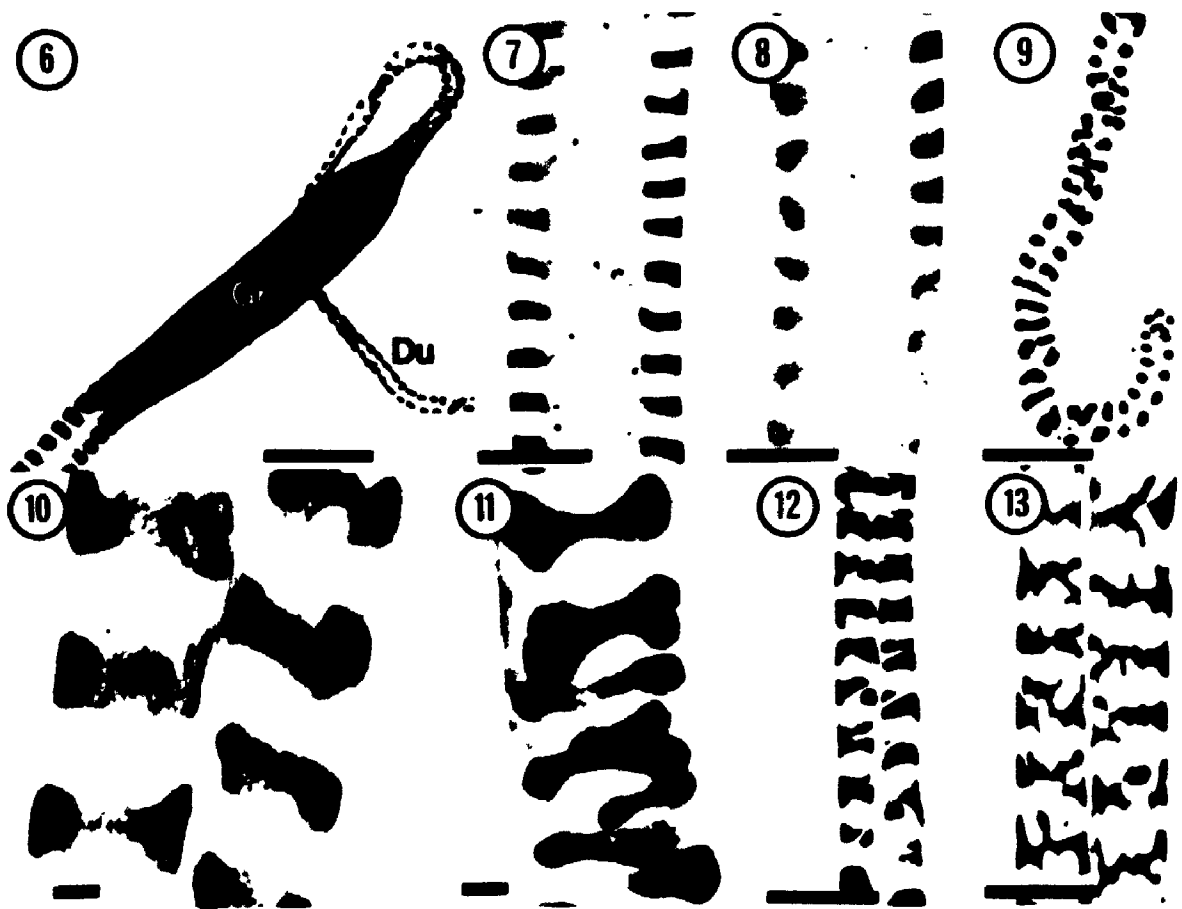
Early in the third stadium, furrows appeared along the long axes of nuclei in the anterior region (fig. 12) and lateral projections extended from nuclei in the mid region (fig. 13). By the fourth stadium, the gland had differentiated into five regions (duct, green, anterior, mid, and posterior (Wiley & Lai-Fook, 1974)), distinguishable by the form of their highly branched nuclei.

By the middle of the fifth stadium, the nuclei had branched to their greatest extent. In the anterior-most region, the duct had relatively small, slightly branched nuclei (fig. 14). The green region had simple C-shaped nuclei (figs. 14 & 15) which only branched slightly at their ends late in the stadium (fig. 14). There was an abrupt transition in nuclear shape between the duct and the green region (fig. 14). A similar abrupt transition occurred in nuclear shape between the green and anterior regions (fig. 15). The anterior gland region had slightly branched nuclei (fig. 16), larger and more branched than those of the duct and green regions. The largest and most elaborately branched nuclei occurred in the mid region (fig. 17), where the nuclei were several hundred micrometres across (approximately 200  $\mu\text{m}$  by

**Figs. 6 to 18.** The silk gland nuclei grow and branch gradually throughout larval life to form regionally characteristic arborescent shapes. Silk glands were stained with Feulgen stain for DNA.

**Figs. 6 to 11.** Silk gland nuclei from early larval stadia are smooth and ovoid. Early in the second stadium, there is little difference in structure between the duct (Du) (fig. 6), green (Gr) (fig. 6), anterior (fig. 7), mid (fig. 8) and posterior (fig. 9) regions of the gland. The first signs of branching appear late in the second larval stadium. Nuclei in the mid region of the gland have lateral bumps (fig. 10). Nuclei in the posterior region form dumbbell shapes (fig. 11). Scale bars = 100  $\mu\text{m}$  (figs. 6-9); 10  $\mu\text{m}$  (figs. 10,11)

**Figs. 12 & 13.** The first signs of nuclear branching appear during the third larval stadium. Furrows develop along the length of the nuclei in the anterior region of the silk gland at this time (fig. 12). The position of the furrow is similar in many cells. At the same time, lateral branches project from the mid region nuclei during the third larval stadium (fig. 13). Scale bars = 100  $\mu\text{m}$



**Figs. 14 to 18. Regionally characteristic nuclear shapes are most elaborate by the middle of the fifth stadium. Nuclei of the duct (Du) are relatively small and simple in their branching pattern (fig. 14). Nuclei of the green region (Gr) (posterior to the duct) are C-shaped and show little or no branching (figs. 14,15). The transition between the duct and the green region (fig. 14) and the transition between the green region and the anterior region (fig. 15) of the silk gland are marked by a sudden changes in nuclear morphology. Nuclei of the anterior region are moderately branched (fig. 16). Nuclear morphology is most complex in the mid region of the gland (fig. 17). Mid region nuclei are several hundred micrometres across and extensively branched. Posterior region nuclei (fig. 18) are moderately branched (more so than the nuclei of the anterior region) but are compacted within the cells. The nuclear branching pattern is more three-dimensional in this region than the two-dimensional branching in the mid and anterior regions. Feulgen stained fat body nuclei (arrowheads) which appear adjacent to the silk gland indicate the relative difference in size between nuclei of the silk gland and fat body.**

**Scale bars = 100  $\mu$ m**



1,000  $\mu\text{m}$ ) with several hundred small branches. The nuclei of the posterior region were more compact but with 3-dimensional branching (fig. 18).

Even in the largest nuclei, the diameter of branches remained about the same as that of whole nuclei from earlier stadia (10 to 20  $\mu\text{m}$ ; compare figs. 7-9 & 17), and only slightly greater than nuclei from other large cells (fig. 18). This kind of nuclear growth results in the nuclear contents never being separated from the cytoplasm by more than a 10  $\mu\text{m}$  distance.

During the larval moults, large Feulgen-negative patches appeared in the nuclei of the anterior region of the gland (fig. 19). Initially, these patches were thought to correspond to spherical nuclear bodies which appear in the anterior region nuclei at the same time (fig. 20). Preliminary investigations with confocal microscopy, however, indicated that these patches were extranuclear, and are probably formed by the compression of the nuclear surface by cytoplasmic vacuoles (figs. 21 & 22).

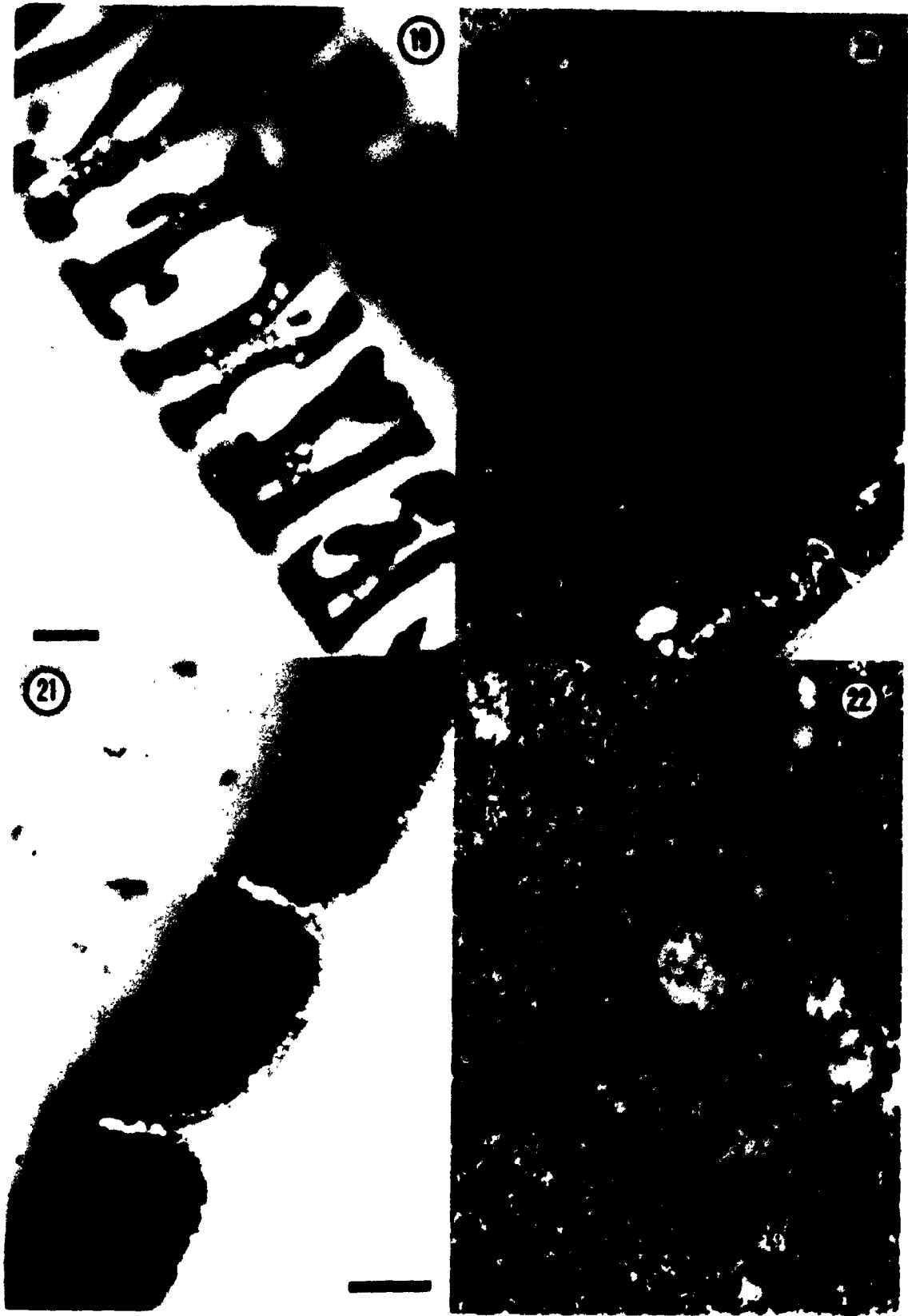
### **3.2.2 The 3-dimensional arrangement of the nuclear matrix resembles the shape of intact nuclei**

If the nuclear matrix plays a role in the branching of silk gland nuclei then it is expected that the orientation of matrix components would reflect the orientation of growth of the branches. SEM of silk glands extracted *in situ* with Triton X-100, nucleases, and high salt solutions (fig. 23) showed that the residual nuclear matrices had shapes similar to those of intact Feulgen stained nuclei. The nuclear lamina formed a 3-dimensional meshwork of filaments with a bias in their orientation parallel to the long axes of the nuclear branches.

TEM of thin sections of the nuclear matrix fraction revealed discrete structural components. Whole nuclei never occurred in these preparations because the technique used for isolation caused shredding of the branches. Yet the ends of the branches often remained intact. Intranuclear filaments were oriented normal to sheets of nuclear lamina at the nuclear surface. These filaments are presumed to be terminating at the ends of branches. The filaments were arranged parallel to each other and to the long axes of the branches (fig. 24).

Epifluorescent imaging of H $\ddot{a}$ echst stained cells showed DNA had a similar alignment in strands parallel to the long axes of the branches (fig.

**Figs. 19 to 22.** Feulgen-negative patches which form in the anterior region nuclei during the 4<sup>th</sup> moult are probably caused by nuclear compression. During the fourth larval moult, large feulgen-negative patches form in the nuclei of the anterior region of the gland (fig. 19). Initially, these patches were thought to correspond to spherical nuclear bodies (NB) which also form during the moult (fig. 20). The nuclear bodies are more regular in profile than nucleoli (compare with fig. 3). Saggital sections (stained with Toludine blue) through the lumen of the gland show that the nuclei in this region are compressed by large cytoplasmic bodies or vacuoles (v) (fig. 21). Similar depressions in the nuclear surface by cytoplasmic vacuoles (v) can be seen in thin sections of nuclei of this region (fig. 22). Scale bars = 25  $\mu\text{m}$  (fig. 19); 1  $\mu\text{m}$  (fig. 20); 25  $\mu\text{m}$  (fig. 21); 0.5  $\mu\text{m}$  (fig. 22).





**Fig. 23.** The nuclear skeleton of silk gland cells conforms to the elaborate shape of the nucleus. Silk gland cells extracted *in situ* and examined by SEM show the meshwork of the nuclear lamina (NL) forms shapes which are similar to shapes of Feulgen stained silk gland nuclei. In some regions the filaments of the lamina have a bias in their orientation which is parallel to the long axis of the branch. Some extranuclear cytoskeletal elements (arrows) resist extraction *in situ*. Scale bar = 1  $\mu\text{m}$

**Fig. 24.** Intranuclear filaments of the silk gland nuclear matrix are arranged parallel to each other. Silk gland nuclei contain an intranuclear matrix even when isolated in the presence of DTT. The filaments of this matrix are aligned parallel to each other and are oriented parallel to the long axis of the nuclear branch. This arrangement of filaments occurs at the ends of the nuclear branches. Further into the nuclear interior, the matrix is coarser and randomly arranged (see fig. 66). Scale bar = 1  $\mu\text{m}$

**Fig. 25.** The spatial arrangement of DNA within the silk gland nuclei reflects the arrangement of the nuclear matrix. Silk gland nuclei stained with Hoechst 33258 for DNA show the DNA arranged in strands parallel to the long axis of the nuclear branch. Scale bar = 10  $\mu\text{m}$



25). DNA is therefore arranged in strands parallel to the nuclear matrix filaments.

Homogenization and extraction often produced isolated sheets of nuclear laminae in the matrix fraction (fig. 26) which were identified by labelling with the monoclonal antibody (P1) to peripherin (fig. 27) and by the structural features that they shared with the nuclear envelope. They contained densely packed nuclear pore complexes, some of which retained the electron dense plug seen in sections of unextracted cells (figs. 27 & 28).

It can be concluded that silk gland nuclei do possess a skeleton which, at least, maintains their branched shapes. Furthermore, there is an intranuclear matrix in which arrays of parallel filaments extend from the nuclear lamina at the ends of nuclear branches. Thus, the nuclear lamina and the intranuclear matrix are arranged in an architecture appropriate for maintaining (if not generating) nuclear shape.

### 3.2.3 The polypeptides forming the nuclear matrix

If nuclear branching is the result of an hypertrophy of a process occurring in most nuclei, then there may be an abundance of particular nuclear matrix polypeptides common to all nuclei. If, on the other hand, nuclear branching is a consequence of a unique specialization within silk gland nuclei, then there may be an abundance of equally unique polypeptides for the purpose. There might also be an increased synthesis of the particular polypeptides needed for incorporation into the matrix during or preceding branching. To determine which proteins incorporate into the matrix of growing nuclei, silk glands from 4<sup>th</sup> stage larvae (*i.e.* when the nuclei were growing and branching (Morimoto *et al.*, 1968)) were labelled with <sup>35</sup>S-methionine. The nuclear matrices were then isolated and analyzed by two dimensional SDS-polyacrylamide gel electrophoresis and fluorography. Since the composition of the matrix can be affected by the order of extraction steps (Kaufmann *et al.*, 1981), two different protocols were used (figs. 29-32).

Components of the matrix fraction common to both extraction procedures included: a polypeptide (76 kD, pI 5.9) similar in molecular weight and pI to *Drosophila* lamin (Smith & Fisher, 1989); a polypeptide (43 kD, pI 6.45) similar in molecular weight to actin (see Chapter 4); and

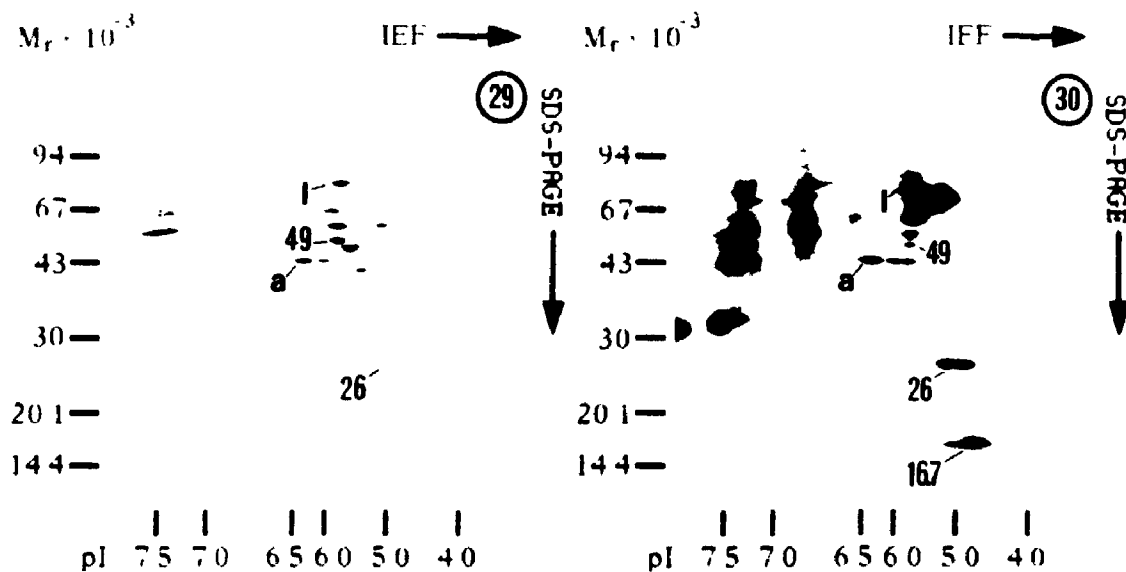
**Figs. 26 to 28. Sheets of nuclear laminae label with P1.** Nuclear matrices isolated from silk gland cells often contain isolated sheets of nuclear laminae (fig. 26). The identification of these structures as nuclear lamina is based upon the presence of nuclear pore complexes (NP) (which contain electron dense plugs (arrows) similar to those seen in unextracted cells) (figs. 27,28) and labelling with colloidal gold tagged anti-peripherin (P1) (fig. 27). Scale bars = 0.5  $\mu\text{m}$  (fig. 26); 0.1  $\mu\text{m}$  (figs. 27,28)



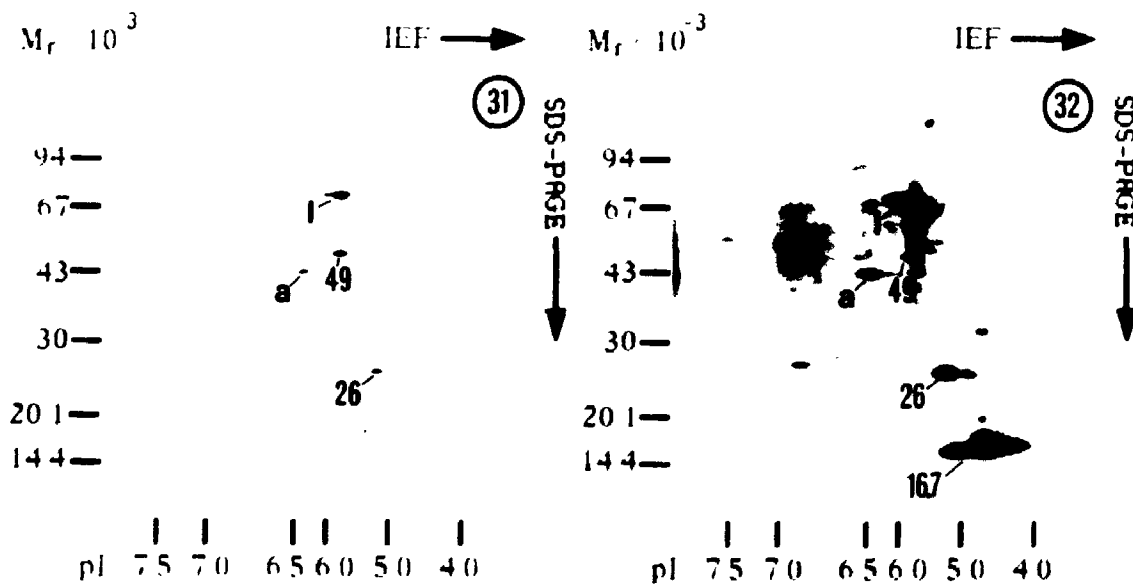
2

**Figs. 29 to 32.** The silk gland nuclear matrix fraction is characterized by an abundance of a very few polypeptides. Nuclear matrices were isolated from <sup>35</sup>S-methionine labelled silk glands dissected from 4<sup>th</sup> instar *Calpodes* larvae. Nuclei during this stage of development are still growing and branching (Morimoto *et al.*, 1968). Nuclear matrices were prepared by two different methods in order to determine if the presence of any of the structural components is affected by the order or ionic strength of the extraction steps (Kaufmann *et al.*, 1981). Polypeptides common to both of the nuclear matrix fractions revealed by Coomassie stained 2-D polyacrylamide gels (figs. 29, 31) and corresponding fluorograms (figs. 30,32) include: a polypeptide (76 kD, pI 5.9) which is similar in molecular weight and pI to *Drosophila* lamin (l) (Fisher, 1988); a 43 kD polypeptide (pI 6.45) which is similar in molecular weight to actin (a); a 49 kD polypeptide (pI 5.9) and a 26 kD polypeptide (pI 5.0-5.2). One polypeptide (16.7 kD, pI 4.9-5.1) forms a large proportion of the newly synthesized polypeptides associated with the matrix but is barely detected in Coomassie stained gels.

SGNAF (by method of Fisher *et al.* (1982))



SGNAF (by method of Berezney and Coffey (1974))



polypeptides of 26 kD (pI 5.0-5.2) and 49 kD (pI 5.9). Some polypeptides (e.g. 16.7 kD, pI 4.9-5.1; 73 kD, pI 5.2) formed a large proportion of the newly synthesized polypeptides associated with the matrix but a small proportion of the total protein complement of the matrix. The presence of a few polypeptides (45, 55, & 63 kD) was affected by the order and/or ionic strength of the extraction steps.

Therefore, the nuclear matrix is formed mainly from a few proteins, some of which are not unique to silk glands.

### **3.2.4 Antigens found in other eukaryote nuclei also occur in silk gland nuclei**

The small number of polypeptides found in the silk gland nuclear matrix did not preclude the possible existence of other minor proteins in these nuclei not detected by electrophoresis. To see if silk gland nuclei contained other proteins in addition to those detected by electrophoresis and to determine the localization of these proteins during development, silk gland nuclei were probed with antibodies to nuclear proteins found in more typical, unbranched, vertebrate nuclei. Anti-nuclear matrix monoclonal antibodies P1 and PI1 but not P12 were bound by the silk gland nucleus. PI1 (figs. 33 & 35) and P1 (figs. 34 & 36) were localized at the nuclear periphery both early in development, when the nuclei were simple in shape and later, when nuclei formed many branches. The localization of these antigens did not change during development (figs. 33-36).

Silk gland nuclei also reacted with anti-nuclear antibodies from human auto-immune sera (fig. 62) to snRNPs.

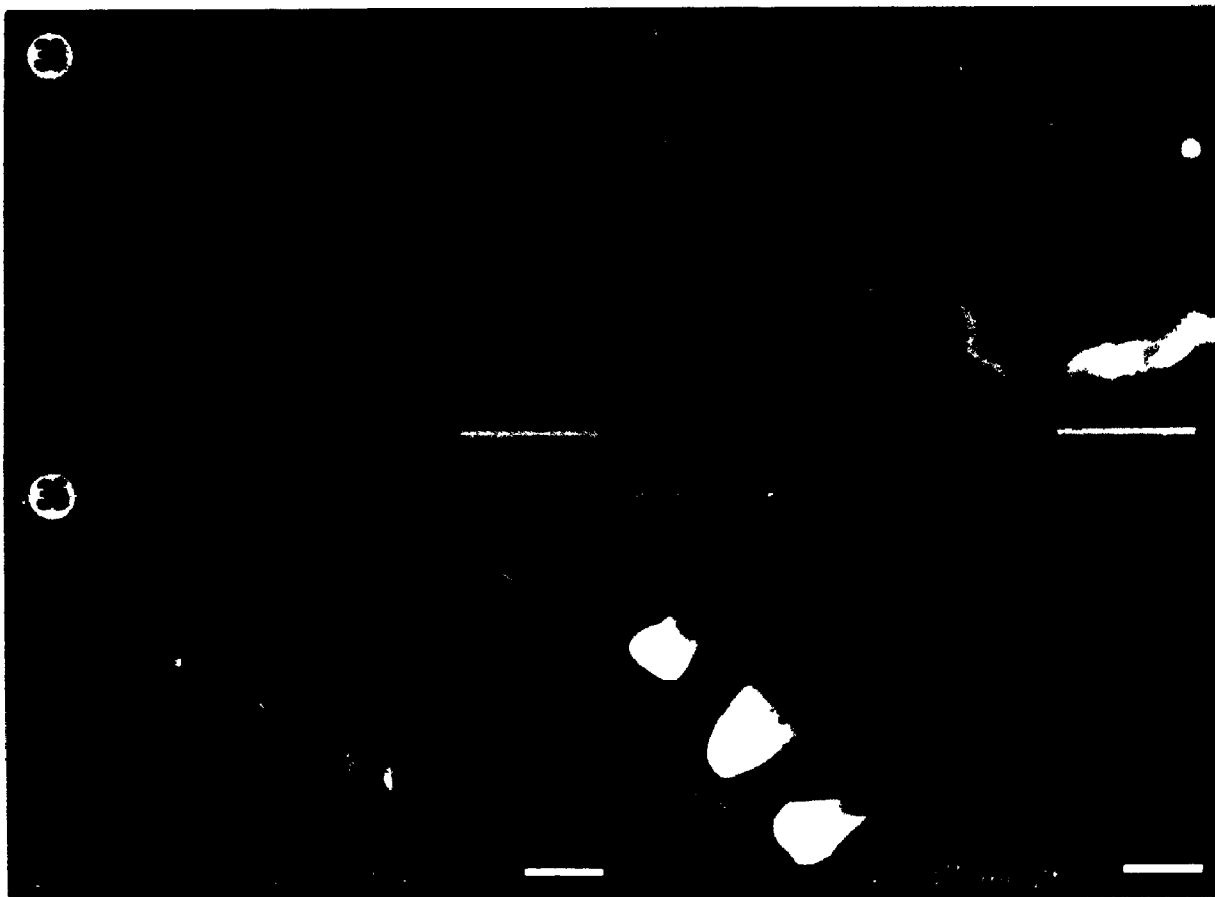
It can be concluded that silk gland nuclei contain many antigens found in smaller, more regularly shaped nuclei. Thus, branching may be accomplished by the selective use of processes present in most cells and/or by the use of elements present in proportionately small amounts not detected by electrophoresis.

### **3.3 Discussion**

Silk gland cells of *Calpodes ethlius* have nuclei that branch in patterns characteristic for each part of the gland. Although the nuclear shapes are not identical between adjacent cells, there are general similarities



**Figs. 33 to 36. Silk gland nuclei label with monoclonal antibodies to nuclear matrix antigens found in more typical nuclei. Crushed/fractured silk glands were probed with monoclonal antibodies P11 (figs. 33,35) and P1 (figs. 34,36) to nuclear matrix antigens (Chaly *et al.*, 1984) followed by FITC-conjugated anti-mouse IgG. The localization of these antigens does not change with development. Both antibodies label the nuclear periphery early in larval life, when nuclear morphology is simple (figs. 33,34), and later, when the nuclei have many branches (figs. 35,36). Figs. 33 & 34: Silk gland nuclei from 3<sup>rd</sup> instar larvae. Figs. 35 & 36: Silk gland nuclei from 4<sup>th</sup> moult larvae. Photographed using a Zeiss Photomicroscope II. Scale bars = 25  $\mu$ m**



in the branching patterns within each region. These regionally characteristic branching patterns suggest that some factor is responsible for controlling nuclear shape. SEM and TEM of extracted nuclei show that silk gland cells have a nuclear matrix which conforms to the three-dimensional shape of the nucleus. The nuclear lamina is a meshwork of filaments similar to that found in vertebrate nuclei (Aebi *et al.*, 1986) except that the lamina filaments have a bias in the direction of the long axes of nuclear branches. The orientation of the nuclear matrix filaments (both laminar and intranuclear) makes them unlike those found in other cells. The matrix arrangement is consistent with the hypothesis that the oriented growth of nuclear branches may be (in part) the result of polarized growth of the lamina and intranuclear filaments. The role of the matrix in maintaining shape is confirmed by the finding that nuclei isolated from the silk glands of *Bombyx mori* maintain their shapes even in salt solutions which extract DNA (Ichimura *et al.*, 1985).

In silk gland nuclear matrices, intranuclear filaments persist in the presence of DTT. In this respect, the silk gland nuclear matrix is similar to other insect cells (Fisher, 1988; Fisher *et al.*, 1982) and is unlike that in mammals. The stability of the intranuclear matrix is not dependent upon oxidative cross-linking (Dijkwel & Wenink, 1986; Fields *et al.*, 1986; Kaufmann *et al.*, 1986).

Typical nuclear matrix preparations from vertebrate cells may contain several polypeptides (Peters & Comings, 1980). The polypeptide composition of the silk gland nuclear matrix fraction is simpler; it contains an abundance of a very few polypeptides. One polypeptide is similar in molecular weight and pI to *Drosophila* lamin (Smith & Fisher, 1989; Smith *et al.*, 1987). Lamin is expected to be abundant given the large surface area of the nucleus. There are other polypeptides which form part of the nuclear matrix (49 kD & 26 kD) whilst some are only temporarily associated with it (16.7 kD). One polypeptide which maintains its association with the nuclear matrix and is similar in molecular weight to actin will be discussed in more detail below and in Chapter 4.

Although exceptional in size and shape, silk gland nuclei contain elements common to all nuclei. They bind monoclonal antibodies (P1 and P11) (Chaly *et al.*, 1984) to nuclear matrix antigens which occur in many eukaryotic nuclei: both plant and animal (Chaly *et al.*, 1986). The antigen

detected by P1 (anti-peripherin) is associated with chromatin (Chaly *et al.*, 1984; Chaly *et al.*, 1985) and with the nuclear lamina (Chaly *et al.*, 1989). The nuclear matrix antigen detected by P11 is part of a glycoprotein associated with the nuclear pore complex (Dabauvalle *et al.*, 1988). The surfaces of branched nuclei are not specialized with respect to the distribution of these antigens. Confocal microscopy shows that both antigens are evenly distributed over the entire nuclear periphery without regard for branching. The exclusively peripheral distribution of P11 labelling in silk gland nuclei was similar to that found in *Drosophila* Kc cells (Chaly *et al.*, 1986) and *Xenopus* oocytes (Dabauvalle *et al.*, 1988).

Actin is capable of polarized growth and known to regulate shape in cells (Clark & Spudich, 1977; DeBiasio *et al.*, 1988). Actin in the nuclear fractions was a likely candidate for the parallel intranuclear matrix filaments. However, the intranuclear matrix filaments did not label with antibodies to actin or heavy meromyosin (results not shown). A lamina-like component of the silk gland nuclear fraction, different from the nuclear lamina, did bind antibodies to actin and myosin as well as heavy meromyosin (Chapter 4). This structure, which is referred to as the nuclear shell, is found at the nucleocytoplasmic interface. The nuclear shell may work in conjunction with polarized growth of the nuclear matrix to shape silk gland nuclei.

It can be concluded that silk gland nuclei have a matrix which conforms to the nuclear shape and which may therefore be responsible for maintaining (and perhaps generating) the regionally specific shapes. The branched pattern is associated with the amplification of a few main matrix components which are also found in other cells. Other components, which are present in small or undetectable amounts, may also play some role in nuclear ramification. The oriented arrangement of the matrix filaments is a unique feature of these branched nuclei and suggests a role for them in the growth of nuclear branches.

## CHAPTER 4

### A Shell of F-actin Surrounds the Branched Nuclei of Silk Gland Cells

#### 4.1 Introduction

Although actin has been found within interphase nuclei, the existence of functional nuclear actin is controversial (Goldstein *et al.*, 1977b; LeStourgeon, 1978). It has been suggested that actin found in the nucleus may be cytoplasmic contamination (Comings & Okada, 1976). Actin has been found to form a filamentous matrix throughout the nucleoplasm (Clark & Rosenbaum, 1979; Crowley & Brasch, 1987; Nakayasu & Ueda, 1985b; Parfenov & Galaktionov, 1987) and may even exist as unique nuclear isoforms (Bremer *et al.*, 1981; Kumar *et al.*, 1984; Nakayasu & Ueda, 1986). Nuclear actin (or nuclear-associated actin) has been implicated in a variety of cellular functions including: nucleocytoplasmic transport (Schindler & Jiang, 1986; Ueyama *et al.*, 1987), condensation of chromatin (Goldstein *et al.*, 1977a; Rubin *et al.*, 1978; Rungger *et al.*, 1979), snRNP attachment (Carmo-Fonseca *et al.*, 1989; Nakayasu & Ueda, 1984), DNA attachment (Valkov *et al.*, 1989), transcription (Nakayasu & Ueda, 1985a; Scheer *et al.*, 1984; Schröder *et al.*, 1987), chromosome movement during mitosis (Forer, 1988), and viral nucleocapsid assembly (Vo'kman, 1988). It has even been suggested that actin may be responsible for the maintenance of nuclear structure (*i.e.* nuclear shape) (Fukui, 1978; Fukui & Katsumara, 1980; Heslop-Harrison & Heslop-Harrison, 1989a; LeStourgeon, 1978; Nakayasu & Ueda, 1983).

The association of actin with the silk gland nuclear matrix fraction suggested that it may play a role in nuclear ramification. The presence and distribution of actin in such extraordinarily shaped nuclei might confirm the possibility of its involvement in the determination of their shape.

It was found that silk gland nuclear matrix fractions contain a nuclear isoform (43 kD, pI 6.45) of a polypeptide similar in molecular weight to actin. The association of actin with these highly branched nuclei was confirmed by immunofluorescence and by immunogold and heavy meromyosin labelling of the nuclear-associated fraction. A myosin-like

antigen was also found to be associated with the branched nuclei. Both antigens occur in a peripheral nuclear layer called the nuclear shell.

Thus, both actin and myosin of the nuclear shell may participate in nuclear growth and shape change in much the same way that cell shape may be controlled by cytoplasmic actin and myosin (Conrad *et al.*, 1989; DeBiasio *et al.*, 1988; Fukui *et al.*, 1989).

## 4.2 Results

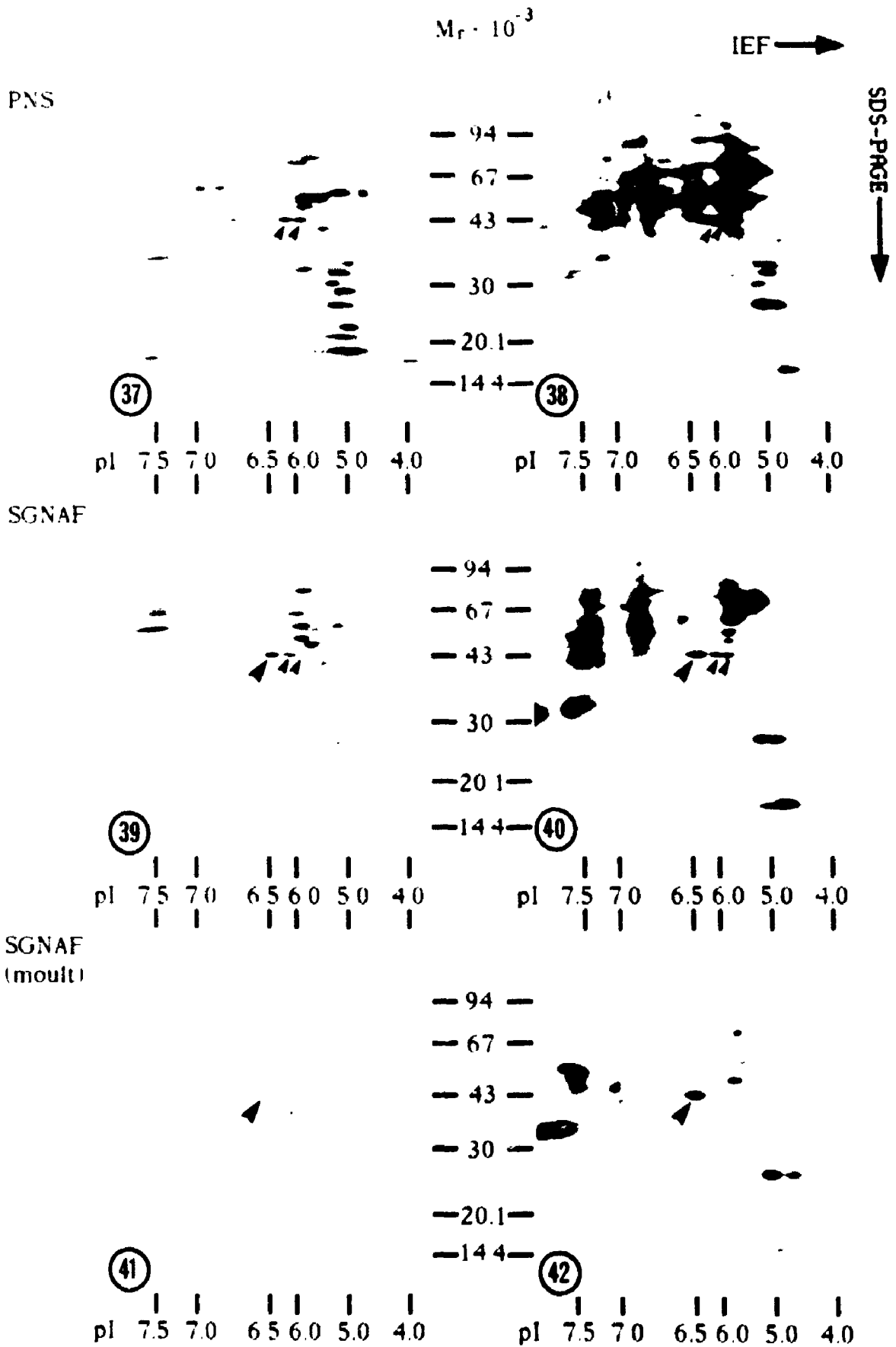
### 4.2.1 Silk gland sub-nuclear fraction has an isoform of actin

Comparison of the polypeptides found in the silk gland nuclear-associated fraction (SGNAF; *i.e.* nuclear matrix - fig. 39) and the post-nuclear fraction (PNS - fig. 37) showed that the nuclear fraction contained an isoform of a polypeptide (43 kD, pI 6.45) that is similar in molecular weight to actin. Small amounts of the two more acidic isoforms found in the cytosolic fraction were also found in the nuclear-associated fraction. Since extensive bundles of f-actin are a major part of the cytoskeleton at this time (Chapter 6), they may have contaminated the nuclear-associated fraction to a small extent. Analysis of the fluorograms of the <sup>35</sup>S-methionine labelled polypeptides also showed the same "actin" isoform (43 kD, pI 6.45) present in the nuclear matrix (fig. 40) but not the cytosolic (fig. 38) fractions. The pI 6.45 isoform of newly synthesized actin is therefore associated preferentially with the nuclear matrix of growing nuclei.

When the nuclear-associated fraction was isolated from silk glands dissected from moulting larvae (at a time when secretory protein synthesis has stopped and only housekeeping protein synthesis is maintained (Couple *et al.*, 1983)) only the pI 6.45 isoform of the polypeptide was detected in both the Coomassie-stained gel (fig. 41) and the fluorogram (fig. 42). Studies on the cytoskeleton in moulting larvae showed that the cytoplasmic f-actin bundles had dissociated during this time (Chapter 6).

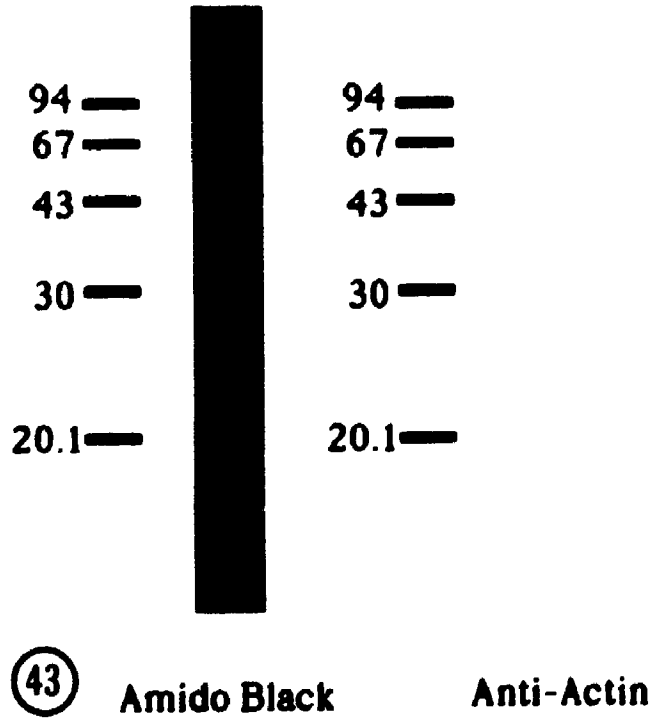
Immunoblots of the silk gland nuclear-associated fraction isolated from moulting larvae (in which only the pI 6.45 isoform was detected) showed a narrow band with a relative mobility of 43 kD bound antibodies to actin (fig. 43). Thus, the nucleus, or nuclear-associated material present in

**Figs. 37 to 42.** The silk gland nuclear-associated fraction contains an isoform of a polypeptide which is similar in molecular weight to actin. Nuclear matrices were prepared from <sup>35</sup>S-methionine labelled silk glands dissected from 4<sup>th</sup> instar larvae. The fractions were separated by isoelectric focusing in the first dimension and SDS-polyacrylamide gel electrophoresis in the second dimension. Comparison of the polypeptide patterns obtained from the post-nuclear supernatant (PNS - fig. 37) and nuclear-associated fractions (SGNAF - fig. 39) indicates that one polypeptide has a nuclear-associated isoform (43 kD, pI 6.45) which is not present in detectable amounts in the cytosolic fraction. This isoform (large arrow) is more basic than the two cytosolic isoforms (small arrows). Similar patterns are obtained for the incorporation of the newly synthesized polypeptides into the nuclear matrix fraction (figs. 38,40). The nuclear matrix fraction prepared from <sup>35</sup>S-methionine labelled silk gland dissected at the time of the fourth larval moult (when secretory protein synthesis ceases) shows that only the more basic isoform of the 43 kD polypeptide is present in detectable amounts in the nuclear-associated fraction (fig. 41). Fluorograms indicate that this isoform is continuously synthesized and incorporated into the nuclear matrix of growing nuclei even during the moult (fig. 42).





**Fig. 43. Western blots of the silk gland nuclear-associated fraction bind antibodies to actin.** The silk gland nuclear-associated fraction isolated from moulting larvae was separated by SDS-PAGE and transferred to nitrocellulose. Longitudinal strips cut from the blot were either stained with amido black or were probed with antibodies to actin followed by alkaline phosphatase-conjugated anti-rabbit IgG. Development of the blot revealed a band (with a relative mobility of 43,000) that had bound antibodies to actin.



this fraction, contains its own isoform of actin. The following experiments attempted to show its location.

#### **4.2.2 Silk gland nuclei label with antibodies to actin and myosin**

Late in larval life, the nuclei of the silk gland cells were several hundred micrometres across and highly branched (fig. 44). Antibodies to actin labelled structures similar in appearance to these arborescent nuclei (fig. 45). To confirm that the anti-actin labelled structures were nuclear and to determine the location of actin within the nuclei, silk glands were double labelled with antibodies to actin and to a nuclear matrix antigen (PI1) (Chaly *et al.*, 1985). Both antibodies labelled the nucleus early in development, when the lobes were beginning to form (figs. 46 & 47), and later when there were many branches (figs. 48 & 49). The labelling for actin was most intense at the nuclear periphery, indistinguishable in its location from the nuclear matrix antigen detected by PI1. Antibodies to myosin also labelled the nuclear lobes both early (figs. 50 & 51), and late in development (figs. 52 & 53). The localization of actin and myosin at the periphery of the nuclear lobes was confirmed by confocal microscopy (figs. 54 & 55).

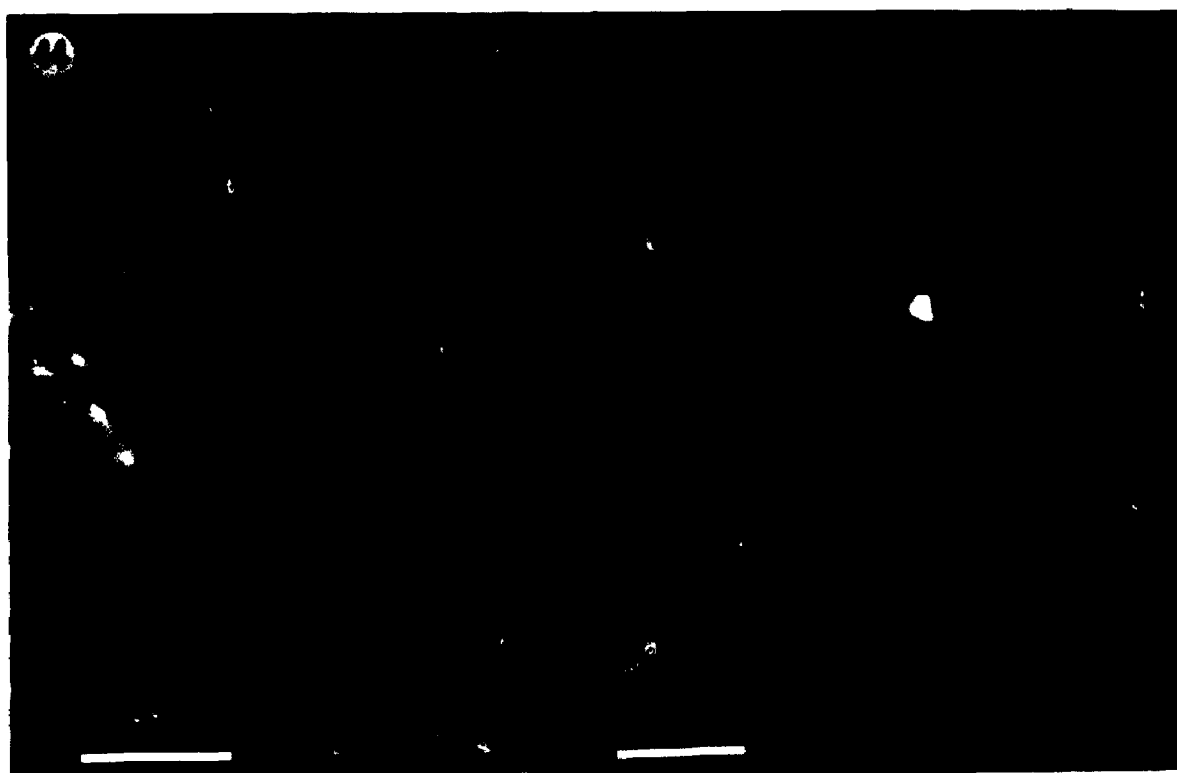
These studies showed that the nucleus has a peripheral layer which contains actin and myosin. Unlike cytoskeletal actin structures that form and disperse with the moult cycle (Chapter 6), this nuclear actin/myosin layer persists throughout larval life (including the moults) and is not formed only at particular phases of development.

#### **4.2.3 The silk gland nuclear-associated fraction contains the nuclear shell which labels with antibodies to actin and myosin**

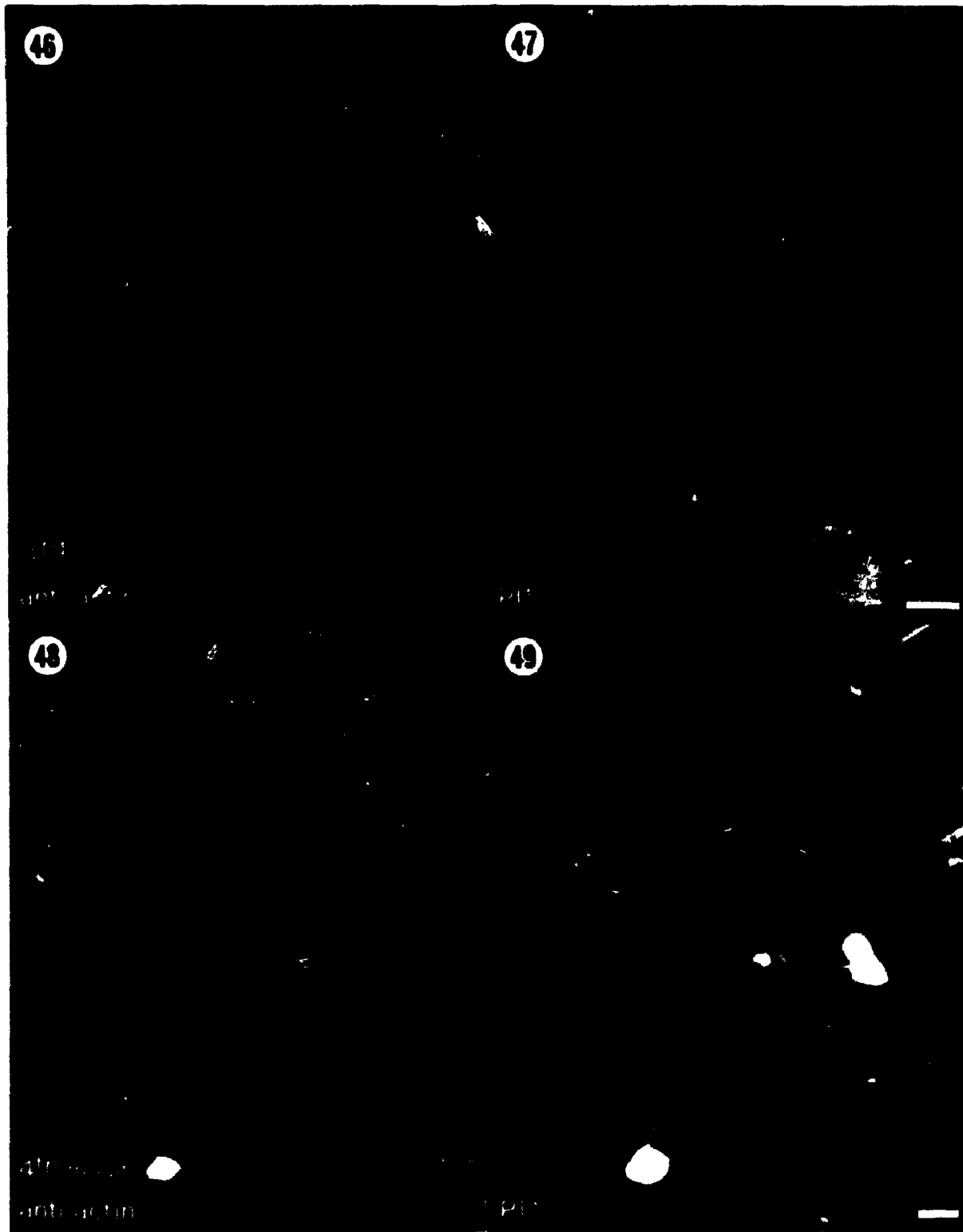
Sections of the silk gland nuclear-associated fraction examined by electron microscopy revealed two different lamina-like structures, one more electron-dense (figs. 56 & 57) than the other (figs. 58 & 59). The denser structure contained many nuclear pore-like elements, and bound a monoclonal antibody to the nuclear matrix antigen - peripherin (figs. 56 & 57) (Chaly *et al.*, 1989) but not actin (fig. 57). This structure is most likely the nuclear lamina from inside the nuclear envelope (Chapter 3). The less dense lamina-like structure did not label with anti-peripherin but labelled with antibodies to both actin (fig. 58) and myosin (fig. 59). Although it had

**Fig. 44. Silk gland nuclei are highly branched and several hundred micrometres across by the time of the 4<sup>th</sup> larval moult. Whole silk glands were stained with Hœchst 33258 for DNA. Scale bar = 100 µm**

**Fig. 45. Silk gland nuclei label with antibodies to actin. Fractured silk glands were probed with a polyclonal antibody to actin and then with FITC-conjugated anti-rabbit IgG. The arborescent nuclei bind the anti-actin antibodies. Scale bar = 100 µm**



**Figs. 46 to 49. Antibodies to actin and the nuclear matrix co-localize to the silk gland nuclear lobes.** Anti-actin labelling correlates with the P11 labelling both early in larval development (figs. 46,47) when nuclear branching is in its initial stages and late in larval development (figs. 48,49) when nuclei are highly branched. Fig. 46: Mid third stage silk gland labelled with polyclonal anti-actin followed by FITC-conjugated anti-rabbit IgG. Fig. 47: Same tissue labelled with monoclonal antibody P11 to nuclear matrix followed by rhodamine-conjugated anti-mouse IgGAM. Fig. 48: Fourth moult silk gland labelled with polyclonal anti-actin followed by rhodamine-conjugated anti-rabbit IgG. Fig. 49: Same tissue labelled with monoclonal antibody P11 to nuclear matrix followed by FITC-conjugated anti-mouse IgG. Photographed using a Zeiss Photomicroscope II. Scale bars = 10  $\mu\text{m}$



**Figs. 50 to 53. Antibodies to myosin and the nuclear matrix co-localize to the silk gland nuclear lobes.** Fractured silk glands were probed with a polyclonal antibody to myosin and then with an anti-nuclear matrix monoclonal antibody (PI1). As was found with anti-actin labelling, anti-myosin labelling correlates with the PI1 labelling both early in larval development when nuclear branching is in its initial stages (figs. 50,51) and later in larval development (figs. 52,53) when nuclei are highly branched. Fig. 50: Third stage silk glands labelled with anti-myosin + rhodamine-conjugated anti-rabbit IgG. Fig. 51: Same tissue labelled with PI1 + FITC-conjugated anti-mouse IgG. Fig. 52: Fourth moult silk glands labelled with anti-myosin + FITC-conjugated anti-rabbit IgG. Fig. 53: Same tissue labelled with PI1 + rhodamine-conjugated anti-mouse IgGAM. Photographed using a Zeiss Photomicroscope II. Scale bars = 10  $\mu$ m



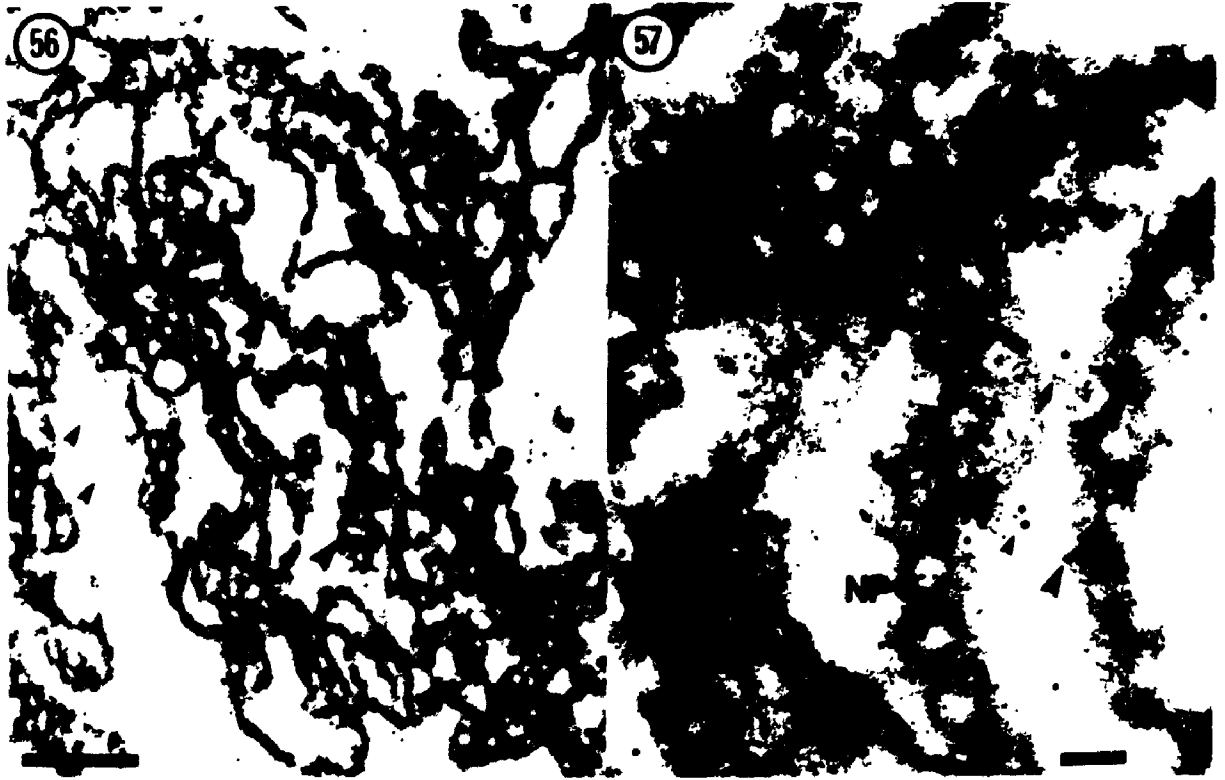


**Fig. 54. Antibodies to actin localize to the nuclear periphery.** Fractured silk glands were probed with a polyclonal antibody to actin and then with FITC-conjugated anti-rabbit IgG. Optical sectioning by confocal microscopy (Leitz CSLM) confirms that anti-actin antibodies label the periphery of silk gland nuclear lobes. Scale bar = 25  $\mu\text{m}$

**Fig. 55. Antibodies to myosin localize to the nuclear periphery.** Fractured silk glands were probed with a polyclonal antibody to myosin and then with FITC-conjugated anti-rabbit IgG. Optical sectioning by confocal microscopy (Leitz CSLM) confirms that anti-myosin antibodies label the periphery of silk gland nuclear lobes.  
Scale bar = 10  $\mu\text{m}$

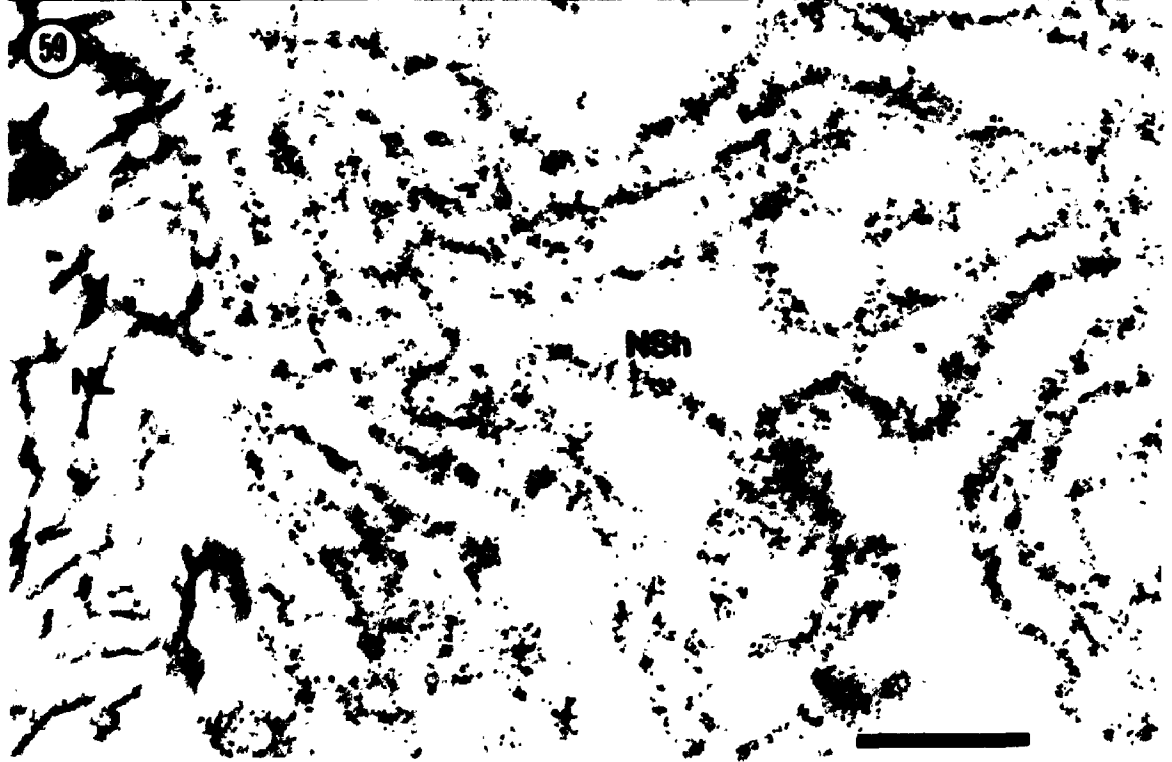


**Figs. 56 & 57. One of the lamina-like structures of the silk gland nuclear-associated fraction labels with a monoclonal antibody to the nuclear matrix antigen - peripherin (P1) but not with antibodies to actin. Sections of LR White embedded silk gland nuclear-associated fraction were labelled with a polyclonal antibody to actin followed by 5 nm gold-conjugated anti-rabbit IgG. The sections were then labelled with an anti-nuclear matrix monoclonal antibody (P1) followed by 10 nm gold-conjugated anti-mouse IgG. Antibodies to peripherin (large arrow) label the lamina-like structures which contain nuclear pores (NP). Antibodies to actin (small arrow) do not label these structures. Scale bars = 0.5  $\mu\text{m}$  (fig. 56); 0.1  $\mu\text{m}$  (fig. 57)**



**Fig. 58. A less electron-dense lamina-like structure of the silk gland nuclear-associated fraction labels with an antibody to actin.** Sections of LR White embedded silk gland nuclear-associated fraction were labelled with a polyclonal antibody to actin and then with 5 nm gold-conjugated anti-rabbit IgG. Antibodies to actin label the less electron-dense structures (nuclear shell, NSh) but do not label the electron dense nuclear lamina (NL). Scale bar = 0.5  $\mu$ m

**Fig. 59. The less electron-dense lamina-like nuclear shell of the silk gland nuclear-associated fraction labels with antibodies to myosin.** Sections of LR White embedded silk gland nuclear-associated fraction were labelled with a polyclonal antibody to myosin and then with a 5 nm gold-conjugated anti-rabbit IgG. Antibodies to myosin label the nuclear shell (NSh) but not the nuclear lamina (NL). Scale bar = 0.5  $\mu$ m



traces of nuclear pore-like structures it was not associated with the nuclear lamina in the pellets of the nuclear-associated fraction. This less electron-dense structure, containing actin and myosin-like antigens but not the nuclear matrix antigen-peripherin, likely corresponds to the peripheral nuclear layer which reacts with antibodies to actin and myosin viewed by light microscopy. This layer is referred to as the nuclear shell. The greater density of the lamina compared to the nuclear shell agrees with the relative densities of the layers proposed to correspond with them in conventional electron microscope preparations (figs. 70 & 71).

#### 4.2.4 Silk gland nuclear branches label for f-actin

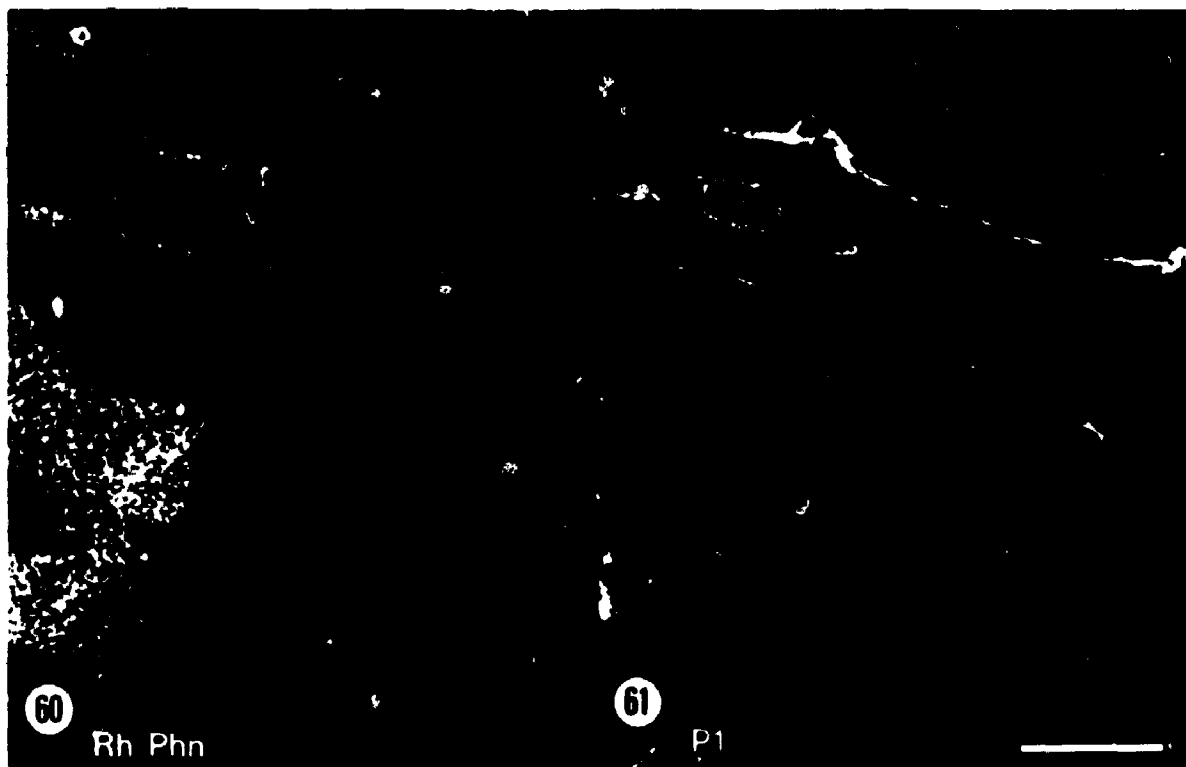
To determine the morphological state of the nuclear shell actin (*i.e.* filamentous or globular), silk glands were double labelled with antibodies to a nuclear antigen (PI 1 (fig. 60) or ANA (fig. 61) with a fluorescein-tagged 2° antibody) and rhodamine-conjugated phalloin (figs. 60 & 62) (which preferentially labels f-actin (Wieland & Govindan, 1974; Wieland *et al.*, 1983)). Silk gland nuclear branches, identified by their positive reaction with the nuclear antibodies, labelled weakly with phalloin. Confocal microscopy showed phalloin labelling at the periphery of the branches indistinguishable in its location from that of antigens detected by PI1 (figs. 60 & 61). The f-actin had the same distribution as the anti-actin antibody localization in the nuclear shell at the nuclear periphery (figs. 60 & 63). Thus, at least part of the actin in the nuclear shell is present as f-actin, which forms a layer so close to the nuclear matrix periphery that it cannot be resolved separately by light microscopy.

#### 4.2.5 Nuclear shells contain f-actin

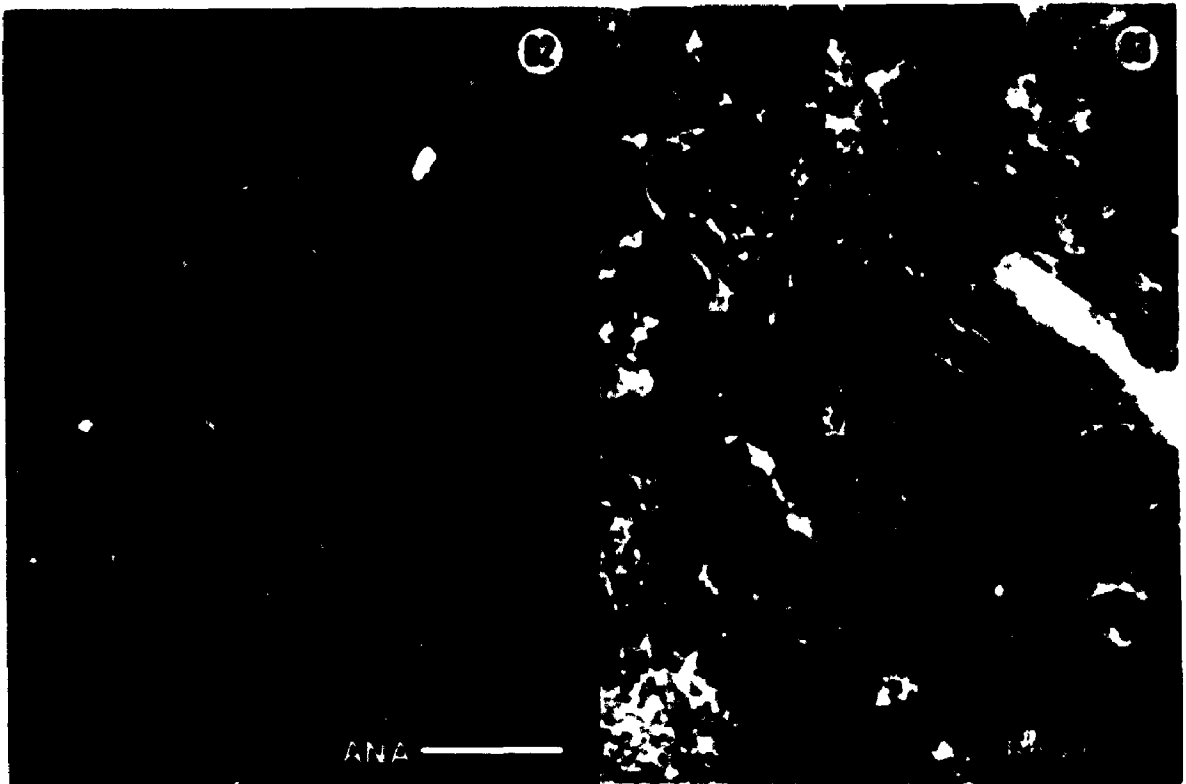
The presence of f-actin in the nuclear shell has been confirmed by heavy meromyosin labelling. The silk gland nuclear-associated fraction was incubated with heavy meromyosin prior to embedding. Layers which labelled with HMM (fig. 64) and contained nuclear pore-like gaps (figs. 65-67) are presumed to be sheets of the nuclear shell. Other nuclear components bound no HMM (fig. 65). The nuclear shell was often isolated from the rest of the matrix with much of the nuclear contents extracted. The nuclear and cytoplasmic faces were still recognizable because the shell usually collapsed



**Figs. 60 & 61. Silk gland nuclear branches label specifically for f-actin.** Fractured silk glands were probed with rhodaminyl-phalloin (fig. 60) and an antibody to the nuclear matrix antigen - peripherin (P1) (fig. 61) followed by FITC-conjugated anti-mouse IgG. Optical sections were taken by confocal microscopy (BioRad Lasersharp 500). Anti-peripherin labelling and phalloin labelling co-localized to the periphery of the nuclear branches. Scale bar = 25  $\mu$ m



**Figs. 62 & 63. A shell of f-actin surrounds the nuclear periphery.** Fractured silk glands were probed with anti-nuclear antibodies followed by an FITC-conjugated anti-human IgG with Evan's Blue (fig. 62) and rhodaminyl-phalloin (fig. 63). Optical sections taken with a confocal microscope (BioRad Lasersharp 500) suggest that a line of fluorescence around the periphery of the nuclear lobe corresponds to the nuclear shell (NSh). Fluorescence of comparable intensity is found along longitudinal fibres (arrowheads) inside the nucleus. This may correspond to intranuclear actin bundles or may be some other intranuclear elements (fig. 24) stained by the Evan's blue (see fig. 127). Scale bar = 25  $\mu\text{m}$



**Figs. 64 to 67. A lamina-like structure of the silk gland nuclear-associated fraction labels with heavy meromyosin. The silk gland nuclear-associated fraction was labelled with heavy meromyosin prior to embedding in araldite for TEM. A collapsed lamina-like structure (which correlates in shape to the nuclear shell) binds the HMM (fig. 64). HMM binding is restricted to the nuclear shell; the intranuclear matrix (INM) remains unlabelled (fig. 65). Periodically, the shell is perforated (figs. 66,67, arrows) in a manner which is similar to the perforation of the nuclear lamina by nuclear pores. Scale bars = 0.5  $\mu\text{m}$  (fig. 64); 0.1  $\mu\text{m}$  (figs. 65-67)**



NSH



on itself (fig. 64). Labelling was asymmetrical. Most of the HMM projected without a preferred orientation from the plane of the cytoplasmic side of the nuclear surface; the other face (which interacts with the nuclear envelope) was less ragged (figs. 64-67). These HMM labelled structures are presumed to be the nuclear shell because: 1) the HMM labelling of a perinuclear layer confirms the LM and EM localization by phalloin and antibodies to actin; 2) they lie apart from the intranuclear matrix; 3) they contain nuclear pore-like gaps; and 4) they have one smoother surface which could have been derived from or associated with the nuclear envelope.

These results gave no information about the shell's normal appearance or its location with respect to the nuclear envelope, although the nuclear pore-like openings in the shell suggested that it must be closely apposed to or part of the structure of the envelope.

#### 4.2.6 The location of the nuclear shell

TEM of unextracted silk glands showed similar features at the nucleocytoplasmic boundary in different regions of the gland during different stages of development (figs. 68-71). A region 25-150 nm wide outside the nuclear envelope was free of ribosomes and ER (fig. 68). It had a slightly fibrous texture (figs. 68-71) but no oriented arrays of microfilaments, even after tannic acid fixation that showed them in microvilli (fig. 86). Within the nuclear envelope the nuclear lamina was about 25 nm wide and stained more densely than the nearby nucleoplasm (figs. 70 & 71). The nuclear lamina had a slightly fibrous texture, like the region just outside the envelope. These layers on either side of the nuclear envelope probably correspond to the two layers seen in the nuclear fractions. The denser layer that bound antibodies to peripherin is the nuclear lamina and the less dense, more fibrous actin-binding nuclear shell is the layer outside the nuclear envelope (fig. 72). The low antigenic activity of nuclei fixed well enough to identify components has so far not allowed direct confirmation by the immunolabelling of sections of unextracted silk gland cells.

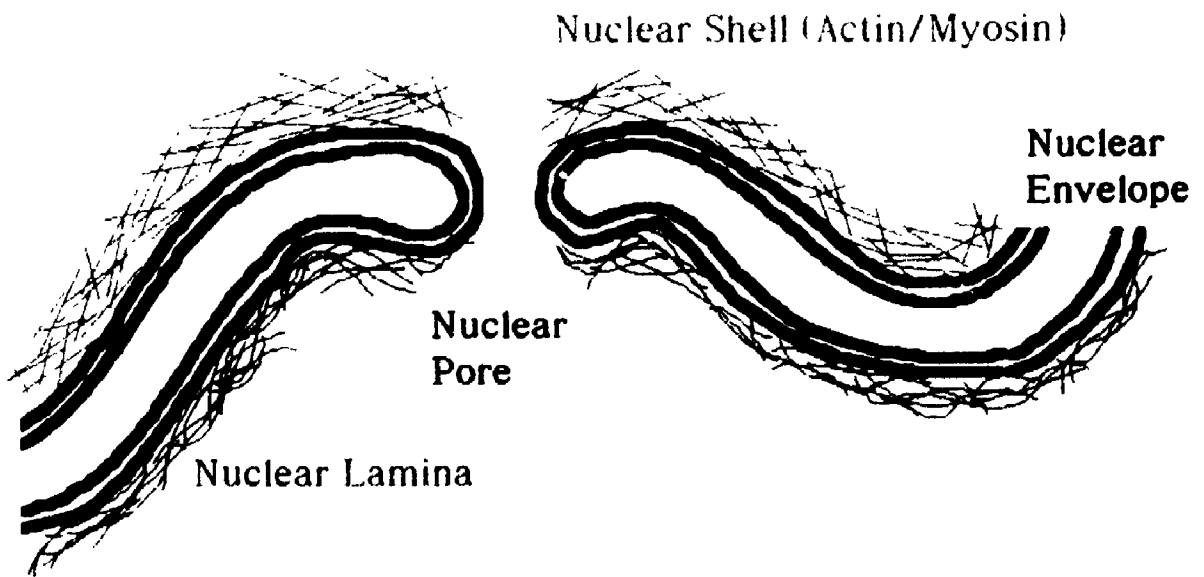
Although electron microscopy of conventionally fixed tissue is limited by uncertain preservation at the molecular level, the results suggest that the shell lies outside the nucleus, associated with the outer membrane of the nuclear envelope. Electron microscopy supports the idea that both

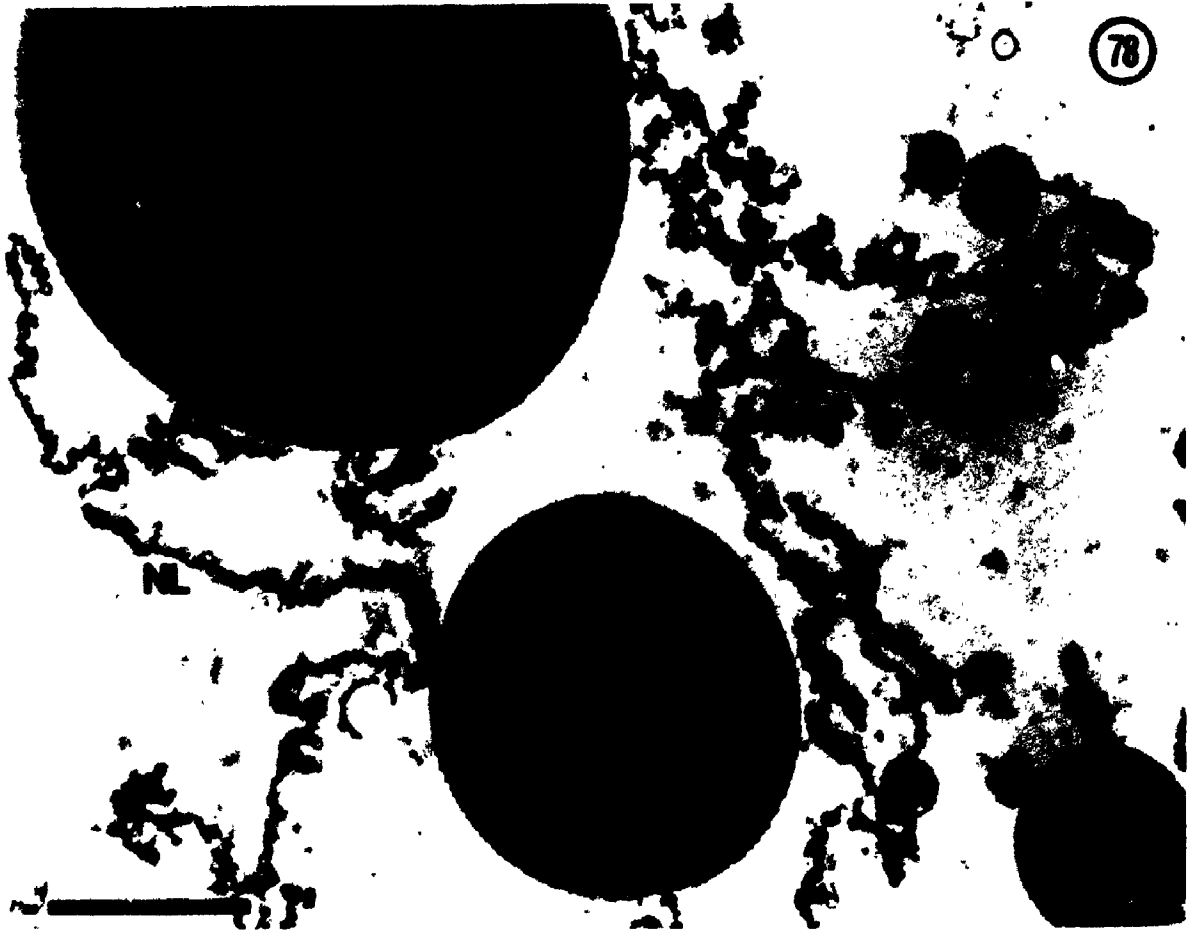
**Figs. 68 to 71. Silk gland nuclei are surrounded by a fibrous zone of exclusion.** A 25 to 150  $\mu\text{m}$  zone of exclusion (ZE) surrounds the branched nuclei in all regions of the gland (figs. 68 to 71). This zone, which is on the cytoplasmic side of the nuclear envelope, often contains randomly oriented microfilaments (MF) and occasionally microtubules (MT). The nuclear lamina (NL), which is located on the nuclear side of the envelope, is not as thick as the shell and is more electron dense. Fig. 68: Anterior region, mid 5<sup>th</sup> stadium (from a block prepared by M. Locke; photographed by S.C. Henderson). Fig. 69: Mid region, 4<sup>th</sup> moult. Fig. 70: Green region, late 5<sup>th</sup> stadium. Fig. 71: Mid region, late 5<sup>th</sup> stadium. Scale bars = 0.1  $\mu\text{m}$





**Fig. 72. The probable location of the nuclear shell.** The nuclear shell of f-actin most likely corresponds to the randomly oriented microfilaments in the zone of exclusion on the cytoplasmic side of the nuclear envelope. The nuclear lamina corresponds to the electron-dense region which is intimately associated with the inner layer of the nuclear envelope. (Drawing not to scale).





*et al.*, 1988; Ankenbauer *et al.*, 1989). Different actin binding proteins could bind to specific actin isoforms, polymerizing each into its own structural network.

Immunofluorescence microscopy localized actin to the periphery of the branched nuclei both early and late in development (*i.e.* when the nuclei are relatively unbranched and extensively branched). Labelling of silk gland cells with rhodaminy-phalloin, which binds preferentially to f-actin (Wieland & Govindan, 1974; Wieland *et al.*, 1983), indicated that some of the peripheral nuclear actin was filamentous. The weakness of the perinuclear labelling compared to that of the apical periluminal circumferential microfilament bundles (Chapter 6) may reflect different properties of the actin isoforms, since some types of f-actin bind phalloidin weakly or not at all (Hirono *et al.*, 1989).

The filamentous nature of the perinuclear actin was confirmed by labelling a lamina-like shell (which binds antibodies to actin) in the nuclear-associated fraction with heavy meromyosin. Silk gland nuclear-associated actin is in a filamentous form in spite of isolation in the presence of DNase 1, a treatment which sometimes (Hitchcock *et al.*, 1976), but not always (Clark & Merriam, 1977), causes the depolymerization of f-actin.

Myosin-like antigens were also localized to the silk gland nuclear periphery by immunofluorescence microscopy and to the nuclear shell of the nuclear-associated fraction by immunogold labelling. Several studies have localized actin and myosin-like proteins to the nuclear surface (Berrios & Fisher, 1986; Butt & Heath, 1988; Heslop-Harrison & Heslop-Harrison, 1989a; Heslop-Harrison & Heslop-Harrison, 1989b; Schindler & Jiang, 1986). Many activities may be attributed to nuclear surface-associated actin and myosin. Actin and myosin may play a role in nuclear movement such as nuclear migration (Heslop-Harrison & Heslop-Harrison, 1989a; Heslop-Harrison & Heslop-Harrison, 1989b; Kaminskyj *et al.*, 1989) or nuclear rotation (Paddock & Albrecht-Buehler, 1986). ATPases have been localized to the nuclear lamina or nuclear pore complexes (Berrios *et al.*, 1983; Berrios & Fisher, 1986; Kalinich & Douglas, 1989) suggesting that nuclear actin and myosin may be involved in nucleocytoplasmic transport, an ATP-dependent process. Since messages for silk proteins are produced and exported in large quantities during larval life, the nuclear shell might be a structural adaptation to enhance nucleocytoplasmic transport by increasing

the surface to volume ratio and/or actively participating in the translocation of packaged messages across the pores.

A molecular force-generating element is needed to form nuclei into the regionally specific shapes occurring within the gland. Actin and myosin are known to generate force in the cytoplasmic lamellipodia of migrating cultured cells (Conrad *et al.*, 1989; DeBiasio *et al.*, 1988). Silk gland nuclear branching may be similar to the nuclear lobe elongation involving actin and myosin in the vegetative nuclei of pollen tubes. The vegetative nuclei are surrounded by cytoskeletal f-actin. The extended nuclear shapes which form during migration contract after treatment with cytochalasin D (Heslop-Harrison & Heslop-Harrison, 1989a). The lack of nuclear shape change in silk glands treated with cytochalasin D (data not shown) was likely due to the presence of the nuclear skeleton which maintains the shape.

Myosin, which has been shown to bind to membrane lipids (Adams & Pollard, 1989), may serve as the actin-binding protein to connect actin in the nuclear shell to the nuclear envelope. The insertion of cytoskeletal elements onto one side of the nuclear envelope through the shell, and the insertion of the nuclear skeleton through the nuclear lamina onto the other side (connected by elements which span the nuclear envelope) gives nuclei the structure needed for generating and transmitting forces for controlling nuclear shape.

## CHAPTER 5

### Cytoplasmic Actin Storage Bodies in Silk Gland Cells

#### 5.1 Introduction

In the previous chapter, it was shown that the arborescent nuclei are surrounded by a shell of actin. This nuclear actin shell may be, in part, responsible for maintenance and/or generation of nuclear shape changes. The nuclear-associated actin is expressed as a different isoform which presumably plays some role in the function of the nuclear shell and/or separation of the shell from the cytoplasmic actin networks. Unlike the cytoplasmic actin bundles (Chapter 6), the nuclear actin shell persists during the larval moults. This suggests that the two actin networks are regulated in different ways.

Coinciding with the dissociation of the periluminal f-actin bundles and its redistribution around vacuoles (Chapter 6) is the appearance of large spherical protein bodies in the cytoplasm near the nucleus. Similar bodies occasionally appear in the nuclear matrix fraction prepared from silk glands of moulting larvae. In both occurrences, the bodies label with antibodies to actin. These bodies may be stores of actin to be incorporated into the shell of the growing nucleus.

#### 5.2 Results

##### 5.2.1 Actin storage bodies appear in the silk gland cytoplasm during the larval moults

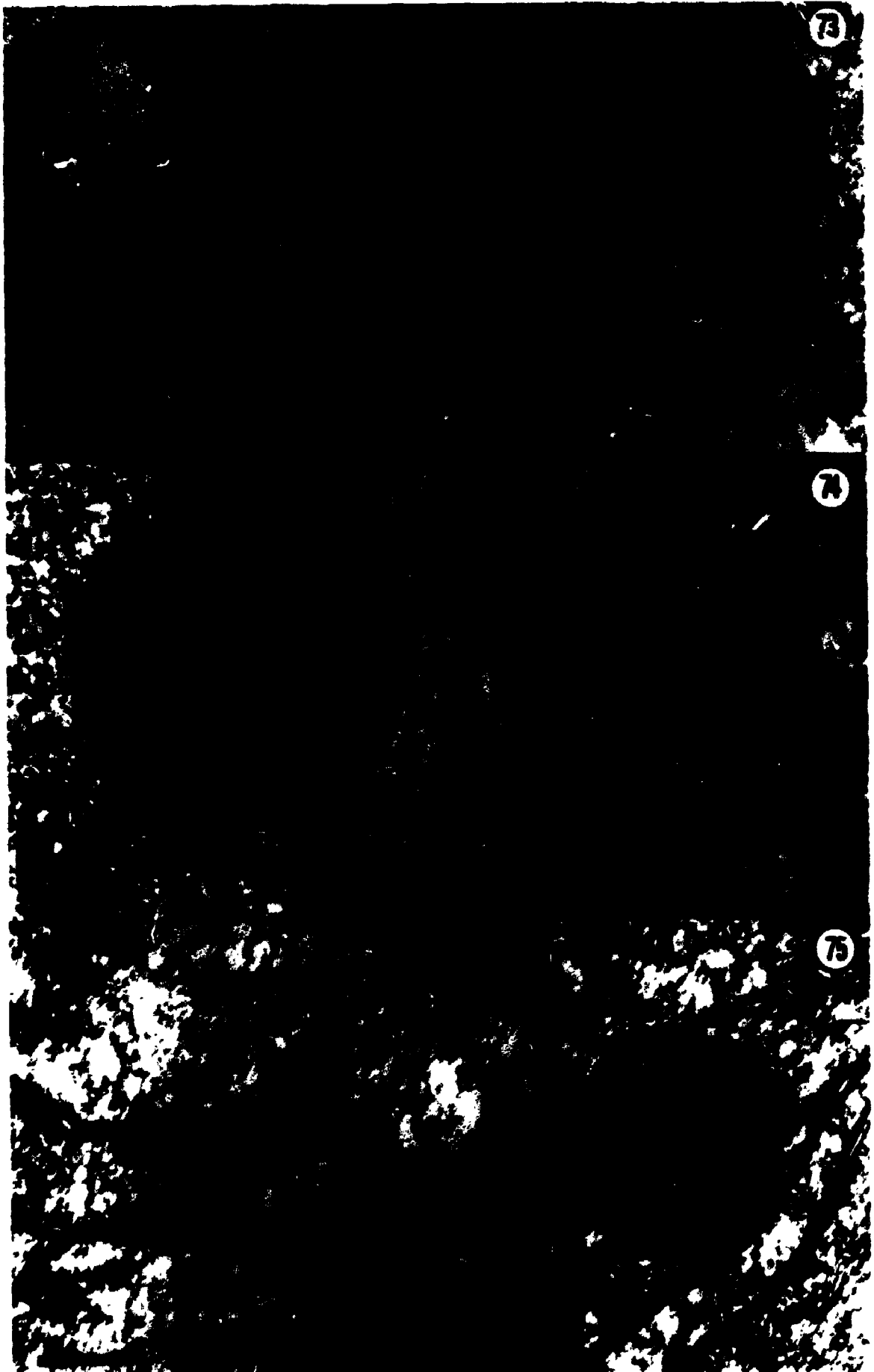
Dense spherical globules, 0.5 to 5  $\mu\text{m}$  in diameter, appeared in the cytoplasm of all regions during each larval moult (figs. 73-75). They were often found in close proximity to the nucleus. These globules disappeared following ecdysis. Antibodies to actin bound to these spheres (figs. 76 & 77) but not to luminal silk (fig. 87) or silk in vacuoles and vesicles that are found in the cytoplasm (fig. 96).

It can be concluded that the cytoplasmic bodies are large actin-containing concretions which accumulate during the moult.

**Figs. 73 to 75. Electron-dense spherical bodies appear in the cytoplasm during the larval moults. During the larval moults, granular electron dense spheres appear in the cytoplasm. These spheres occur in each of the gland regions (figs. 73,74: mid; fig. 75: duct) and during each of the larval moults (figs. 73,75: fourth moult; fig. 74: third moult).**

**(N = nucleus). Scale bars = 0.5  $\mu\text{m}$  (fig. 73); 0.25  $\mu\text{m}$  (figs. 74,75)**





**Figs. 76 & 77. Moulting-associated cytoplasmic bodies label with antibodies to actin.** Crushed/fractured silk glands were incubated with antibodies to actin followed by FITC-conjugated anti-rabbit IgG (fig. 76). Both the nucleus (N) and cytoplasmic bodies (arrows) in the same focal plane near the nucleus label with antibodies to actin. Sections of LR White-embedded silk glands dissected from fourth moulting larvae were probed with antibodies to actin followed by 5 nm gold-conjugated anti-rabbit IgG (fig. 77). The electron-dense spherical bodies bound antibodies to actin.  
Scale bars = 25  $\mu\text{m}$  (fig. 76); 0.25  $\mu\text{m}$  (fig. 77)



### **5.2.2 Spheres resembling the cytoplasmic actin storage bodies co-isolate with the nuclear matrix**

When nuclear matrices were prepared from fourth moult silk glands, electron-dense protein spheres occasionally co-isolated with the nuclear matrix fraction (fig. 78). These spheres were absent from silk gland nuclear matrix fractions isolated from feeding fourth stage larvae. Other components present in the fraction included fragments of nuclear laminae.

The similarity in size, appearance and time of occurrence, between the spheres in the nuclear matrix fraction and the cytoplasmic actin bodies suggested that they might be the same structure.

### **5.2.3 Nuclear matrix-associated bodies label for actin**

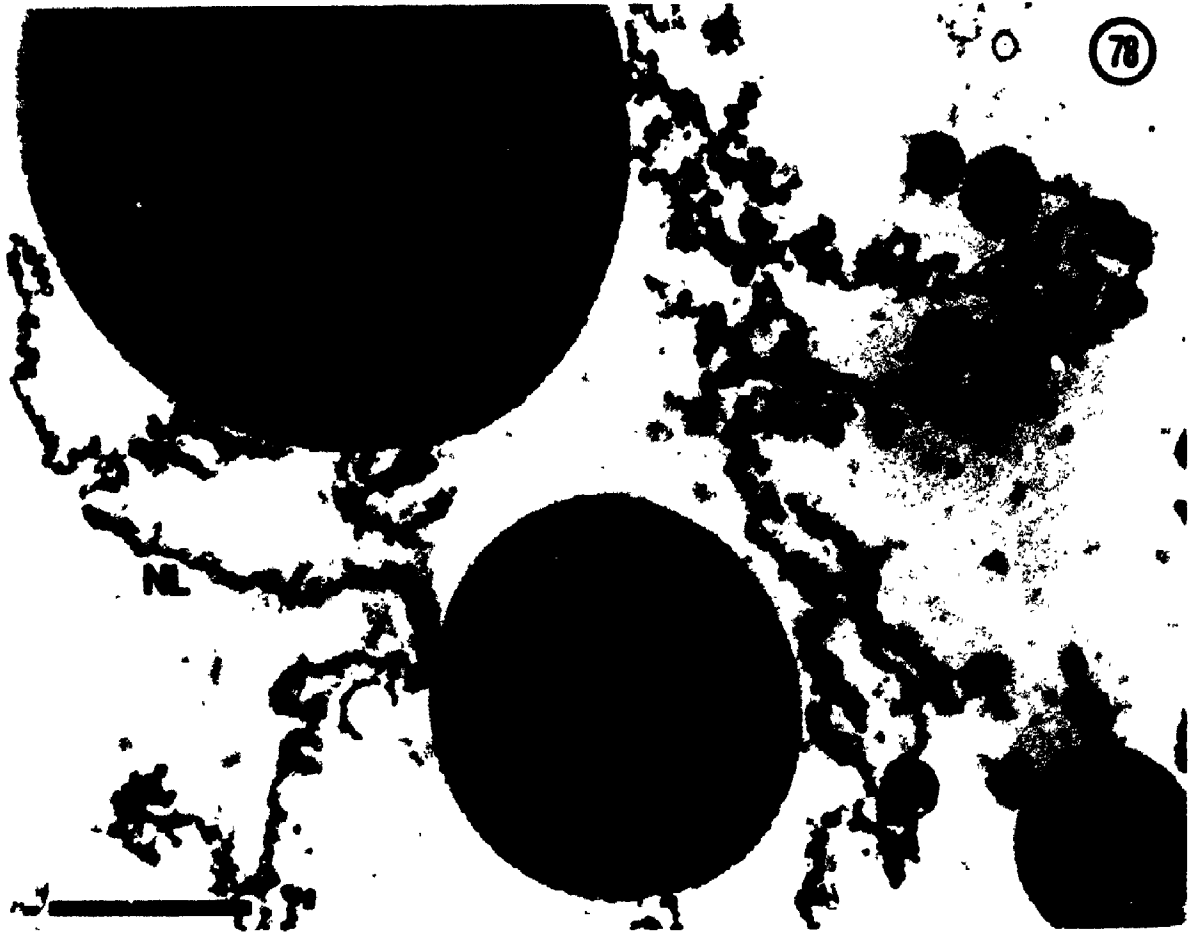
Sections of the nuclear matrix fraction were double labelled with a polyclonal antibody to actin and with a monoclonal antibody to a nuclear matrix antigen-peripherin (P1). The protein bodies which co-isolated with the nuclear matrix labelled uniformly with antibodies to actin, whereas the surrounding short fragments of nuclear laminae labelled only with P1 (fig. 79). Sections of the same material probed with antibodies to myosin (which bound intensely to the perinuclear shell that is also found in this fraction; fig. 59), showed little binding of anti-myosin to the protein bodies (fig. 80).

Thus, the protein bodies in the nuclear matrix fraction are probably the cytoplasmic actin storage globules seen in sections of intact cells.

## **5.3 Discussion**

Actin-containing bodies form in the cytoplasm of silk gland cells during larval moults. They are probably storage bodies of actin for use by the cell during growth in the next feeding stage. In this respect, they are similar to the actin storage bundles in *Calpodes* dermal glands (Delhanty & Locke, 1990), mammalian lens epithelia (Liou & Rafferty, 1988; Rafferty & Scholz, 1985), and pollen grains (Heslop-Harrison *et al.*, 1986). Silk glands differ in that the actin storage bodies are uniformly spherical rather than rod shaped, presumably reflecting the hydrophobicity of component proteins other than actin. The globular form of the bodies may also reflect the storage of non-filamentous actin rather than the f-actin in the fibrous, rod

**Fig. 78. Spherical protein bodies co-isolate with the nuclear matrix prepared from silk glands of moulting larvae. Nuclear matrices prepared from the silk glands dissected from moulting larvae contain large spherical bodies. These bodies are presumably protein in composition since they survive extraction with Triton X-100, DNase I, RNase A, and 1 normal NaCl. Other components of the silk gland nuclear matrix fraction include sheets of nuclear lamina (NL). Scale bar = 1  $\mu$ m**



**Figs. 79 & 80. Moulting-associated protein bodies which co-isolate with the nuclear matrix fraction label with antibodies to actin.** Nuclear matrices prepared from silk glands dissected from moulting larvae were embedded in LR White and probed with gold tagged antibodies. Thin sections were double labelled with a polyclonal antibody to actin (followed by 5 nm gold-conjugated anti-rabbit IgG) (small arrows) and a monoclonal antibody (P1) to a nuclear matrix antigen (followed by 10 nm gold-conjugated anti-mouse IgG) (large arrows). The protein spheres label for actin whereas the nuclear lamina labels with P1 (fig. 79). Similar sections show little binding with antibodies to myosin (fig. 80). Scale bars = 0.25  $\mu\text{m}$  (fig. 79); 0.5  $\mu\text{m}$  (fig. 80)





shaped storage bundles. Spherical rather than rod shaped stores of actin may also be the result of different types of actin binding proteins (Nishida *et al.*, 1987; Weeds, 1982; Weihing, 1985).

Evidence for the function of these actin storage bodies is circumstantial. They form during the moults, when other cytoplasmic structures regress. The loss of periluminal actin also coincides with the formation of f-actin coated vacuoles (Chapter 6). It is therefore not clear why the cell might require another temporary storage location for its actin. A possible answer comes from the finding that the nuclear-associated fraction at moulting does not contain detectable amounts of the two isoforms present in the cytoplasmic fraction during the intermoult. This indicates that actin in the globules which co-isolate with the nuclear matrix must be the nuclear-associated isoform.

Storage bodies (cytoplasmic globules) which act as reservoirs of actin for the nuclear shell may therefore be different from those structures which recycle cytoplasmic periluminal actin (*i.e.* coats on the vacuoles). Separate stores of isoforms for structures having different purposes may also be required because of the different timing of their assembly. Periluminal bundles reform after ecdysis whereas nuclear growth continues throughout the stadium.

## CHAPTER 6

### The Redeployment of F-actin in Silk Gland Cells During Moulting

#### 6.1 Introduction

A general problem in cell biology concerns the mechanism by which similar cytoskeletal elements may simultaneously form separate networks within the same cell. As an example of this phenomenon, different f-actin networks exist concurrently in embryos of *Drosophila melanogaster* (Miller *et al.*, 1985). One network is associated with the plasma membrane while the other surrounds the nucleus. The separate development of actin networks is presumed to be a consequence of different actin binding proteins (Ankenbauer *et al.*, 1988; Ankenbauer *et al.*, 1989; Weeds, 1982) and/or different actin isoforms (Bremer *et al.*, 1981; Kumar *et al.*, 1984; Nakayasu & Ueda, 1986).

Most of the microfilaments in silk glands occur in a network around the lumen at the apical cell surface (Couble *et al.*, 1984; Sasaki *et al.*, 1981; Tashiro *et al.*, 1982). It has been hypothesized that they may play a role in the exocytosis of silk-containing secretory vesicles (Couble *et al.*, 1984; Sasaki *et al.*, 1981; Tashiro *et al.*, 1982) or in the propagation of peristaltic contractions for the movement of silk down the lumen (Sasaki, 1977; Sasaki & Tashiro, 1976).

One of the difficulties in studying nuclear-associated actin in silk gland cells is that the cytoplasmic actin (*i.e.* luminal actin) undergoes its own set of changes during the moult (*i.e.* at the same time that actin storage bodies form). This chapter describes the developmental changes of the cytoskeletal f-actin. The apical actin cytoskeleton consists of parallel bundles which surround the lumen of the gland. The bundles dissociate during the moults and the f-actin redistributes through the cytoplasm as coats to vacuoles and occasionally in variably oriented strands. After moulting there is a return to the distribution of f-actin in the apical periluminal bundles. Thus, the regulation of cytoplasmic actin assembly differs from that of the nuclear-associated actin during development.

## 6.2 Results

### 6.2.1 Periluminal circumferential f-actin bundles

Whole silk glands labelled with rhodaminyl-phalloin showed most f-actin was arranged in parallel bundles around the lumen, perpendicular to the long axis of the gland. Often, there was an impression of continuity in some of the bundles between opposing cells (figs. 81-83, 100 & 101). Stereo imaging of "stacked" optical sections generated by confocal microscopy showed that the apparent continuity in bundles between cells is, in fact, an overlap of bundles projecting from the two opposing cells (fig. 85). The arrangement of f-actin bundles was similar during each larval feeding stage (figs. 81-84).

The bundles lay immediately beneath the plasma membrane (fig. 86). Identification of the microfilament bundles as clusters of actin filaments was confirmed by immunogold labelling with antibodies to actin (fig. 87). Microfilaments in microvilli were oriented perpendicular to the bundles (fig. 86). Secretory vesicles containing silk occurred in these regions during the feeding stages.

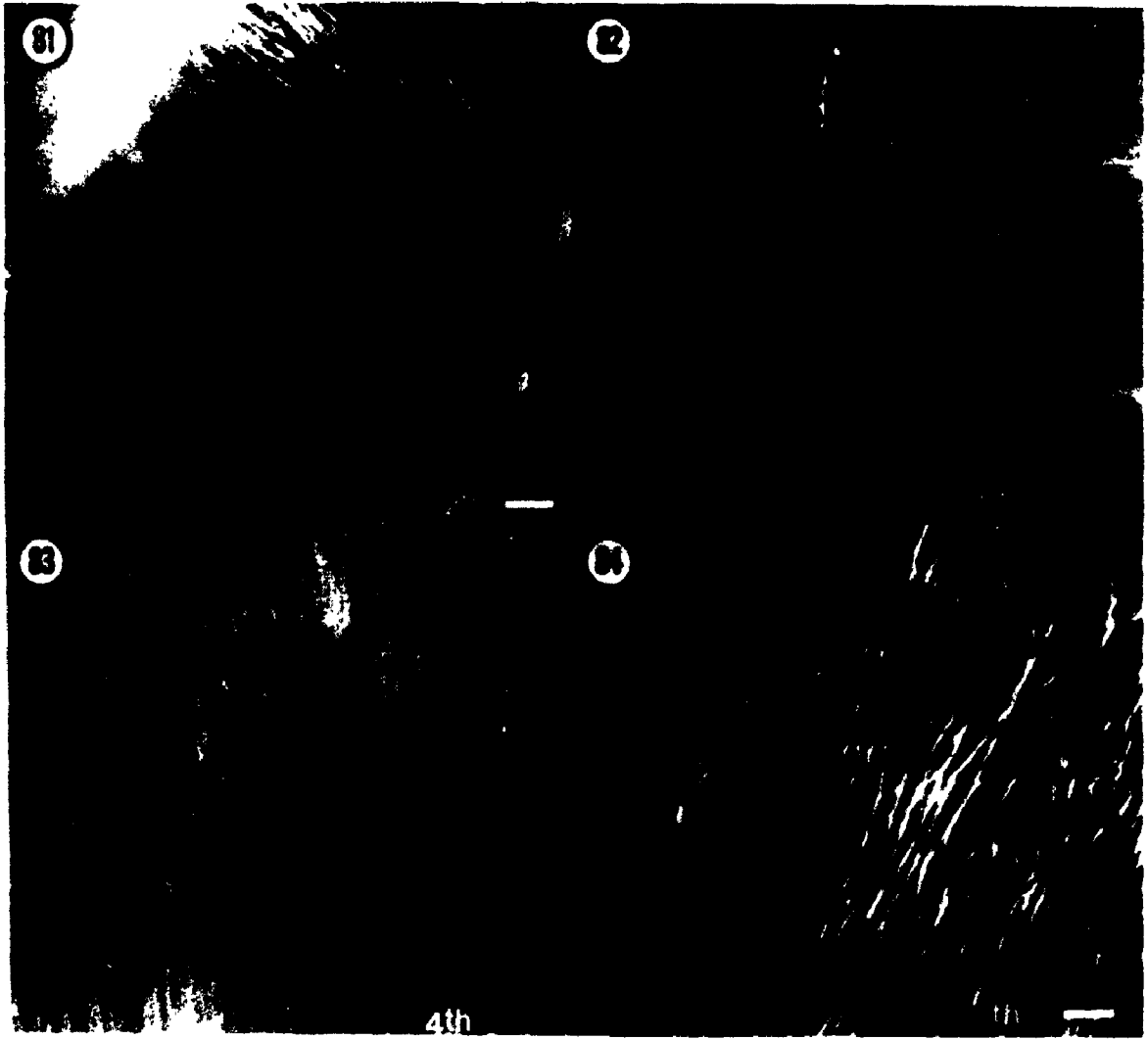
Thus, through the intermoult period of silk spinning, the apical cytoskeletal structure allowed for both secretion into the lumen and the subsequent containment or constriction of the newly secreted silk.

### 6.2.2 F-actin-coated vacuoles form during the larval moults

During each larval moult, when silk secretion stopped, the circumferential actin bundles dissociated and were replaced by f-actin-coated vacuoles which were sometimes as large as 20  $\mu\text{m}$  in diameter (figs. 88-90). Transition stages showed the dissolution of actin bundles and the concurrent formation of the actin-coated vacuoles (fig. 91). The state of the actin filaments could change abruptly from one cell to the next. Sometimes cells with apical bundles and cells with actin-coated vacuoles were side by side. In addition to the f-actin coating vacuoles, f-actin occasionally appeared as strands throughout the cytoplasm where previously, during the intermoult, it had been absent (fig. 92).

The vacuoles arise from the lumen or from vesicles about to discharge into the lumen. Optical sectioning by confocal microscopy of

**Figs. 81 to 84. F-actin bundles surround the lumen of the silk gland during each larval intermoult stage. Silk glands from mid-instar larvae were labelled with rhodaminyl-phalloin. Most of the f-actin is located in parallel bundles around the gland lumen perpendicular to the long axis of the gland. The bundles occur during each larval feeding stage when silk is secreted. Representative examples are shown for f-actin labelling in the mid region of the silk glands from second (fig. 81), third (fig. 82), fourth (fig. 83), and fifth (fig. 84) stage larvae. Scale bar = 10  $\mu$ m**

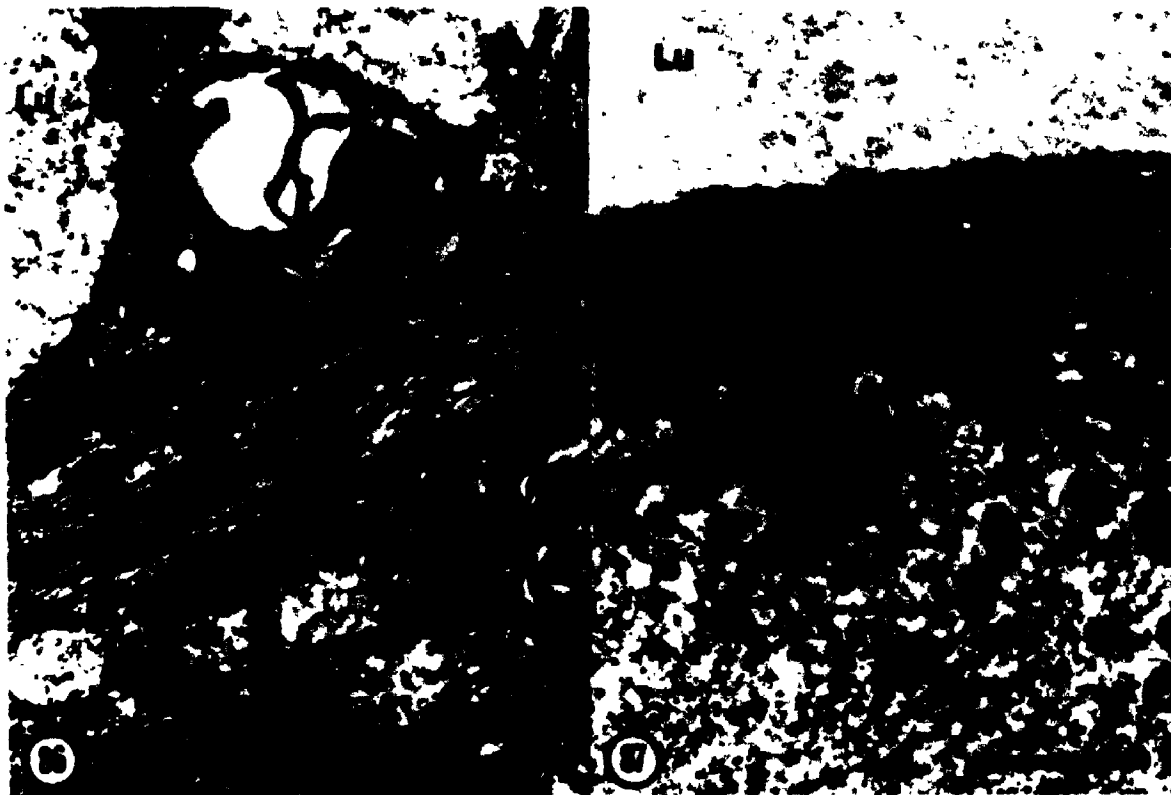


**Fig. 85. F-actin bundles overlap between opposing cells.** Stereo pairs of extended focus reconstructions generated from optical sections (taken by Leitz CSLM) of rhodaminy-phalloin labelled silk glands show that the apparent continuity in f-actin bundles between opposing cells (see figs. 81-83, 100-102) is created by the overlap of bundles which extend in interdigitating processes from the opposing cells. Scale bar = 10  $\mu\text{m}$



**Figs. 86 & 87. Bundles of microfilaments found in the apical cytoplasm of silk gland cells label with antibodies to actin. Thick bundles of microfilaments (MB) are found immediately beneath the plasma membrane in the apical cytoplasm of silk gland cells (fig. 86). The bundles are oriented parallel to the apical surface of the cells and perpendicular to the microfilaments found within the microvilli (mv). Secretory vesicles (sv) are often found near the bundles of microfilaments and microtubules (MT). The microfilaments in the apical region of the cell immunogold label with antibodies to actin (arrows) (fig. 87). No labelling was found in the gland lumen (Lu). Scale bars = 0.5  $\mu$ m**





**Figs. 88 to 90. F-actin-coated vacuoles form during each of the larval moults. During the larval moults, the periluminal circumferential actin bundles (figs. 81 to 84) dissociate and are replaced by large f-actin-coated vacuoles and small rhodaminyI-phalloin labelling spots (arrows). Fig. 88: 2<sup>nd</sup> moult - mid region. Fig. 89: 3<sup>rd</sup> moult - anterior region. Fig. 90: 4<sup>th</sup> moult - posterior region. Photographed using a Zeiss Photomicroscope II. Scale bar = 10  $\mu$ m**



**Fig. 91.** F-actin-coated vacuoles (large arrows) form as the periluminal circumferential actin bundles (small arrows) dissociate. Scale bar = 100  $\mu\text{m}$

**Fig. 92.** The f-actin bundles occasionally redistribute throughout the cytoplasm. (Lu = lumen) Scale bar = 100  $\mu\text{m}$

**Fig. 93.** Optical sectioning by confocal microscopy (Leitz CSLM) reveals that the f-actin is at the periphery of the moult-associated vacuoles.  
Scale bar = 25  $\mu\text{m}$

**Fig. 94.** F-actin-coated vacuoles in the silk glands of *Pieris rapae* appear to bud from the apical surface as oblong pockets. (Lu = lumen)  
Scale bar = 10  $\mu\text{m}$



*Calpodex* silk glands confirmed that the f-actin was in a thin coat around the vacuoles which were usually detached from the surface (fig. 93). In another Lepidopteran, *Pieris rapae*, the f-actin-coated vacuoles were elongated and kept their connections with the luminal surface of the cell (fig. 94). Electron microscopy showed that the vacuoles are larger than secretory vesicles and have contents similar to the gland lumen (fig. 95). The actin coating of these vacuoles was confirmed by immunogold labelling with antibodies to actin (fig. 96).

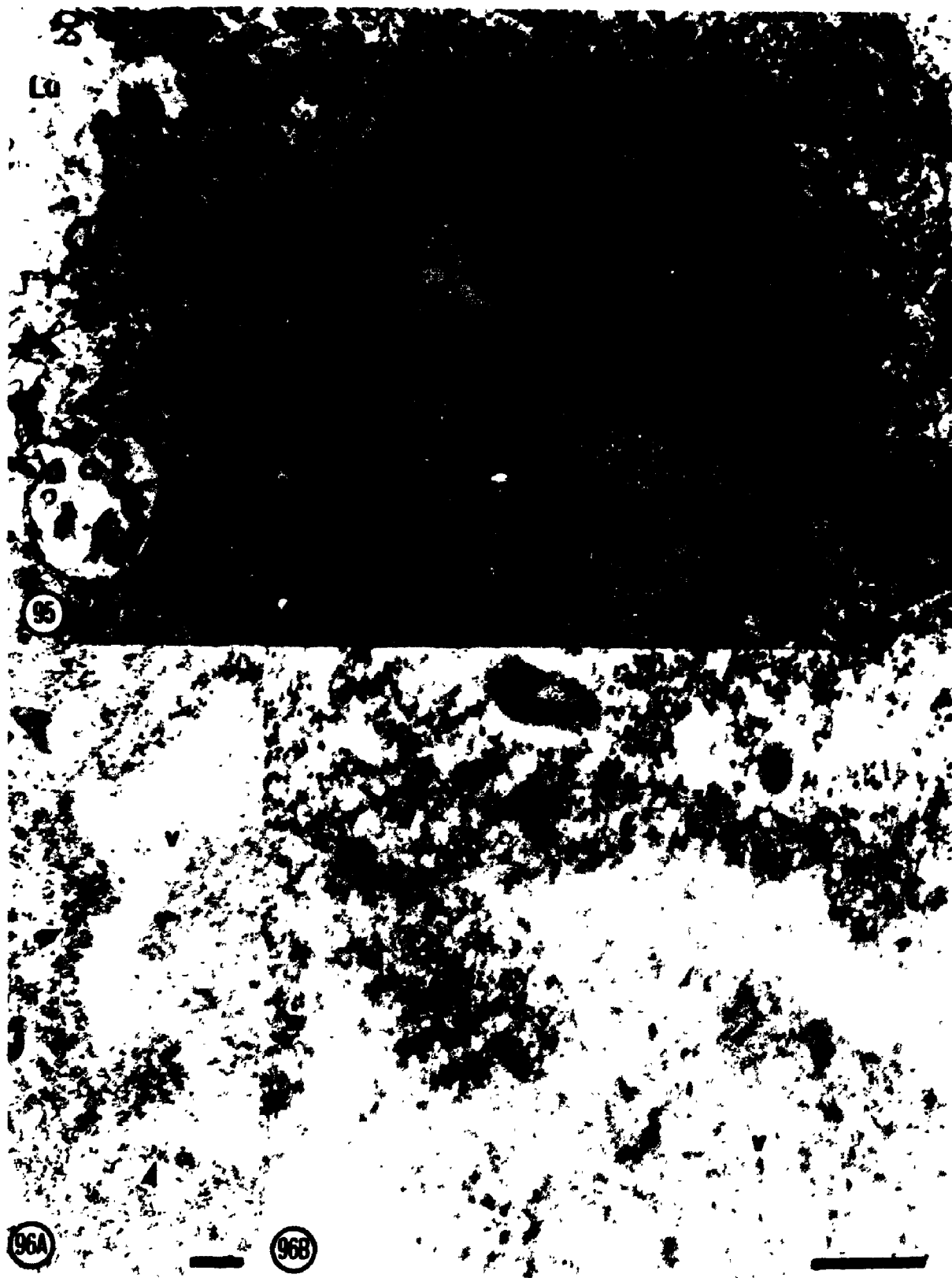
### 6.3 Discussion

A cytoskeleton of actin arranged in parallel bundles surrounds the lumen of the silk glands of *Calpodex*. This apical location is similar to the microfilament network in *Bombyx mori* (Couple *et al.*, 1984; Tashiro *et al.*, 1982). All of the f-actin is aligned perpendicular to the gland lumen; there are no longitudinal actin bundles. The apparent continuity of some bundles between cells is caused by the overlap of bundles in extensions from opposing cells. These lateral projections which are formed from the actin bundles are similar to the feet which occur at the basal end of epidermal cells (Delhanty & Locke, 1989; Locke, 1985).

It has been suggested that the apical microfilament network may play a role in the secretion of silk proteins (Couple *et al.*, 1984; Sasaki, 1977; Sasaki *et al.*, 1981; Sasaki & Tashiro, 1976). Cytochalasin treatment of silk glands gave contradictory results. In one study, cytochalasin treatment inhibited the release of silk proteins into the lumen of the gland (Couple *et al.*, 1984) whereas in another investigation, cytochalasin treatment enhanced the release of silk proteins into the gland lumen (Sasaki *et al.*, 1981).

Actin has been implicated in secretion in a variety of cell types including the dermal glands of *Calpodex* (Delhanty & Locke, 1990), mammalian salivary gland (Segawa & Yamashina, 1989) and pancreatic acinar cells (Bendayan, 1985). A number of models have been developed for the role of f-actin in the secretory process. In one model, f-actin coats the secretory vesicles (via interactions with actin binding proteins in or attached to the vesicle membrane) and facilitates the transport of the secretory vesicle to the apical surface of the cell (Bendayan, 1985; Fowler & Pollard, 1982). By this model, cytochalasin treatment should inhibit secretory vesicle release.

**Figs. 95 & 96. Large silk-containing spheres in the apical cytoplasm of silk gland cells from moulting larvae immunogold label at their periphery with antibodies to actin. Fig. 95: Mid region of silk gland from 4<sup>th</sup> moult was embedded in araldite. Large vacuoles (v) form in the apical cytoplasm of silk gland cells during the moult and have contents that are similar in appearance to the contents of the lumen (Lu). Fig. 96: Anterior region of silk gland from 4<sup>th</sup> moult was embedded in LR White. Sections were incubated with anti-actin followed by 5 nm gold-conjugated anti-rabbit IgG. The vacuoles (v) which appear in the apical cytoplasm of the cells during the moult are surrounded by a slightly denser cortex (large arrow) which immunogold labels with antibodies to actin (small arrows). Scale bars = 0.5  $\mu\text{m}$  (fig. 95); 0.25  $\mu\text{m}$  (figs. 96 a & b)**





Another model suggests that f-actin forms a barrier at the apical end of the cell (Aunis & Bader, 1988; Burgoyne & Cheek, 1987; Lelkes *et al.*, 1986). The microfilament barrier prevents the release of secretory vesicles until the f-actin is disrupted by an influx of calcium which affects the actin-binding proteins. By this model, cytochalasin enhances the release of secretory vesicles (Aunis & Bader, 1988; Lelkes *et al.*, 1986; Sontag *et al.*, 1988). A third model proposes that f-actin initially forms a barrier and then, upon vesicle contact with the apical membrane, forms a shell around the secretory vesicle and facilitates exocytosis of the vesicle (Segawa & Yamashina, 1989).

Two of the above models require the dissolution of the microfilament barrier for secretion and two of the models involve the formation of actin-coated secretory vesicles. In silk glands however, the microfilament bundles are intact during secretory phases and thus do not act as a barrier. Secretory vesicles in silk gland cells are approximately 0.5  $\mu\text{m}$  in diameter (fig. 86) and can easily pass between the periluminal actin bundles (which are separated by a 0.5 to 1.0  $\mu\text{m}$  gap). Furthermore, f-actin coated vacuoles form not at times of secretion, but at times when silk secretion has stopped during the larval moults. Another possible function for the apical f-actin cytoskeleton is suggested by the arrangement of bundles of actin as hoops perpendicular to the long axis of the gland. The apical cytoskeleton is ideally designed to resist or contain luminal hydrostatic pressure. In a cylinder under uniform internal hydrostatic pressure, the hoop stress is twice the axial stress (Locke, 1958; Timoshenko, 1936). That is, the stress to the walls of the lumen is twice that along the length of the lumen. Increasing the reinforcement with circumferential rings counteracts this tendency. Further reinforcement is gained by the interdigitation of some of the bundles between opposing cells which form the lumen.

The function of the f-actin-coated vacuoles which form during the larval moults is unknown. These vacuoles, which are larger than the secretory vesicles, contain material similar in appearance to the contents of the gland lumen. Vacuoles have been observed in the silk glands of *Bombyx mori* during the moults (Akai, 1965; Matsuura & Tashiro, 1976; Morimoto *et al.*, 1968). It has been suggested that the moult-related vacuoles may be formed by the endocytosis of unspun luminal silk (Akai, 1965; Akai, 1971), possibly as a means of providing nutrients for the cells at a time when the larva is not feeding (Morimoto *et al.*, 1968). In this respect, the vacuoles

may be similar to the vacuoles which form when larvae are experimentally starved and do not spin silk (Blaes *et al.*, 1980).



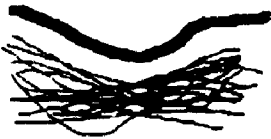
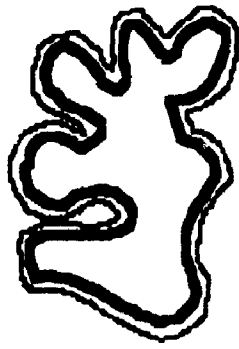

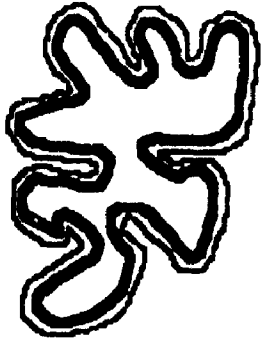
Thus, instead of participating in exocytosis, f-actin in silk glands may be required for the formation of endocytic vacuoles of luminal silk during the larval moults. The pocket-like f-actin-coated depressions observed in the silk glands of *Pieris* show how these vacuoles may be formed.

Another possible function for the f-actin-coated vacuoles is a means by which the apical f-actin can be recycled. Although the hoop reinforcements remain the same through larval life, there is a continuous increase in diameter of the gland lumen. During the intermoult, the actin bundles likely accommodate to the increase in lumen diameter by the incorporation of g-actin into the filaments much in the same way stress fibres increase in length in cultured cells. However, during the larval moults, when there is no need for hydrostatic resistance, the length of the actin bundles may be increased by the dissociation of the filaments and their subsequent reformation in longer bundles. Thus, actin is withdrawn from the old, smaller rings, and is temporarily stored in the body of the cell in the form of coated vacuoles prior to relocation at the new enlarged apical surface.

The cyclical restructuring of the cytoplasmic actin bundles is coincident with the moult/intermoult cycle of larval development. Yet, f-actin in the nuclear shell does not follow this cycle of dissolution and rearrangement. Recycling and re-erection of the apical ring cytoskeleton coincides with the continuous presence of f-actin during growth of the nuclear shell (fig. 97). Thus, the two actin skeletal systems within the cell appear to be independently controlled.

**Fig. 97. Nuclear shell and periluminal actin display different behaviours with respect to the moult/intermoult cycle.** During the larval feeding stages (intermoult), the f-actin is found in the periluminal bundles and in a thin shell around the nuclear periphery. During the larval moults, the periluminal actin dissociates and is recycled in the form of coats around large cytoplasmic vacuoles whereas the nuclear shell actin maintains its structure around the nuclear periphery. At the same time, large spherical concretions of actin, which are thought to be stores for the nuclear shell, form near the nucleus. By the time of the next intermoult stage, the periluminal bundles have reformed as the actin-coated vacuoles have disappeared and the actin storage bodies have disappeared.

(Drawing not to scale).

	Intermoult	Moult	Intermoult
Periluminal Actin			
Nuclear Shell Actin			

## CHAPTER 7

### Regional Differences in the Apical F-actin Cytoskeleton of Silk Gland Cells

#### 7.1 Introduction

In the previous chapters it has been demonstrated that silk gland cells contain two actin networks. These actin networks are separated both by space (*i.e.* around the nucleus and around the lumen) and behaviour (*i.e.* different rearrangements during the moults) (fig. 97). Presumably, the independence of these networks is achieved by the expression of different actin isoforms and/or different actin binding proteins (Pollard & Cooper, 1986; Stossel, 1984; Stossel *et al.*, 1985; Weeds, 1982).

Not only are there differences in actin skeletons within the cell, but also between cells in different regions along the length of the gland. Like the changes in nuclear morphology along the length of the gland (Chapter 3; figs. 14-18), there are regional differences in the apical actin cytoskeleton.

This chapter describes the regional differences in the density of the periluminal bundles of filamentous actin. This regional definition in f-actin density and redeployment presumably reflects a functional or physiological difference within the gland.

#### 7.2 Results

##### 7.2.1 Regional differences in the density of the actin bundles along the length of the gland

By the fifth stadium, the silk glands of *Calpodes* have 5 structurally different segments: the duct, green, anterior, mid, and posterior regions (Wiley & Lai-Fook, 1974) (fig. 4). Rhodaminyl-phalloin staining of whole glands showed that each region had its own pattern and density of actin bundles. Few actin filaments encircled the gland lumen in the duct region; most of the f-actin was distributed throughout the cytoplasm and in a thick shell around the nucleus (fig. 98). There was then an abrupt increase in bundle density around the lumen with the beginning of the green region. The green region contained the greatest density of bundles (fig. 99). The f-actin bundle density declined with the beginning of the anterior

**Figs. 98 to 102. Regional differences exist in the density of periluminal circumferential actin bundles in the silk gland. Rhodaminyl-phalloin labelled silk glands from fifth stage larvae display differences along the length of the gland in the density of the f-actin bundles. In the duct (fig. 98) the f-actin occurs throughout the cytoplasm and forms a shell around the nucleus. The region posterior to the duct (Du), the green region (Gr), is marked by a sudden change in the distribution of f-actin within the cells (fig. 99). The periluminal circumferential actin bundle density is greatest in the green region (fig. 99) and becomes less dense towards the posterior end of the gland. Occasionally, there appears to be a continuity of actin bundles between opposing cells (arrows).**

**Fig. 100: anterior region. Fig. 101: mid region. Fig. 102: posterior region. Photographed using a Zeiss Photomicroscope II. Scale bars = 100  $\mu$ m**



region. The density of bundles then declined gradually through the anterior (fig. 100), mid (fig. 101) and posterior regions (fig. 102).

These differences in density of f-actin bundles were not as conspicuous during earlier larval intermoult stages (figs. 108-111) when the cells are much smaller. In silk glands from the third stadium, the difference in bundle density between the green region and the regions on either side of it was prominent (figs. 108 & 109), but no apparent difference existed in bundle density between the anterior, mid and posterior regions (figs. 109-111).

### **7.2.2 Regional differences in f-actin-coated vacuole formation during moulting**

During each larval moult, the f-actin bundles disappeared at the same time as vacuoles derived from the apical surface became coated with actin. After moulting the bundles reformed (Chapter 6). These changes only occurred in the anterior (figs. 104 & 105), mid (fig. 106), and posterior (fig. 107) regions of the gland. The distribution of bundles in the duct (fig. 103) and the green (figs. 103 & 104) regions remained unchanged through the larval moults. The same regional pattern of f-actin-coated vacuole formation occurred during each of the larval moults (figs. 112-115), regardless of cell size.

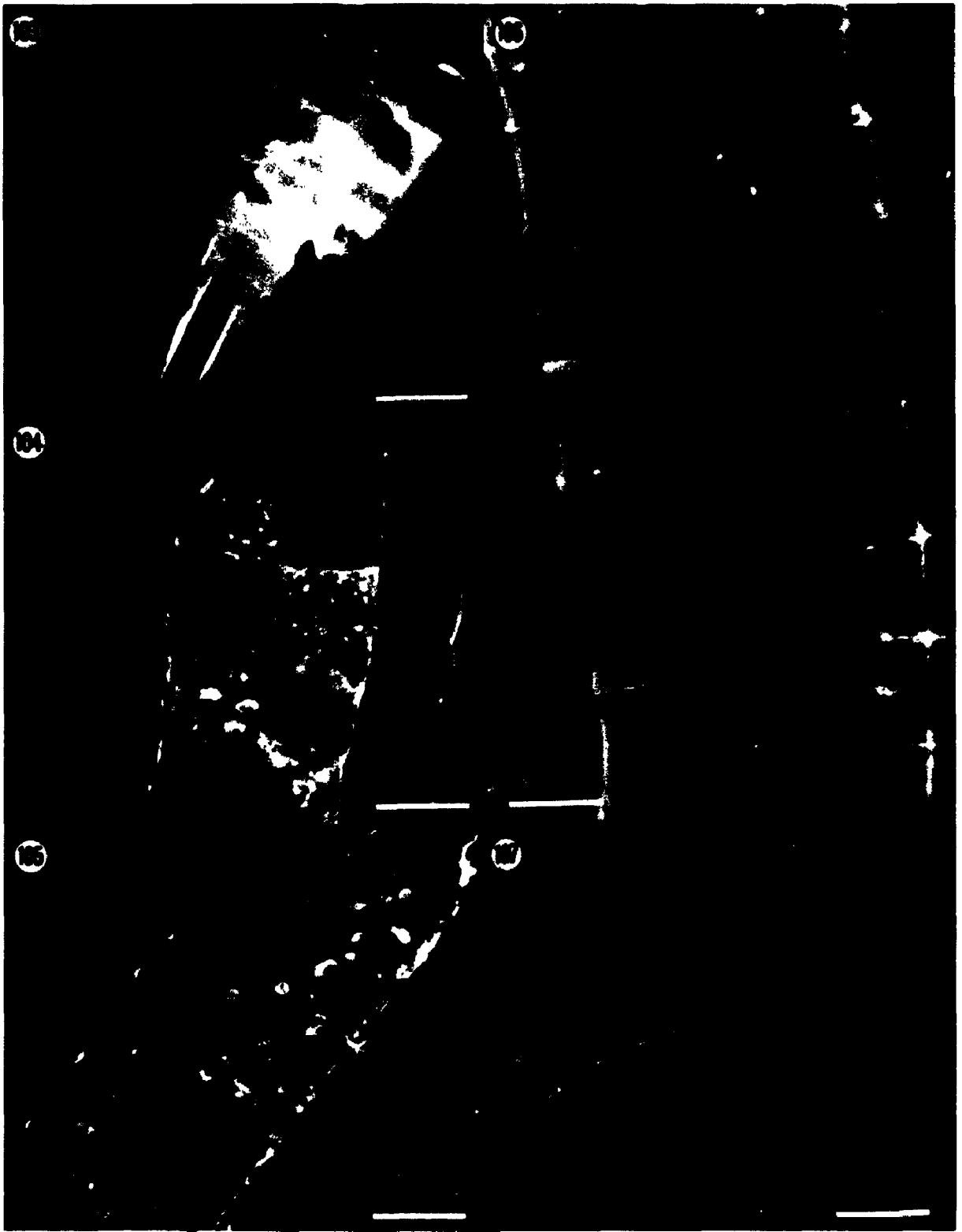
### **7.3 Discussion**

A regionally-dependent pattern exists in the density of the periluminal circumferential actin bundles. The greatest density of bundles occurs in the anterior-most regions of the gland (excluding the duct). These regional differences in the density of microfilament bundles persist throughout larval life and presumably have some functional or physiological significance.

One proposed function for the microfilament network in silk gland cells is to provide peristaltic contractions to propel the silk within the lumen of the gland (Couple *et al.*, 1984; Sasaki & Tashiro, 1976). The arrangement of the bundles in rings around the lumen of the gland (with the bundles of one cell aligned with the bundles of the opposing cell) could provide local constrictions of the lumen if the bundles are contractile.



**Figs. 103 to 107. The formation of actin-coated vacuoles during the larval moults occurs only in certain regions of the gland. Rhodaminyl-phalloin labelling of silk glands from 4<sup>th</sup> moult larvae shows that there is no f-actin-coated vacuole formation in the duct (Du) or green (Gr) regions of the gland (fig. 103). There is an abrupt change in the occurrence of vacuole formation between the green region (Gr) and the anterior region (fig. 104). F-actin-coated vacuoles occur only in the anterior (figs. 104 & 105), mid (fig. 106), and posterior (fig. 107) regions of the silk gland during moult. Photographed using a Zeiss Photomicroscope II. Scale bars = 100  $\mu$ m**

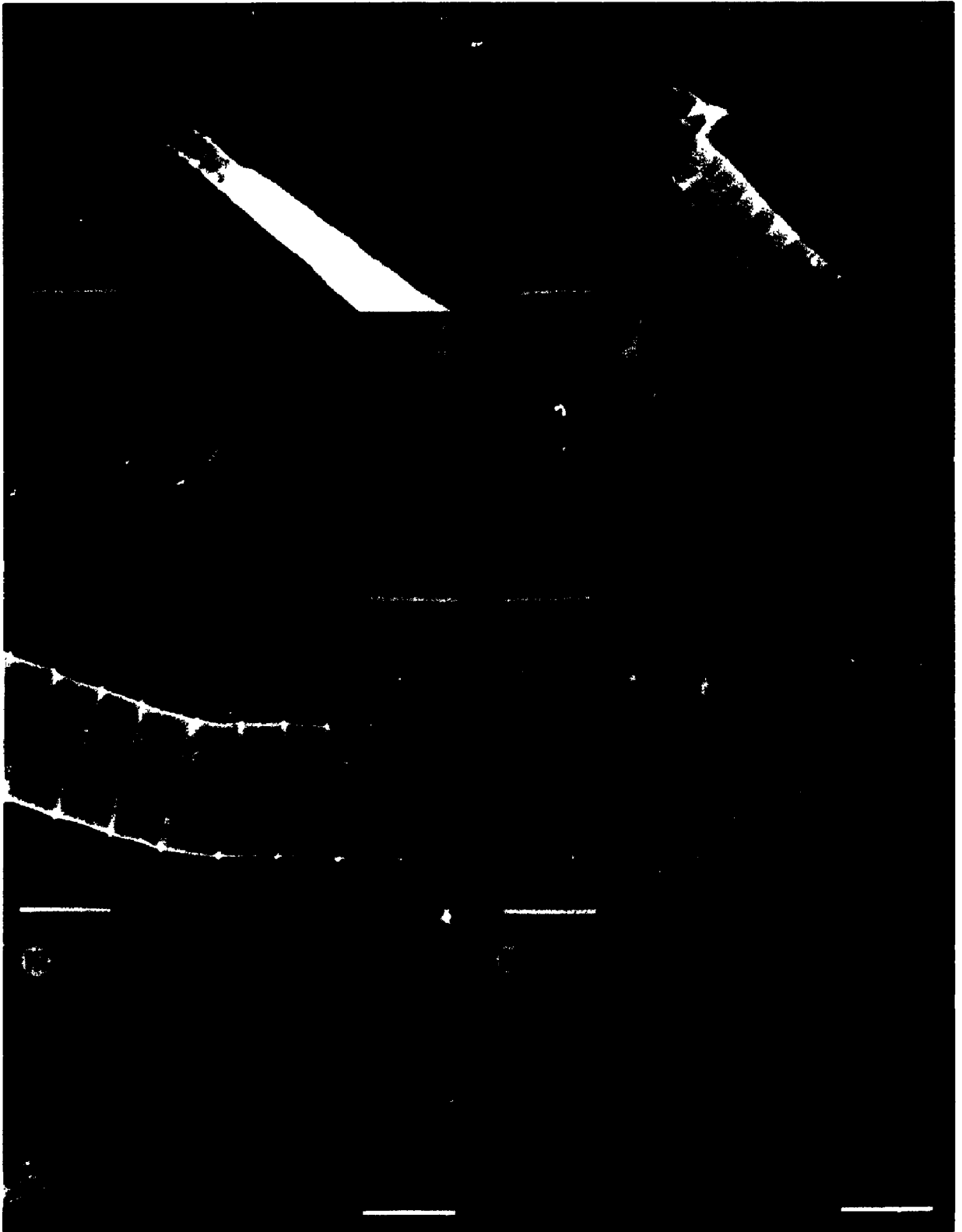


**Figs. 108 to 111.** The regional differences in the density of the periluminal circumferential actin bundles are not as conspicuous in earlier larval intermoult stages. The pattern of f-actin labelling in silk glands from third stage larvae is similar to that found in silk glands from fifth stage larvae in the duct and green regions. The difference in f-actin density is not apparent between anterior, mid, and posterior regions at this stage of development. Fig. 108: duct and green regions. Fig. 109: anterior region. Fig. 110: mid region. Fig. 111: posterior region.

Photographed using a Zeiss Photomicroscope II. Scale bars = 100  $\mu\text{m}$

**Figs. 112 to 115.** The regional patterns of f-actin-coated vacuole formation are similar during each of the larval moults. Silk glands from 3<sup>rd</sup> moult larvae show a lack of vacuole formation in the duct (Du) and green (Gr) regions (fig. 112). F-actin-coated vacuoles form only in the anterior (fig. 113), mid (fig. 114), and posterior (fig. 115) regions.

Photographed using a Zeiss Photomicroscope II. Scale bars = 100  $\mu\text{m}$



However, one might expect the density of bundles to be greatest at the posterior end of the gland in order to propel the silk toward the gland opening. Additionally, peristaltic movement of luminal secretion may not be necessary, since the gland is only open at its anterior end. The continued synthesis and secretion of silk during feeding periods may be sufficient to force the silk along the lumen.

Contractions of periluminal circumferential actin bundles may serve a different purpose. Oscillating contractions of individual actin bundles could compress the luminal silk locally, and thus increase the space between the bundles for exocytosis of silk. This interpretation could also allow the contraction to move in a series of local waves, encouraging peristalsis to a limited degree.

Another possible function for the apical actin bundles, suggested by their arrangement in parallel hoops around the gland lumen and perpendicular to the long axis of the gland, is to resist or contain luminal hydrostatic pressure. This possible function may give a clue to the need for various degrees of reinforcement in the different regions. Uniform hydrostatic pressure in a cylinder produces twice as much stress along the sides as along the length/ends (*i.e.* the hoop stress is twice the axial stress) (Locke, 1958; Timoshenko, 1936), thus, the need for lateral reinforcement. The silk gland, however, is a tube of varying luminal diameter. Assuming a constant flow rate of silk, by Poiseuille's law<sup>1</sup> for flow of viscous liquids through a tube (Sears *et al.*, 1980), the hydrostatic pressure in a tube is inversely proportional to the cross sectional area of the flow through it. Posterior regions have lower cross sectional areas and are flowing into wider tubes. Their need for circumferential reinforcement is correspondingly low. From the mid region towards the anterior of the

---

<sup>1</sup> Poiseuille's law:

$$\text{volume rate of flow } Q = \frac{\pi r^4 \Delta p}{8 \eta l}$$

where:  $r$  = radius  
 $\Delta p$  = change in pressure  
 $l$  = length  
 $\eta$  = viscosity

gland, the diameter of the gland narrows into the green region which requires correspondingly more reinforcing bundles to resist the hoop stress. Although the duct is narrower still, it is lined by cuticle (Akai, 1984), which would take the place of the luminal cytoskeleton in resisting the pressure from within.

During the larval moults, the periluminal circumferential actin bundles dissociate and the f-actin is redistributed in the apical cytoplasm in the form of actin-coated vacuoles. The differences in the density of f-actin-coated vacuoles between the anterior, mid, and posterior regions merely reflects the regional differences in density of the periluminal circumferential actin bundles during the intermoult. However, the lack of vacuole formation in the green region suggests that its actin bundles continue to be needed during moulting. The actin in this region maintains a constant structure whilst that in other regions is rearranged between stages. The green region, which has the greatest density of actin bundles, may act as a sphincter for flow regulation during the intermoult.

## SUMMARY AND CONCLUSIONS

### **The development of silk gland nuclei: the silk gland nuclear matrix**

Nuclear ramification in *Calpodes* silk gland cells is a gradual process throughout larval life. In early stages, the nuclei are small and ovoid. Branching becomes conspicuous early in the third stadium and is most extensive by the middle of the fifth stadium.

There are regionally-specific patterns of nuclear branching. Nuclei are most branched in the mid region. Little branching is apparent in the green region even though branching occurs in the regions on either side of it. Thus, arborescent nuclear shapes are determined.

Silk gland nuclei possess a structural skeleton which conforms to the nuclear shapes. Nuclear matrices prepared *in situ* are similar in shape to nuclei in unextracted glands. Therefore, nuclear shape is maintained by a nuclear skeleton.

Filaments which form the silk gland nuclear matrix have a bias in their orientation which suggests a role in nuclear branching. SEM of the outer nuclear lamina and TEM of profiles of the intranuclear filaments reveal that their arrangement is parallel to the long axes of the nuclear branches. Thus, matrix elements are arranged in an architecture which is appropriate for elongation of nuclear branches.

The polypeptide complement of the silk gland nuclear-associated (nuclear matrix) fraction is characterized by an abundance of a few polypeptides including actin and lamin.

Silk gland nuclei label for matrix antigens which are found in smaller, more typically shaped mammalian nuclei. P1 (anti-peripherin) and P11 both label the nuclear periphery. The distribution of these antigens is uniform over the entire nuclear periphery. Anti-peripherin labels the nuclear lamina in the nuclear-associated fraction.

### **A shell of f-actin surrounds the branched nuclei in silk gland cells**

The silk gland nuclear-associated fraction contains an isoform of a polypeptide (43 kD, pI 6.45) similar in relative mobility to actin.

Actin antibodies bind to a band with a relative mobility of 43 kD on Western blots of the silk gland subnuclear fraction.

Silk gland nuclei label at their periphery with antibodies to actin and myosin at all stages of nuclear branching (*i.e.* both early and late in larval development). The distribution of these antigens does not change during the larval moults.

Silk gland nuclei label weakly at their periphery with rhodaminyl-phalloin which specifically binds to f-actin.

A lamina-like element of the nuclear-associated fraction binds antibodies to both actin and myosin. This component of the fraction is not the nuclear lamina and is referred to as the nuclear shell.

The nuclear shell of the nuclear-associated fraction binds heavy meromyosin without any preferred orientation.

A perinuclear zone of exclusion, which contains randomly oriented fibrils, on the cytoplasmic side of the nuclear envelope corresponds to the nuclear shell.

Therefore, the nuclear shell contains f-actin and a myosin-like protein. These components, which are known to generate force, may participate, along with the intranuclear elements, in nuclear ramification.

### **Cytoplasmic actin storage bodies in silk gland cells**

During larval moults, large spherical protein concretions which bind antibodies to actin occur in the cytoplasm near the nuclei. These are likely actin storage bodies maintained during the larval moults.



Large spherical protein bodies occasionally co-isolate with the nuclear-associated fraction prepared from silk glands from moulting larvae. These bodies bind antibodies to actin but not to myosin or peripherin. These are probably the same actin storage bodies which occur in the cytoplasm. These bodies most likely act as reserves of actin to be incorporated into the nuclear shell during nuclear growth.

### **The redeployment of f-actin in silk glands during moulting**

Most of the cytoplasmic f-actin is restricted to the apical end of the cell in the form of parallel bundles which encircle the gland lumen. These bundles persist throughout the intermolt and present no barrier to exocytosis of silk. The function of the bundles may be to provide resistance to the luminal hydrostatic pressure.

During the larval moults, the periluminal circumferential actin bundles dissociate as the f-actin forms coats around large vacuoles in the apical cytoplasm. Molt-related cytoplasmic vacuoles label with rhodaminy-phalloin and with gold-tagged anti-actin antibodies. The formation of f-actin-coated vacuoles may facilitate the endocytosis of unspun luminal silk or may act as a temporary store of f-actin during the larval moults.

### **Regional differences in the apical f-actin cytoskeleton of silk gland cells**

Regional differences exist in the density of the periluminal circumferential actin bundles within the gland. The greatest density is in the green region. The bundle density becomes less towards the posterior end of the gland. These regional differences reflect the need for varying degrees of resistance to the luminal hydrostatic pressure along the length of the gland.

Regional differences occur in the formation of f-actin-coated vacuoles during the larval moults. F-actin coated vacuoles form in the anterior, mid and posterior gland regions but not in the green or duct regions. The density of f-actin coated vacuoles is greatest in the anterior region and least in the posterior region.

## APPENDIX 1

### Controls for Immunofluorescence Microscopy

#### Autofluorescence controls

Unlabelled whole silk glands were examined by epifluorescence microscopy for autofluorescence. The glands were examined with the filters used in this study to detect fluorescence from either rhodamine or fluorescein. With the rhodamine excitation and band pass filters, only a faint autofluorescence could be detected in the cytoplasm of the green region of the gland (figs. 116-118). No autofluorescence occurred in the regions on either side of the green region or in any other part of the gland (figs. 116-120). No autofluorescence was detected in or near the lumen in any region of the gland.

Examination of the glands with the fluorescein excitation and band pass filters revealed autofluorescence from the luminal contents of the gland (*i.e.* the silk) (fig. 121).

Figures 117, 118, 120, and 121 were all exposed and printed under conditions which matched those used for immunofluorescent images.

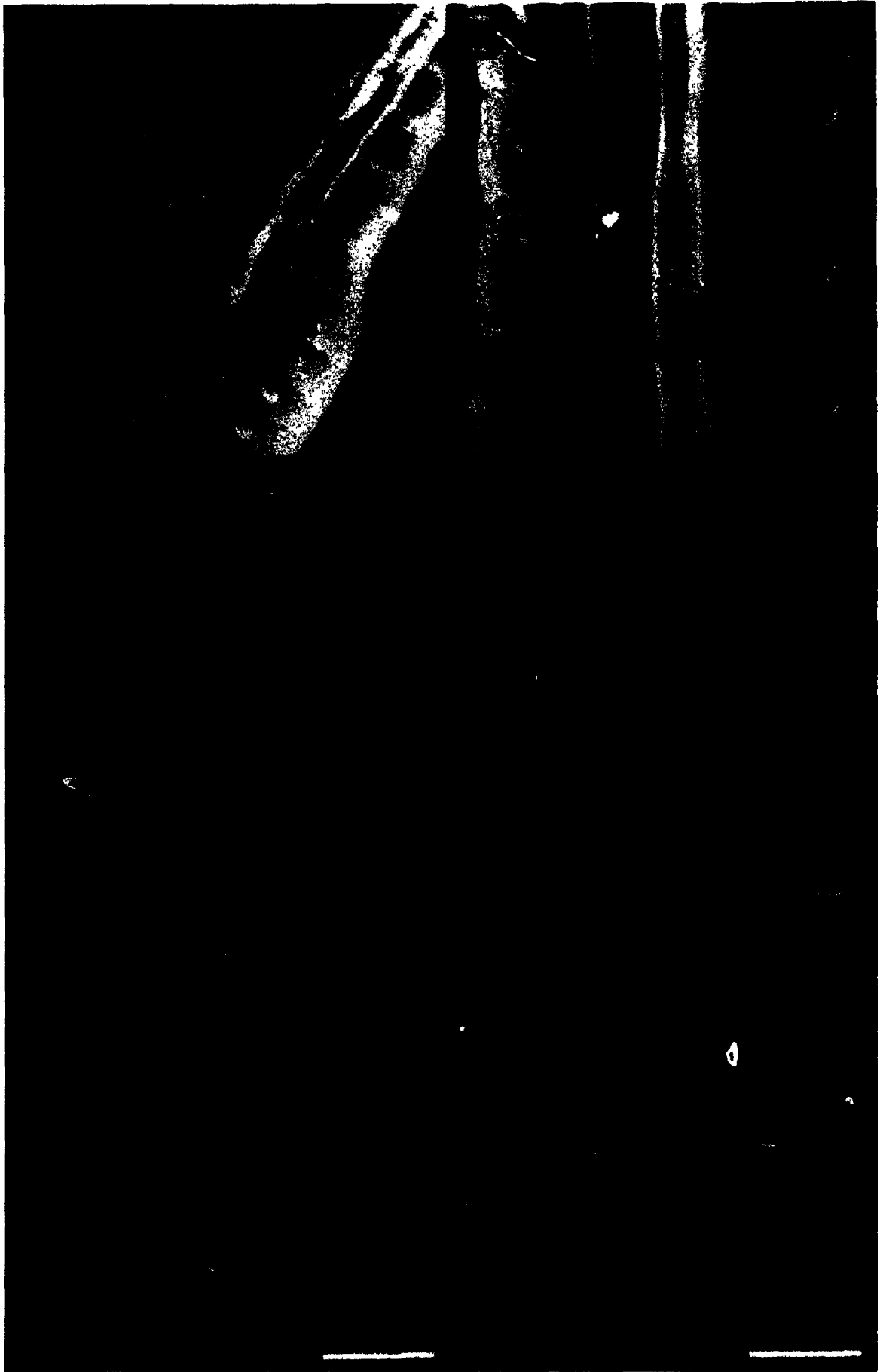
#### 2° Antibody controls (immunofluorescence)

As a control for false positive labelling, fractured silk glands were incubated with only the 2° antibodies (under the conditions outlined in Chapter 2). The only detectable fluorescence in slides incubated with FITC-conjugated anti-rabbit IgG was from linear structures thought to be the tracheoles which penetrate the glands (fig. 122). Since no fluorescence was detected in slides incubated with rhodamine-conjugated anti-rabbit IgG (fig. 123), the fluorescence in figure 122 probably represents autofluorescence from the tracheoles. Similar results were obtained when slides were incubated with FITC-conjugated anti-mouse IgG (fig. 124) and rhodamine-conjugated anti-mouse IgGAM (fig. 125).

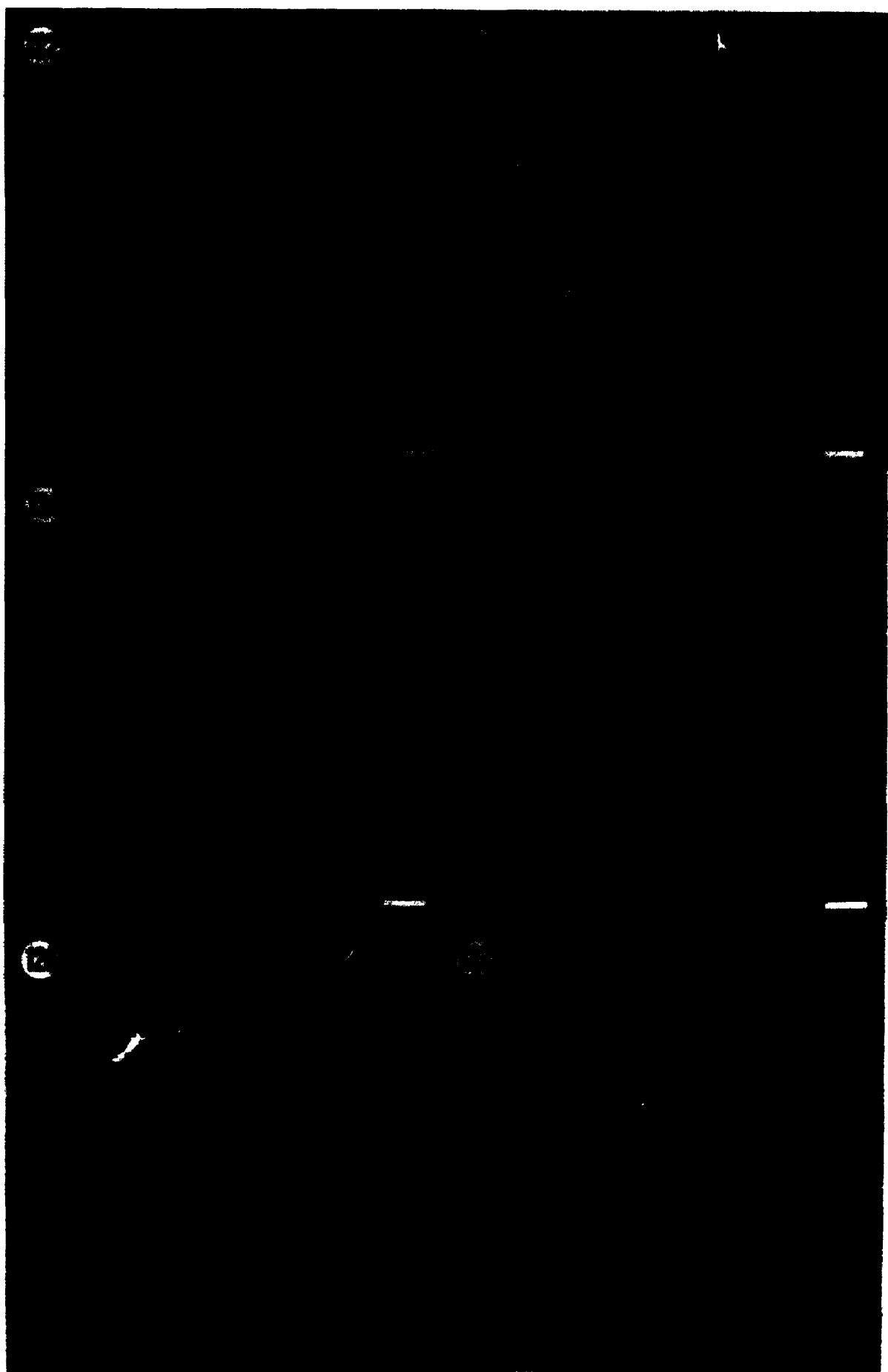
Slides incubated with FITC-conjugated anti-human IgG were examined with the filters to detect both fluorescein- and rhodamine-like fluorescence because of the inclusion of an Evan's Blue counterstain. With the FITC filters, spheres which stain with Evan's Blue (*i.e.* they fluoresce

**Figs. 116 to 121. No autofluorescence occurs within the cells of the anterior, mid, and posterior regions of the silk glands. Whole unlabelled silk glands were examined by epifluorescence microscopy with filters used to detect rhodamine fluorescence. Comparison of the phase contrast image (fig. 116) of duct/green region (Du/Gr) from early 5<sup>th</sup> instar with corresponding epifluorescent image (fig. 117) indicates a weak autofluorescence is apparent only in the green region (Gr) of the gland. The junction between the duct and the green region is marked by large arrows. No increased autofluorescence occurs around the gland lumen in the green region or in any other region. The weak autofluorescence disappears at the junction between the green and anterior regions (small arrow) (fig. 118). Autofluorescence does not occur in any other region of the gland under conditions used to detect rhodamine fluorescence. Fig. 119: Phase contrast image of anterior region from early 5<sup>th</sup> instar. Fig. 120: Corresponding epifluorescent image.**

With filters used to detect FITC fluorescence, the luminal content (Lu) of the silk glands (*i.e.* the silk) is autofluorescent (fig. 121). No structures within the cell appear to be autofluorescent under these conditions. Fig. 121: Epifluorescent image of the anterior region from early 5<sup>th</sup> instar. Scale bars = 100  $\mu$ m



**Figs. 122 to 127. Fluorescent-tagged secondary antibodies do not bind to any sites within silk gland cells.** Fractured silk glands (see section 2.4) were probed with only the secondary antibodies under the same conditions which gave positive results when the primary antibodies were included. In glands labelled with FITC-conjugated anti-rabbit IgG (fig. 122) or FITC-conjugated anti-mouse IgG (fig. 124) only a small amount of fluorescence occurs from the tracheoles (Tr) which penetrate the glands. The fluorescence is thought to be due to autofluorescence of the tracheoles since a similar fluorescence does not occur when glands are labelled with rhodamine-conjugated anti-rabbit IgG (fig. 123) or rhodamine-conjugated anti-mouse IgGAM (fig. 125). Glands were also labelled with FITC-conjugated anti-human IgG and Evan's blue. Vacuoles (v) which stain with Evan's blue are only detected when using the filters for FITC fluorescence (fig. 126). Fluorescence from the cytoplasm which stains with Evan's blue is detected under conditions used to detect both FITC (fig. 126) and rhodamine fluorescence (fig. 127). In both cases, only the red fluorescence from the Evan's blue was detected. Scale bars = 10  $\mu$ m



red, not green) were detected (fig. 126). With the rhodamine filters, only a background fluorescence from the Evan's Blue was detected (fig. 127). The intensity of the fluorescence was less than that detected with the fluorescein filters.

Thus, under the conditions used, fluorescence from the 2° antibody appears to represent a true binding of the 1° antibody to the antigen.

### **Specificity of antibodies and filters**

Double labelling of cells for immunofluorescence presents 2 problems:

- 1) the possibility of non-specific binding of the 1° antibodies; and
- 2) the possibility of "cross-talk" between the excitation and/or barrier filters (*i.e.* the excitation or detection of fluorescence of a label with an inappropriate filter).

The excitation (430-500 nm) and emission (500-560 nm) of fluorescein can excite rhodamine (excitation = approximately 450-600 nm). Therefore, a short wave band pass filter (KP 490) was used for the excitation of FITC. This filter allows for the transmission of light with wavelengths between 400 and 490 nm (with a sharp cut off at 490 nm). A long pass barrier (emission) filter which blocks wavelengths below 500 nm was used to detect FITC fluorescence.

For the excitation of rhodamine, a band pass excitation filter (BP 510-560) (*i.e.* transmission of wavelengths between 510 and 560 nm) was used to prevent the excitation of FITC. To detect rhodamine fluorescence, a long pass barrier (emission) filter (LP 590) (*i.e.* cuts off wavelengths below 590 nm) was used.

The co-localization of actin (or myosin) and P1 (or P11) to the nuclear periphery was detected with both combinations of 2° tags (*i.e.* FITC-P1/Rh-actin(myosin) (figs. 50-51) and Rh-P1/FITC-actin(myosin) (figs. 46,47,52 & 53)). Furthermore, each of the antibodies labelled the nucleus independently (figs. 36 & 45).

The specificity of antibody binding was indicated by the labelling of the apical actin bundles with anti-actin (fig. 131) but not P1 (fig. 130) in the same cell in which both antibodies labelled the nucleus (figs. 128 & 129).

Furthermore, immunogold labelling of sections of nuclear matrix fractions showed that each antibody binds to a separate nuclear structure (*i.e.*

**Fig. 128 to 131. The binding of primary antibodies is specific.** Fractured silk glands from 3rd instar larvae were double labelled with an antibody to actin followed by rhodamine-conjugated anti-rabbit IgG and with a monoclonal antibody (P1) to the nuclear matrix antigen-peripherin (Chaly *et al.*, 1985) followed by FITC-conjugated anti-mouse IgG. Optical sections were taken by confocal microscopy in two different planes within the cell: at the nuclear surface (figs. 128,129) and at the lumen (figs. 130, 131). Antibodies to actin label the periluminal bundles (fig. 131) which are known to contain actin (Couple *et al.*, 1984) as well as the cell nucleus (fig. 129). Antibodies to peripherin label the cell nucleus (fig. 128) but not the periluminal bundles (fig. 130). Scale bars = 10  $\mu$ m



**Figs. 134 to 136. Gold-tagged secondary antibodies alone do not bind to nuclear or cytoplasmic structures which label for actin or peripherin.** Sections of silk glands or of silk gland nuclear matrices were incubated with only the gold-tagged secondary antibodies under the same conditions which gave positive results when the primary antibodies were included. Structures which labelled strongly when the primary antibodies were included were examined for binding of only the secondary antibody. Nuclear laminae which bound antibodies to peripherin (see figs. 27,56,57, & 79) did not bind 10 nm gold-conjugated anti-mouse IgG (fig. 134). Storage bodies, found either in nuclear matrix preparations (fig. 135) or *in situ* (fig. 136), bound antibodies to actin (see figs. 77,79) but did not bind 5 nm gold conjugated anti-rabbit IgG. Scale bars = 0.2  $\mu$ m

anti-actin bound to the nuclear shell (fig. 58) and actin storage bodies (figs. 77 & 79); P1 bound to the nuclear lamina (figs. 27,56,57, & 79)).

### **Controls for fracture technique**

Due to a thick impermeable basal lamina, the silk glands had to be fractured in order to expose the internal structures to antibodies. The glands were gently compressed between two gelatin-coated slides, frozen on dried ice, and then pried apart. Such a treatment introduces the possibility of structural rearrangement of the antigens. To test for this possibility, the fractured glands were probed with antibodies to antigens of a known distribution within the cell.

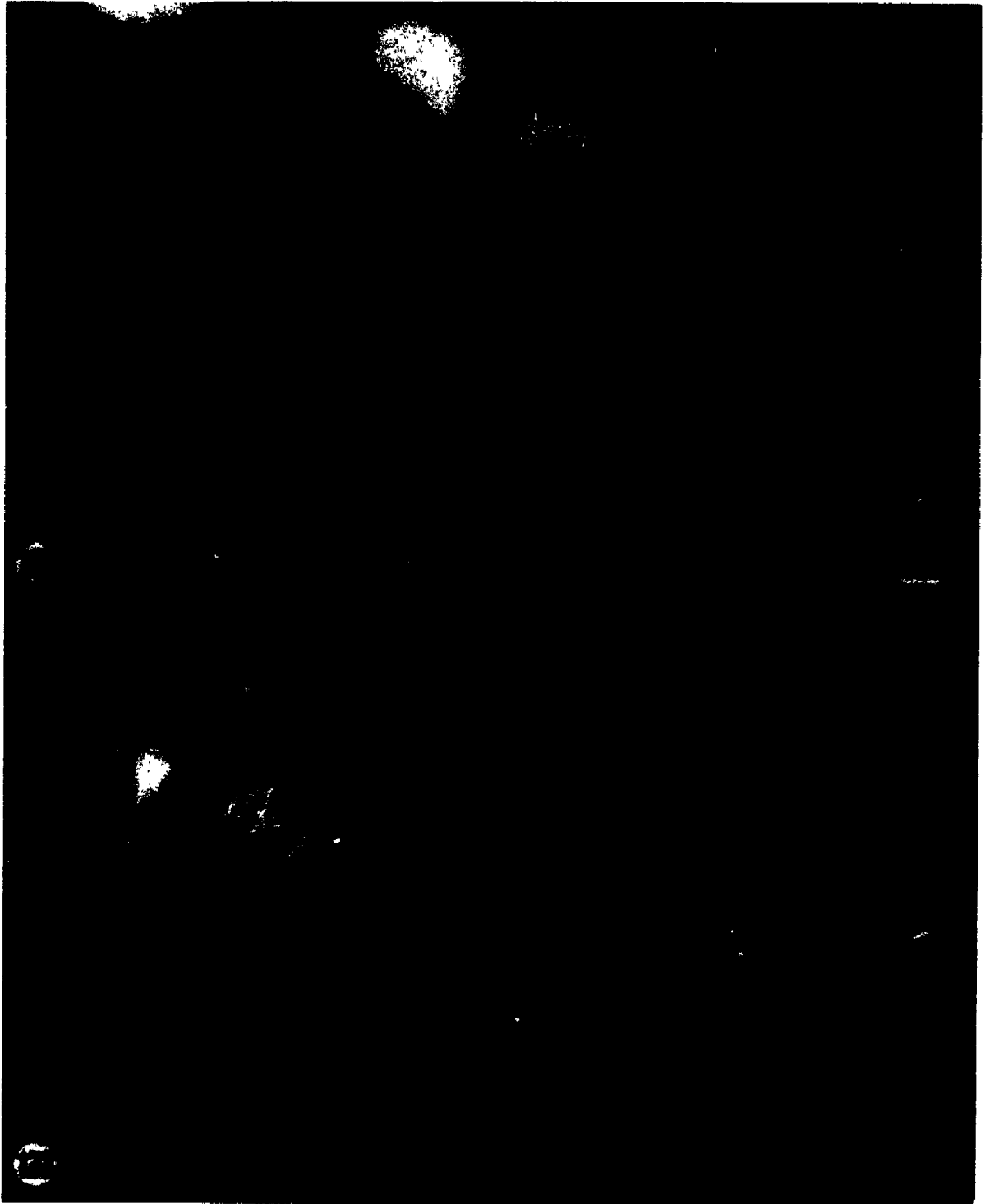
The parallel bundles of f-actin around the lumen of intact glands (figs. 100-102) were preserved in the fractured preparations (figs. 84 & 131). This distribution correlated with the distribution of microfilament bundles observed by TEM (fig. 86).

The distribution of nuclear antigens detected by P1 (figs. 34,36, & 61) and anti-nuclear antibodies (fig. 62) in fractured glands correlated with the previously established distribution in other cells (Chaly *et al.*, 1984; Chaly *et al.*, 1985; Chaly *et al.*, 1986; Chaly *et al.*, 1989).

Fractured glands probed with an antibody to tubulin showed that the microtubules extended from the nucleus to the luminal end of the cell (figs. 132 & 133). Thus, the radial microtubule system, similar to that found in *Bombyx mori* (Sasaki, 1977; Sasaki *et al.*, 1981; Sasaki & Tashiro, 1976; Tashiro *et al.*, 1982), is preserved in fractured silk glands.

It can be concluded that there is no appreciable alteration in the distribution of 4 different antigens within fractured silk gland cells.

**Figs. 132 & 133.** The technique used to expose intracellular regions does not alter the distribution of microtubules in silk gland cells. Access of antibodies to intracellular antigens in silk glands is prevented by a thick basal lamina. To overcome this problem, silk glands were crushed, frozen, and fractured to expose the interior of the cell (see section 2.4). Glands from 4th moult larvae were fractured and incubated with a monoclonal antibody to sea urchin  $\beta$ -tubulin (Leslie *et al.*, 1984; Scholey *et al.*, 1984) followed by rhodamine-conjugated anti-mouse IgGAM. The slides were also incubated with H $\ddot{o}$ chst 33258 to label the nuclei (N) (fig. 132). The microtubules (MT) (fig. 133) are arranged parallel to each other and are oriented towards the apical/luminal face of the cell. This arrangement of the microtubules is similar to that found in the silk gland cells of *Bombyx mori* (Sasaki, 1977; Sasaki *et al.*, 1981; Sasaki & Tashiro, 1976). Thus, the protocol used to expose the cell interior does not cause structural rearrangements. Scale bar = 10  $\mu$ m



## APPENDIX 2

### Controls for Immunogold Labelling

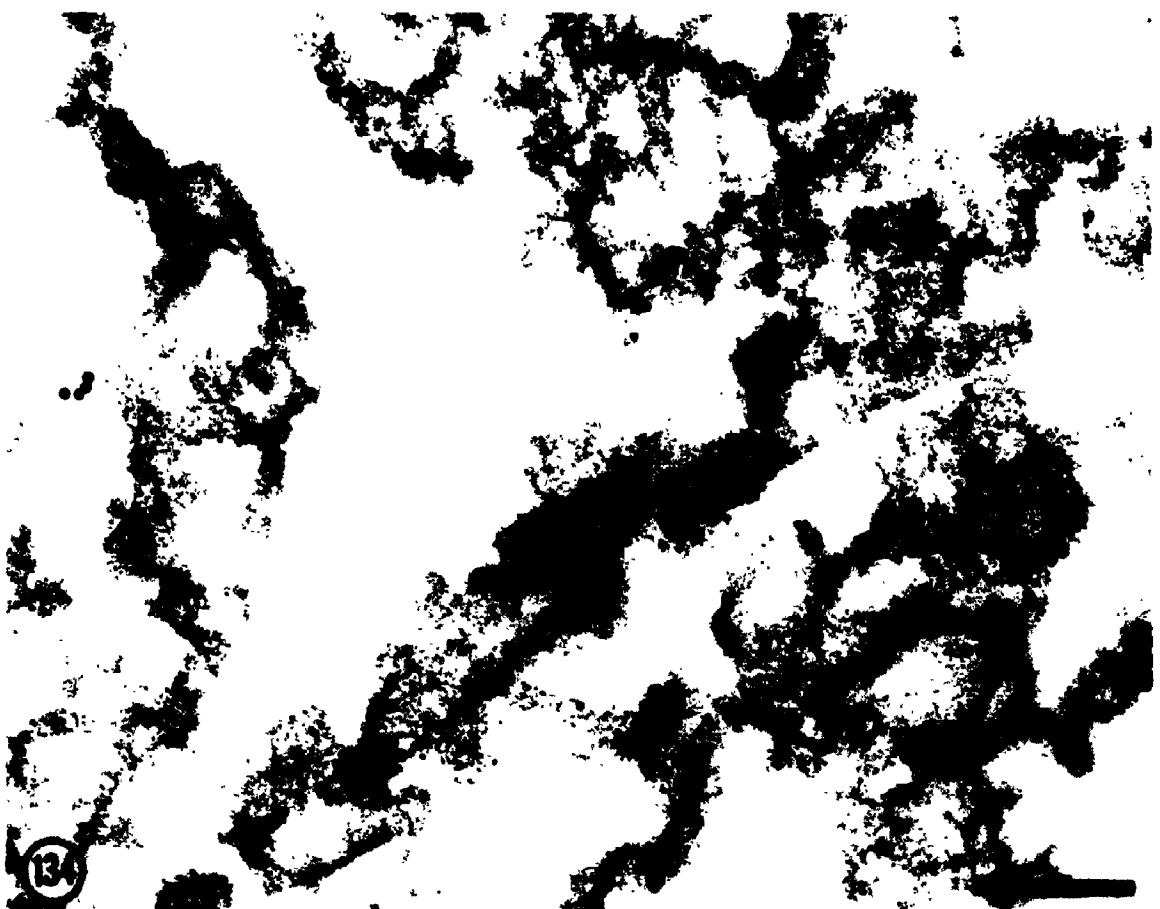
#### 2° Antibody controls (immunogold)

As a control for false positive labelling, sections of silk glands or silk gland nuclear matrices were incubated with only the gold-tagged 2° antibody (under the conditions outlined in Chapter 2). Structures known to bind 1° antibodies strongly were examined for binding of the 2° antibody only. Little or no antibody was detected in nuclear laminae probed with 10 nm gold-conjugated anti-mouse IgG (fig. 134) or in actin storage bodies (either associated with the nuclear matrix fraction (fig. 135) or *in situ* (fig. 136)) probed with 5 nm gold-conjugated anti-rabbit IgG. Thus, under the conditions used, labelling appears to represent true binding of the antibody to the antigen.

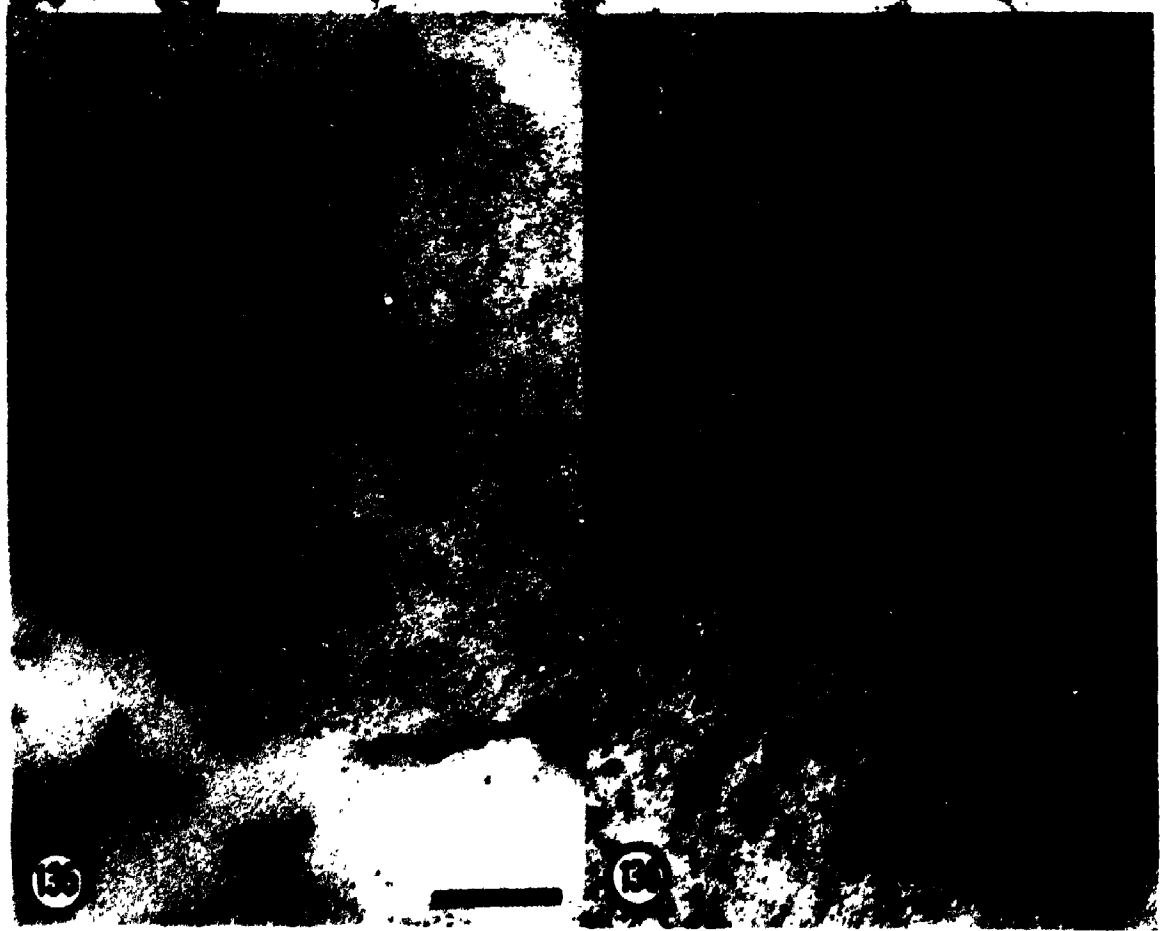
#### Mouse liver nuclear matrices

Nuclear matrices prepared from mouse liver extracted (in the presence of DTT) by the protocol used in this study possessed a nuclear lamina but no intranuclear filaments (figs. 137 & 138). The remnant intranuclear structures may represent residual nucleoli or collapsed parts of the intranuclear matrix. These nuclear matrices label with antibodies to peripherin (P1) (fig. 137) but not with antibodies to actin (fig. 138).

**Figs. 134 to 136. Gold-tagged secondary antibodies alone do not bind to nuclear or cytoplasmic structures which label for actin or peripherin. Sections of silk glands or of silk gland nuclear matrices were incubated with only the gold-tagged secondary antibodies under the same conditions which gave positive results when the primary antibodies were included. Structures which labelled strongly when the primary antibodies were included were examined for binding of only the secondary antibody. Nuclear laminae which bound antibodies to peripherin (see figs. 27,56,57, & 79) did not bind 10 nm gold-conjugated anti-mouse IgG (fig. 134). Storage bodies, found either in nuclear matrix preparations (fig. 135) or *in situ* (fig. 136), bound antibodies to actin (see figs. 77,79) but did not bind 5 nm gold conjugated anti-rabbit IgG. Scale bars = 0.2  $\mu$ m**



134

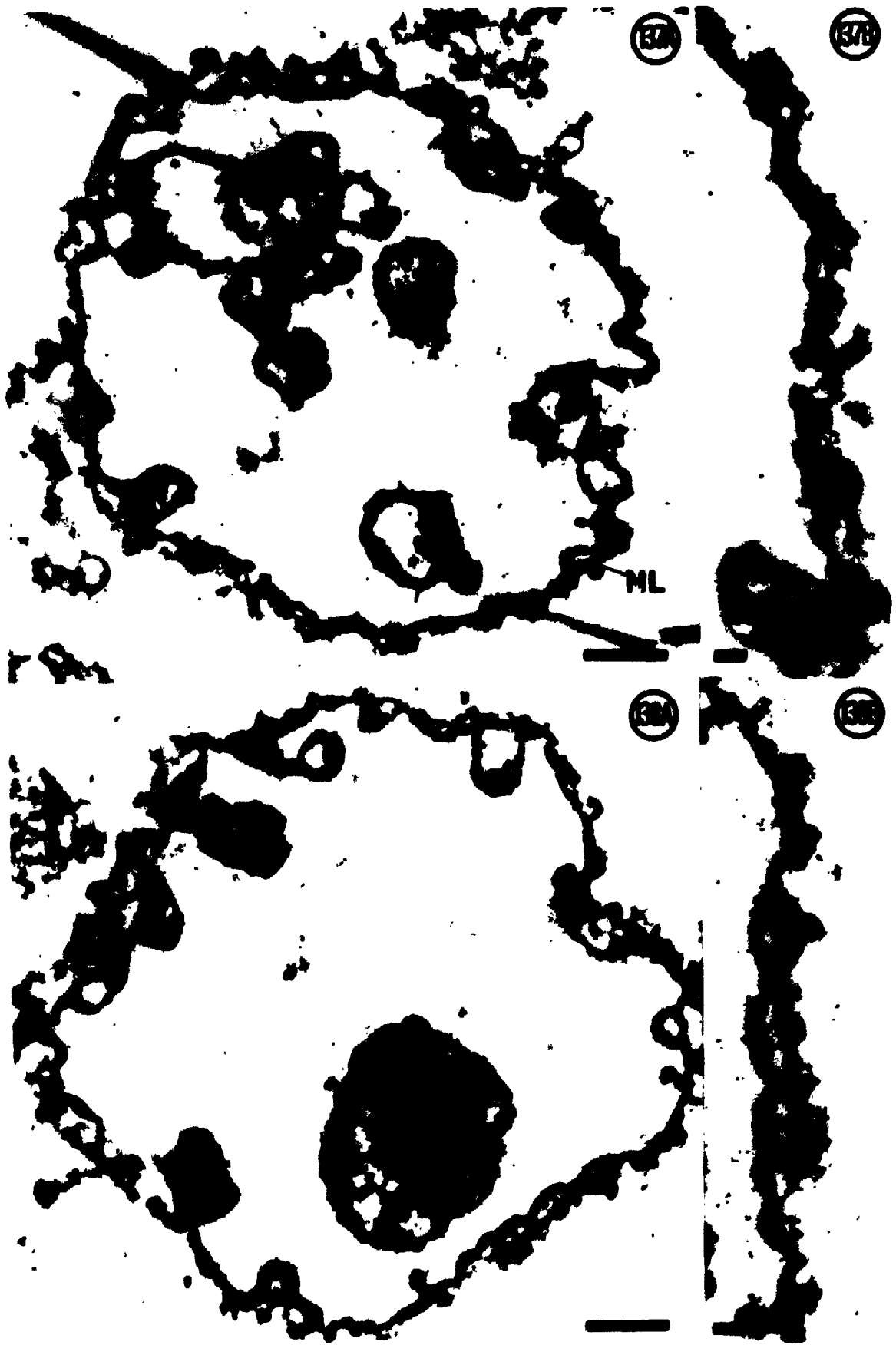


135

135

**Figs. 137 & 138. Nuclear matrices prepared from mouse liver label with antibodies to peripherin but not with antibodies to actin. Nuclear matrices prepared from mouse liver by the method of Fisher *et al.* (1982) in the presence of a reducing agent (DTT) contain only a peripheral nuclear lamina (NL). Structures that remain in the nuclear interior may be either the nucleolar skeleton or the collapsed intranuclear matrix. The isolated nuclear lamina from rat liver labels with monoclonal antibodies to peripherin (fig. 137 a,b) but not with antibodies to actin (fig. 138 a,b). Scale bars = 0.5  $\mu\text{m}$  (figs. 137a & 138a); 0.1  $\mu\text{m}$  (figs. 137b & 138b).**





## REFERENCES

- Achong, B. G. & Epstein, M. A. (1966). Fine structure of the Burkitt tumor. *J. Natl. Cancer Inst.* **36**, 877-897.
- Adams, R. J. & Pollard, T. D. (1989). Binding of myosin I to membrane lipids. *Nature* **340**, 565-568.
- Aebi, U., Cohn, J., Buhle, L. & Gerace, L. (1986). The nuclear lamina is a meshwork of intermediate-type filaments. *Nature* **323**, 560-564.
- Ahearn, M. J., Trujillo, J. M., Cork, A., Fowler, A. & Hart, J. S. (1974). The association of nuclear blebs with aneuploidy in human acute leukemia. *Cancer Res.* **34**, 2887-2896.
- Akai, H. (1965). Studies on the ultrastructure of the silk gland in the silkworm, *Bombyx mori* L. *Bull. Sericul. Exp. Sta.* **19**, 375-484.
- Akai, H. (1971). An ultrastructural study of changes during molting in the silk gland of larvae of the Eri-silkworm, *Philosamia cynthia ricini* Boisduval (Lepidoptera: Saturniidae). *Appl. Ent. Zool.* **6**, 27-39.
- Akai, H. (1983). The structure and ultrastructure of the silk gland. *Experientia* **39**, 443-449.
- Akai, H. (1984). The ultrastructure and functions of the silk gland cells of *Bombyx mori*. In *Insect Ultrastructure*, 2 (ed. H. Akai & R. C. King), pp. 323-364. New York: Plenum Press.
- Alexander, R. B., Greene, G. L. & Barrack, E. R. (1987). Estrogen receptors in the nuclear matrix: direct demonstration using monoclonal antireceptor antibody. *Endocrinology* **120**, 1851-1857.
- Ankenbauer, T., Kleinschmidt, J. A., Vandekerckhove, J. & Franke, W. W. (1988). Proteins regulating actin assembly in oogenesis and early embryogenesis of *Xenopus laevis*: gelsolin is the major cytoplasmic actin-binding protein. *J. Cell Biol.* **107**, 1489-1498.
- Ankenbauer, T., Kleinschmidt, J. A., Walsh, M. J., Weiner, O. H. & Franke, W. W. (1989). Identification of a widespread nuclear actin binding protein. *Nature* **342**, 822-825.
- Atkinson, B. G. (1981). Synthesis of heat-shock proteins by cells undergoing myogenesis. *J. Cell Biol.* **89**, 666-673.
- Aubock, V. L. (1976). "Labyrinthkerne" bei einem Dermatofibrosarcoma protuberans und einen Fibroxanthom. *Exp. Path.* **12**, 1-18.

- Aunis, D. & Bader, M.-F. (1988). The cytoskeleton as a barrier to exocytosis in secretory cells. *J. Exp. Biol.* **139**, 253-266.
- Barrack, E. R. (1987). Steroid hormone receptor localization in the nuclear matrix: interaction with acceptor sites. *J. Steroid Biochem.* **27**, 115-122.
- Barrack, E. R. & Coffey, D. S. (1982). Biological properties of the nuclear matrix: steroid hormone binding. *Recent Prog. Hormone Res.* **38**, 133-195.
- Bartnik, E. & Weber, K. (1989). Widespread occurrence of intermediate filaments in invertebrates; common principles and aspects of diversion. *Eur. J. Cell Biol.* **50**, 17-33.
- Benavente, R. & Franke, W. W. (1985). Changes of the karyoskeleton during spermatogenesis of *Xenopus*: expression of lamin I<sub>IV</sub>, a nuclear lamin protein specific for the male germ line. *Proc. Natl. Acad. Sci. USA* **82**, 6176.
- Benavente, R. & Krohne, G. (1986). Involvement of the nuclear lamins in post mitotic reorganization of chromatin as demonstrated by microinjection of lamin antibodies. *J. Cell Biol.* **103**, 1847-1854.
- Benavente, R., Krohne, G. & Franke, W. W. (1985). Cell type-specific expression of nuclear lamin proteins during development in *Xenopus laevis*. *Cell* **41**, 177-190.
- Benavente, R., Krohne, G., Stick, R. & Franke, W. W. (1984). Electron microscopic immunolocalization of a karyoskeletal protein of molecular weight 145,000 in nucleoli and perinucleolar bodies of *Xenopus laevis*. *Exp. Cell Res.* **151**, 224-235.
- Bendayan, M. (1985). Ultrastructural localization of cytoskeletal proteins in pancreatic secretory cells. *Can. J. Biochem. Cell Biol.* **63**, 680-690.
- Berezney, R. (1980). Fractionation of the nuclear matrix. I. Partial separation in matrix protein fibrils and a residual ribonucleoprotein fraction. *J. Cell Biol.* **85**, 641-650.
- Berezney, R. & Coffey, D. S. (1974). Identification of a nuclear protein matrix. *Biochem. Biophys. Res. Comm.* **60**, 1410-1417.
- Berezney, R. & Coffey, D. S. (1975). Nuclear protein matrix: association with newly synthesized DNA. *Science* **189**, 291-293.
- Berezney, R. & Coffey, D. S. (1977). Nuclear matrix: isolation and characterization of a framework structure from rat liver nuclei. *J. Cell Biol.* **73**, 616-637.

- Berrios, M., Blobel, G. & Fisher, P. A. (1983). Characterization of an ATPase/dATPase activity associated with the *Drosophila* nuclear matrix-pore complex-lamina fraction. *J. Biol. Chem.* **258**, 4548-4555.
- Berrios, M. & Fisher, P. A. (1986). A myosin heavy chain-like polypeptide is associated with the nuclear envelope in higher eukaryotic cells. *J. Cell Biol.* **103**, 711-724.
- Berrios, M., Osheroff, N. & Fisher, P. A. (1985). *In situ* localization of DNA topoisomerase II, a major polypeptide component of the *Drosophila* nuclear matrix fraction. *Proc. Natl. Acad. Sci. USA* **82**, 4142-4146.
- Blaes, N., Couble, P. & Prudhomme, J. C. (1980). The programming of silk gland development in *Bombyx mori*: I. Effects of experimental starvation on growth, silk production, and autolysis during the fifth larval instar studied by electron microscopy. *Cell Tissue Res.* **213**, 311-324.
- Bourgeois, C. A., Bouvier, D., Sève, A.-P. & Hubert, J. (1987). Evidence for the existence of a nucleolar skeleton attached to the pore complex-lamina in human fibroblasts. *Chromosoma* **95**, 315-323.
- Bouvier, D., Hubert, J., Sève, A.-P. & Bouteille, M. (1985). Structural aspects of intranuclear disintegration upon RNase digestion of HeLa cell nuclei. *Eur. J. Cell Biol.* **36**, 323-333.
- Boyle, W. J. & Baluda, M. A. (1987). Subnuclear associations of the *v-myb* oncogene product and actin are dependent on ionic strength during nuclear isolation. *Mol. Cell. Biol.* **7**, 3345-3348.
- Brasch, K. (1982). Fine structure and localization of the nuclear matrix *in situ*. *Exp Cell Res.* **140**, 161-171.
- Bremer, J. W., Busch, H. & Yeoman, L. C. (1981). Evidence for a species of nuclear actin distinct from cytoplasmic and muscle actins. *Biochemistry* **20**, 2013-2017.
- Burgoyne, R. D. & Cheek, T. R. (1987). Reorganisation of peripheral actin filaments as a prelude to exocytosis. *Biosci. Rep.* **7**, 281-288.
- Burns, E. R., Soloff, B. L., Hanna, C. & Buxton, D. F. (1971). Nuclear pockets associated with the nucleolus in normal and neoplastic cells. *Cancer Res.* **31**, 159-165.
- Butt, T. M. & Heath, I. B. (1988). The changing distribution of actin and nuclear behaviour during the cell cycle of the mite-pathogenic fungus *Neozygites* sp. *Eur. J. Cell Biol.* **46**, 499-505.

- Capco, D. G., Munoz, D. M. & Gassmann, C. J. (1987). A method for analysis of the detergent-resistant cytoskeleton of cells within organs. *Tissue Cell* **19**, 607-616.
- Capco, D. G., Wan, K. M. & Penman, S. (1982). The nuclear matrix: three dimensional architecture and protein composition. *Cell* **29**, 847-858.
- Carmo-Fonseca, M., Cidadao, A. J. & David-Ferreira, J. F. (1987). Filamentous cross-bridges link intermediate filaments to the nuclear pore complexes. *Eur. J. Cell Biol.* **45**, 282-290.
- Carmo-Fonseca, M., Pfeifer, K., Schröder, H. C., Vaz, M. F., Fonseca, J. E., Müller, W. E. G. & Bachmann, M. (1989). Identification of La ribonucleoproteins as a component of interchromatin granules. *Exp. Cell Res.* **185**, 73-85.
- Chaly, N., Bladon, T., Setterfield, G., Little, J. E., Kaplan, J. G. & Brown, D. L. (1984). Changes in distribution of nuclear matrix antigens during the mitotic cell cycle. *J. Cell Biol.* **99**, 661-671.
- Chaly, N., Little, J. E. & Brown, D. L. (1985). Localization of nuclear antigens during preparations of nuclear matrices *in situ*. *Can. J. Biochem. Cell Biol.* **63**, 644-653.
- Chaly, N., Sabour, M. P., Silver, J. C., Aitchison, W. A., Little, J. E. & Brown, D. L. (1986). Monoclonal antibodies against nuclear matrix detect nuclear antigen in mammalian, insect, and plant cells: an immunofluorescence study. *Cell Biol. Int. Rep.* **10**, 421-428.
- Chaly, N., St. Aubin, G. & Brown, D. L. (1989). Ultrastructural localization of nuclear antigens during interphase in mouse 3T3 fibroblasts. *Biochem. Cell Biol.* **67**, 563-574.
- Ciampor, F. (1988). The role of the cytoskeleton and nuclear matrix in virus replication. *Acta virol.* **32**, 168-189.
- Clark, M. & Spudich, J. A. (1977). Nonmuscle contractile proteins: the role of actin and myosin in cell motility and shape determination. *Annu. Rev. Biochem.* **46**, 797-822.
- Clark, T. G. & Merriam, R. W. (1977). Diffusible and bound actin in nuclei of *Xenopus laevis* oocytes. *Cell* **12**, 883-891.
- Clark, T. G. & Rosenbaum, J. L. (1979). An actin filament matrix in hand-isolated nuclei of *X. laevis* oocytes. *Cell* **18**, 1101-1108.

- Collard, J.-F. & Raymond, Y. (1990). Transfection of human lamins A and C into mouse embryonal carcinoma cells possessing only lamin B. *Exp. Cell Res.* **186**, 182-187.
- Comerford, S. A., Agutter, P. S. & McLennan, A. G. (1986). Nuclear matrices. In *Nuclear Structures - Isolation and Characterization*, (ed. A. J. MacGillivray & G. D. Birnie), pp. 1-13. London: Butterworths and Co. Ltd.
- Comings, D. E. & Harris, D. C. (1976). Nuclear proteins. III. The fibrillar nature of the nuclear matrix. *Exp. Cell Res.* **103**, 341-360.
- Comings, D. E. & Okada, T. A. (1976). Nuclear proteins. II. Similarity of non-histone proteins in nuclear sap and chromatin, and essential absence of contractile proteins from mouse liver nuclei. *J. Cell Biol.* **70**, 440-452.
- Conforti, A., Medolago-Albani, L. & Alessio, L. (1976). Ultrastructural changes in human leukemic cell nuclei. *Virchows Arch. B Cell Path.* **22**, 143-149.
- Conrad, P. A., Nederlof, M. A., Herman, I. M. & Taylor, D. L. (1989). Correlated distribution of actin, myosin, and microtubules at the leading edge of migrating Swiss 3T3 fibroblasts. *Cell Motil. Cytoskel.* **14**, 527-543.
- Cook, P. R. (1988). The nucleoskeleton: artefact, passive framework or active site? *J. Cell Sci.* **90**, 1-6.
- Corben, F., Butcher, G., Hutchings, A., Wells, B. & Roberts, K. (1989). A nucleolar matrix protein from carrot cells identified by a monoclonal antibody. *Eur. J. Cell Biol.* **50**, 353-359.
- Couble, P., Blaes, N. & Prudhomme, J. C. (1984). Actin microfilaments and fibroin secretion in the silk gland cells of *Bombyx mori*: effects of cytochalasin B. *Exp. Cell Res.* **151**, 322-331.
- Couble, P., Moine, A., Garel, A. & Prudhomme, J. C. (1983). Developmental variations of a non-fibroin mRNA of *Bombyx mori* silk gland, encoding for a low-molecular weight silk protein. *Dev. Biol.* **97**, 398-407.
- Crowley, K. S. & Brasch, K. R. (1987). Does the interchromatin compartment contain actin? *Cell Biol. Int. Rep.* **11**, 537-546.

- Dabauvalle, M. C., Benavente, R. & Chaly, N. (1988). Monoclonal antibodies to a  $M_r$  68,000 pore complex glycoprotein interfere with nuclear protein uptake in *Xenopus* oocytes. *Chromosoma* **97**, 193-197.
- DeBiasio, R., Wang, L. & Taylor, D. L. (1988). The dynamic distribution of fluorescent analogs of actin and myosin in protrusions at the leading edge of migrating Swiss 3T3 fibroblasts. *J. Cell Biol.* **107**, 2631-2645.
- Delhanty, P. & Locke, M. (1989). The development of epidermal feet in preparation for metamorphosis in an insect. *Tissue Cell* **21**, 891-909.
- Delhanty, P. & Locke, M. (1990). The redistribution of F-actin in the dermal glands of an insect in relation to secretion. *J. Cell Sci.* **96**, 303-311.
- Dijkwel, P. A. & Wenink, P. W. (1986). Structural integrity of the nuclear matrix: differential effects of thiol agents and metal chelators. *J. Cell Sci.* **84**, 53-67.
- Dustin, P. (1978). Nuclear and cytoplasmic shaping in spermatogenesis. In *Microtubules*, pp. 232-238. Berlin: Springer-Verlag.
- Earnshaw, W. C., Halligan, B., Cooke, C. A., Heck, M. M. S. & Liu, L. F. (1985). Topoisomerase II is a structural component of mitotic chromosome scaffolds. *J. Cell Biol.* **100**, 1706-1715.
- Earnshaw, W. C. & Heck, M. M. S. (1985). Localization of topoisomerase II in mitotic chromosomes. *J. Cell Biol.* **100**, 1716-1725.
- Fey, E. G., Capco, D. G., Krochmalnic, G. & Penman, S. (1984a). Epithelial structure revealed by chemical dissection and unembedded electron microscopy. *J. Cell Biol.* **99**, 203s-208s.
- Fey, E. G., Krochmalnic, G. & Penman, S. (1986a). The nonchromatin substructures of the nucleus: the ribonucleoprotein (RNP)-containing and the RNP-depleted matrices analyzed by sequential fractionation and resinless section electron microscopy. *J. Cell Biol.* **102**, 1654-1665.
- Fey, E. G., Ornelles, D. A. & Penman, S. (1986b). Association of RNA with the cytoskeleton and the nuclear matrix. *J. Cell Sci. Suppl.* **5**, 99-119.
- Fey, E. G., Wan, K. M. & Penman, S. (1984b). Epithelial cytoskeletal framework and nuclear matrix-intermediate filament scaffold: three-dimensional organization and protein composition. *J. Cell Biol.* **98**, 1973-1984.
- Fields, A. P., Kaufmann, S. H. & Shaper, J. H. (1986). Analysis of the internal nuclear matrix: oligomers of a 38 kD nucleolar polypeptide stabilized by disulfide bonds. *Exp. Cell Res.* **164**, 139-153.

- Fisher, D. Z., Chaudhary, N. & Blobel, G. (1986). cDNA sequencing of nuclear lamins A and C reveals primary and secondary structural homology to intermediate filament proteins. *Proc. Natl. Acad. Sci. USA* **83**, 6450-6454.
- Fisher, P. A. (1987). Disassembly and reassembly of nuclei in cell-free systems. *Cell* **48**, 175-176.
- Fisher, P. A. (1988). Karyoskeletal proteins of *Drosophila*. In *Chromosomes and Chromatin*. III (ed. K. W. Adolph), pp. 119-150. Boca Raton: CRC Press, Inc.
- Fisher, P. A., Berrios, M. & Blobel, G. (1982). Isolation and characterization of a proteinaceous subnuclear fraction composed of nuclear matrix, peripheral lamina and nuclear pore complexes from embryos of *Drosophila melanogaster*. *J. Cell Biol.* **92**, 674-686.
- Forer, A. (1988). Do anaphase chromosomes chew their way to the pole or are they pulled by actin? *J. Cell Sci.* **91**, 449-453.
- Fowler, V. M. & Pollard, H. B. (1982). Chromaffin granule membrane-F-actin interactions are calcium sensitive. *Nature* **295**, 336-339.
- Franke, W. W. (1987). Nuclear lamins and cytoplasmic intermediate filament proteins: a growing multigene family. *Cell* **48**, 3-4.
- Franke, W. W., Kleinschmidt, J. A., Spring, H., Krohne, G., Grund, C., Trendelenburg, M. F., Stoehr, M. & Scheer, U. (1981). A nucleolar skeleton of protein filaments demonstrated in amplified nucleoli of *Xenopus laevis*. *J. Cell Biol.* **90**, 289-299.
- French, S. W., Kawahara, H., Katsuma, Y., Ohta, M. & Swierenga, S. H. H. (1989). Interaction of intermediate filaments with nuclear lamina and cell periphery. *Electron Microsc. Rev.* **2**, 17-51.
- Fukui, Y. (1978). Intranuclear actin bundles induced by dimethyl sulfoxide in interphase nucleus of *Dictyostelium*. *J. Cell Biol.* **76**, 146-157.
- Fukui, Y. & Katsumara, H. (1980). Dynamics of nuclear actin bundle induction by dimethyl sulfoxide and factors affecting its development. *J. Cell Biol.* **84**, 131-140.
- Fukui, Y., Lynch, T. J., Brzeska, H. & Korn, E. D. (1989). Myosin I is located at the leading edges of locomoting *Dictyostelium* amoebae. *Nature* **341**, 328-331.
- Fyrberg, E. A., Kindle, K. L. & Davidson, N. (1980). The actin genes of *Drosophila*: a dispersed multigene family. *Cell* **19**, 365-378.



- Gage, L. P. (1974). Polyploidization of the silk gland of *Bombyx mori*. *J. Mol. Biol.* **86**, 97-108.
- Galigher, A. E. & Kozloff, E. N. (1971). *Essentials of Practical Microtechnique*. Philadelphia: Lea & Febiger., 531 p.
- Georgatos, S. D. & Blobel, G. (1987). Lamin B constitutes an intermediate filament attachment at the nuclear envelope. *J. Cell Biol.* **105**, 117-125.
- Gerace, L. (1986). Nuclear lamina and organization of nuclear architecture. *TIBS* **11**, 443-446.
- Gerace, L. & Blobel, G. (1980). The nuclear envelope lamina is reversibly depolymerized during mitosis. *Cell* **19**, 277-287.
- Goldstein, L., Ko, C. & Errick, J. (1977a). Nuclear actin: an apparent association with condensed chromatin. *Cell Biol. Int. Rep.* **1**, 511-515.
- Goldstein, L., Rubin, R. & Ko, C. (1977b). The presence of actin in nuclei: a critical appraisal. *Cell* **12**, 601-608.
- Gower, D. J. & Tytell, M. (1985). A simplified procedure of evaluation and storage of isoelectric focusing gels prior to second-dimension electrophoresis. *Electrophoresis* **6**, 296-298.
- Gruenbaum, Y., Hochstrasser, M., Mathog, D., Saumweber, H., Agard, D. A. & Sedat, J. W. (1984). Spatial organization of the *Drosophila* nucleus: a three-dimensional cytogenetic study. *J. Cell Sci. Suppl.* **1**, 223-234.
- Gruenbaum, Y., Landesman, Y., Drees, B., Bare, J. W., Saumweber, H., Paddy, M. R., Sedat, J. W., Smith, D. E., Benton, B. M. & Fisher, P. A. (1988). *Drosophila* nuclear lamin precursor Dm<sub>0</sub> is translated from either of two developmentally regulated mRNA species apparently encoded by a single gene. *J. Cell Biol.* **106**, 585-596.
- Haggis, G. H., Schwietzer, I., Hall, R. & Bladon, T. (1982). Freeze fracture through the cytoskeleton, nucleus, and nuclear matrix of lymphocytes studied by scanning electron microscopy. *J. Microsc.* **132**, 185-194.
- Herlan, G., Quevedo, R. & Wunderlich, F. (1978). Structural transformation of the nuclear matrix *in situ*. *Exp. Cell Res.* **115**, 103-110.
- Heslop-Harrison, J. & Heslop-Harrison, Y. (1989a). Conformation and movement of the vegetative nucleus of the angiosperm pollen tube: association with the actin cytoskeleton. *J. Cell Sci.* **93**, 299-308.

- Heslop-Harrison, J. & Heslop-Harrison, Y. (1989b). Myosin associated with the surfaces of organelles, vegetative nuclei and generative cells in angiosperm pollen grains and tubes. *J. Cell Sci.* **94**, 319-325.
- Heslop-Harrison, J., Heslop-Harrison, Y., Cresti, M., Tiezzi, A. & Ciampolini, F. (1986). Actin during pollen germination. *J. Cell Sci.* **86**, 1-8.
- Hirokawa, N., Keller, T. C. S., Chasan, R. & Moosker, M. S. (1983). Mechanism of brush border contractility studied by the quick-freeze, deep-etch method. *J. Cell Biol.* **96**, 1325-1336.
- Hirono, M., Kumagai, Y., Numata, O. & Watanabe, Y. (1989). Purification of *Tetrahymena* actin reveals some unusual properties. *Proc. Natl. Acad. Sci. USA* **86**, 75-79.
- Hitchcock, S. E., Carlsson, L. & Lindberg, U. (1976). Depolymerization of f-actin by deoxyribonuclease I. *Cell* **7**, 531-542.
- Hochstrasser, M., Mathog, D., Gruenbaum, Y., Saumweber, H. & Sedat, J. W. (1986). Spatial organization of chromosomes in the salivary gland nuclei of *Drosophila melanogaster*. *J. Cell Biol.* **102**, 112-123.
- Hochstrasser, M. & Sedat, J. W. (1987a). Three-dimensional organization of *Drosophila melanogaster* interphase nuclei. I. Tissue specific aspects of polytene nuclear architecture. *J. Cell Biol.* **104**, 1455-1470.
- Hochstrasser, M. & Sedat, J. W. (1987b). Three-dimensional organization of *Drosophila melanogaster* interphase nuclei. II. Chromosome spatial organization and gene regulation. *J. Cell Biol.* **104**, 1471-1483.
- Höner, B., Citi, S., Kendrick-Jones, J. & Jockusch, B. M. (1988). Modulation of cellular morphology and locomotory activity by antibodies against myosin. *J. Cell Biol.* **107**, 2181-2189.
- Ichimura, S., Mita, K., Zama, M. & Numata, M. (1985). Isolation of the giant ramified nuclei of the posterior silk glands of *Bombyx mori*. *Insect Biochem.* **15**, 277-284.
- Jackson, D. A. & Cook, P. R. (1985). Transcription occurs at a nucleoskeleton. *EMBO J.* **4**, 919-925.
- Jackson, D. A. & Cook, P. R. (1986). Replication occurs at a nucleoskeleton. *EMBO J.* **5**, 1403-1410.
- Jackson, D. A., McCready, S. J. & Cook, P. R. (1981). RNA is synthesized at the nuclear cage. *Nature* **292**, 552-555.

- Kalinich, J. F. & Douglas, M. G. (1989). *In vitro* translocation through the yeast nuclear envelope. Signal-dependent transport requires ATP and calcium. *J. Biol. Chem.* **264**, 17979-17989.
- Kaminskyj, S. G. W., Yoon, K. S. & Heath, I. B. (1989). Cytoskeletal interactions with post-mitotic migrating nuclei in the oyster mushroom fungus, *Pleurotus ostreatus* : evidence against a force-generating role for astral microtubules. *J. Cell Sci.* **94**, 663-674.
- Katsuma, Y., Swierenga, S. H. H., Marceau, N. & French, S. W. (1987). Connection of intermediate filaments with the nuclear lamina and the cell periphery. *Biol. Cell* **59**, 193-204.
- Kaufmann, S. H., Coffey, D. S. & Shaper, J. H. (1981). Considerations in the isolation of rat liver nuclear matrix, nuclear envelope, and pore complex lamina. *Exp. Cell Res.* **132**, 105-123.
- Kaufmann, S. H., Fields, A. P. & Shaper, J. H. (1986). The nuclear matrix: current concepts and unanswered questions. *Meth. Achiev. exp. Pathol.* **12**, 141-171.
- Kessel, R. G. (1966). The association between microtubules and nuclei during spermiogenesis in the dragonfly. *J. Ultrastruct. Res.* **16**, 293-304.
- Krohne, G. & Benavente, R. (1986). The nuclear lamins: a multigene family of proteins in evolution and differentiation. *Exp. Cell Res.* **162**, 1-10.
- Krohne, G., Stick, R., Kleinschmidt, J. A., Moll, R., Franke, W. W. & Hausen, P. (1982). Immunological localization of a major karyoskeletal protein in nucleoli of oocytes and somatic cells of *Xenopus laevis*. *J. Cell Biol.* **94**, 749-754.
- Kumar, A., Raziuddin, Finlay, T. H., Thomas, J. O. & Szer, W. (1984). Isolation of a minor species of actin from the nuclei of *Acanthamoeba castellanii*. *Biochemistry* **23**, 6753-6757.
- Laemmli, U. K. (1970). Cleavage of structural proteins during the assembly of the head of bacteriophage T<sub>4</sub>. *Nature* **227**, 680-685.
- LaFond, R. E., Woodcock, H., Woodcock, C. L. F., Kundahl, E. R. & Lucas, J. J. (1983). Generation of an internal matrix in mature avian nuclei during reactivation in cytoplasts. *J. Cell Biol.* **96**, 1815-1819.

- Laliberté, J.-F., Dagenais, A., Fillion, M., Bibor-Hardy, V., Simard, R. & Royal, A. (1984). Identification of distinct messenger RNAs for nuclear lamin C and a putative precursor of nuclear lamin A. *J. Cell Biol.* **98**, 980-985.
- Laskey, R. A. & Mills, A. D. (1975). Quantitative film detection of  $^3\text{H}$  and  $^{14}\text{C}$  in polyacrylamide gels by fluorography. *Eur. J. Biochem.* **56**, 335-341.
- Lawrence, J. B., Singer, R. H. & Marselle, L. M. (1989). Highly localized tracks of specific transcripts within interphase nuclei visualized by *in situ* hybridization. *Cell* **57**, 493-502.
- Lebel, S., Lampron, C., Royal, A. & Raymond, Y. (1987). Lamins A and C appear during retinoic acid-induced differentiation of mouse embryonal carcinoma cells. *J. Cell Biol.* **105**, 1099-1104.
- Lebel, S. & Raymond, Y. (1984). Lamin B from rat liver nuclei exists both as a lamina protein and as an intrinsic membrane protein. *J. Biol. Chem.* **259**, 2693-2696.
- Lehner, C. F., Eppenberger, H. M., Fakan, S. & Nigg, E. A. (1986). Nuclear substructure antigens: monoclonal antibodies against components of nuclear matrix preparations. *Exp. Cell Res.* **162**, 205-219.
- Lelkes, P. I., Friedman, J. E., Rosenheck, K. & Oplatka, A. (1986). Destabilization of actin filaments as a requirement for the secretion of catecholamines from permeabilized chromaffin cells. *FEBS Lett.* **208**, 357-363.
- Leslie, R. J., Saxton, W. M., Mitchison, T. J., Neighbors, B., Salmon, E. D. & McIntosh, J. R. (1984). Assembly properties of fluorescein-labeled tubulin *in vitro* before and after fluorescence bleaching. *J. Cell Biol.* **99**, 2146-2156.
- LeStourgeon, W. M. (1978). The occurrence of contractile proteins in nuclei and their possible functions. In *The Cell Nucleus*, 6 (ed. H. Busch), pp. 305-326. New York: Academic Press.
- Leung, H., Palli, S. R. & Locke, M. (1989). The localization of arylphorin in an insect, *Calpodes ethlius*. *J. Insect Physiol.* **35**, 223-231.
- Lewis, C. D., Lebkowski, J. S., Daly, A. K. & Laemmli, U. K. (1984). Interphase nuclear matrix and metaphase scaffolding structures. *J. Cell Sci. Suppl.* **1**, 103-122.

- Liou, W. & Rafferty, N. S. (1988). Actin filament patterns in mouse lens epithelium: a study of the effects of aging, injury, and genetics. *Cell Motil. Cytoskel.* **9**, 17-29.
- Locke, M. (1958). The formation of tracheae and tracheoles in *Rhodnius prolixus*. *Quart. J. Micros. Sci.* **99**, 29-46.
- Locke, M. (1970). The moult/intermoult cycle in the epidermis and other tissues of an insect *Calpodex ethlius* (Lepidoptera, Hesperidae). *Tissue Cell* **2**, 197-223.
- Locke, M. (1985). The structure of epidermal feet during their development. *Tissue Cell* **17**, 901-921.
- Locke, M. & Huie, P. (1980). Ultrastructure methods in cuticle research. In *Cuticle Techniques in Arthropods*, (ed. T. A. Miller), pp. 91-144. New York: Springer-Verlag.
- Locke, M. & Leung, H. (1985). The pairing of nucleolar patterns in an epithelium as evidence for a conserved nuclear skeleton. *Tissue Cell* **17**, 573-588.
- Lourim, D. & Lin, J. J.-C. (1989). Expression of nuclear lamin A and muscle-specific proteins in differentiating muscle cells *in ovo* and *in vitro*. *J. Cell Biol.* **109**, 495-504.
- Maraldi, N. M., Marinelli, F., Cocco, L., Papa, S., Santi, P. & Manzoli, F. A. (1986). Morphometric analysis and topological organization of nuclear matrix in freeze-fractured electron microscopy. *Exp. Cell Res.* **163**, 349-362.
- Matsuura, S., Morimoto, T., Nagata, S. & Tashiro, Y. (1968). Studies on the posterior silk gland of the silkworm *Bombyx mori*. II. Cytolytic processes in posterior silk gland cells during metamorphosis from larva to pupa. *J. Cell Biol.* **38**, 589-603.
- Matsuura, S. & Tashiro, Y. (1976). Ultrastructural changes of the posterior silk gland cells in the early larval instars of the silkworm, *Bombyx mori*. *J. Insect Physiol.* **22**, 967-979.
- Maupin-Szamier, P. & Pollard, T. D. (1978). Actin filament destruction by osmium tetroxide. *J. Cell Biol.* **77**, 837-852.
- McDuffie, N. G. (1967). Nuclear blebs in human leukaemic cells. *Nature* **214**, 1341-1342.

- McKeon, F. D., Kirschner, M. W. & Caput, D. (1986). Homologies in both primary and secondary structure between nuclear envelope and intermediate filament proteins. *Nature* 319, 463-468.
- Miller, K. G., Karr, T. L., Kellogg, D. R., Mohr, I. J., Walter, M. & Alberts, B. M. (1985). Studies on the cytoplasmic organization of early *Drosophila* embryos. *Cold Spring Harb. Symp. Quant. Biol.* 50, 79-90.
- Morimoto, T., Matsuura, S., Nagata, S. & Tashiro, Y. (1968). Studies on the posterior silk gland of the silkworm, *Bombyx mori*. III. Ultrastructural changes of posterior silk gland cells in the fourth larval instar. *J. Cell Biol.* 38, 604-614.
- Mounier, N. & Prudhomme, J.-C. (1986). Isolation of actin genes in *Bombyx mori*: the coding sequence of a cytoplasmic actin gene expressed in the silk gland is interrupted by a single intron in an unusual position. *Biochimie* 68, 1053-1061.
- Nakayasu, H. & Ueda, K. (1983). Association of actin with the nuclear matrix from bovine lymphocytes. *Exp. Cell Res.* 143, 55-62.
- Nakayasu, H. & Ueda, K. (1984). Small nuclear RNA-protein complex anchors on the actin filaments in bovine lymphocyte nuclear matrix. *Cell Struct. Funct.* 9, 317-326.
- Nakayasu, H. & Ueda, K. (1985a). Association of rapidly-labelled RNAs with actin in nuclear matrix from mouse L5178Y cells. *Exp. Cell Res.* 160, 319-330.
- Nakayasu, H. & Ueda, K. (1985b). Ultrastructural localization of actin in nuclear matrices from mouse leukemia L5178Y cells. *Cell Struct. Funct.* 10, 305-309.
- Nakayasu, H. & Ueda, K. (1986). Preferential association of acidic actin with nuclei and nuclear matrix from mouse leukemia L5178Y cells. *Exp. Cell Res.* 163, 327-336.
- Newman, G. R. (1987). The use and abuse of LR White. *Histochem. J.* 19, 118-120.
- Newport, J. (1987). Nuclear reconstitution *in vitro*: stages of assembly around protein-free DNA. *Cell* 48, 205-217.
- Newport, J. & Spann, T. (1987). Disassembly of the nucleus in mitotic extracts: membrane vesicularization, lamin disassembly, and chromosome condensation are independent processes. *Cell* 48, 219-230.

- Nishida, E., Kazuko, I., Yonezawa, N., Koyasu, S., Yahara, I. & Sasaki, H. (1987). Cofilin is a component of intranuclear and cytoplasmic actin rods induced in cultured cells. *Proc. Natl. Acad. Sci. USA* **84**, 5262-5266.
- O'Farrell, P. H. (1975). High resolution two-dimensional electrophoresis of proteins. *J. Biol. Chem.* **250**, 4007-4021.
- Ottaviano, Y. & Gerace, L. (1985). Phosphorylation of the nuclear lamins during interphase and mitosis. *J. Biol. Chem.* **260**, 624-632.
- Paddock, S. W. & Albrecht-Buehler, G. (1986). Distribution of microfilament bundles during rotation of the nucleus in 3T3 cells treated with monensin. *Exp. Cell Res.* **163**, 525-538.
- Parfenov, V. N. & Galaktionov, K. I. (1987). Intranuclear actin microfilaments in the oocytes of *Rana temporaria*. *Tsitologiya* **29**, 142-149.
- Paulin-Levasseur, M., Scherbarth, A., Traub, U. & Traub, P. (1988). Lack of lamins A and C in mammalian hemopoietic cell lines devoid of intermediate filament proteins. *Eur. J. Cell Biol.* **47**, 121-131.
- Perdrix-Gillot, S. (1979). DNA synthesis and endomitosis in the giant nuclei of the silk gland of *Bombyx mori*. *Biochimie* **61**, 171-204.
- Peters, K. E. & Comings, D. E. (1980). Two-dimensional gel electrophoresis of rat liver nuclear washes, nuclear matrix, and hnRNA proteins. *J. Cell Biol.* **86**, 135-155.
- Pollard, T. D. & Cooper, J. A. (1986). Actin and actin-binding proteins. A critical evaluation of mechanisms and functions. *Ann. Rev. Biochem.* **55**, 987-1035.
- Popoff, N. & Ellsworth, R. M. (1969). The fine structure of nuclear alterations in retinoblastoma and in the developing human retina: *in vivo* and *in vitro* observations. *J. Ultrastruct. Res.* **29**, 535-549.
- Pouchelet, M., Anteunis, A. & Gransmuller, A. (1986). Correspondence of two nuclear networks observed *in situ* with the nuclear matrix. *Biol. Cell* **56**, 107-112.
- Rafferty, N. S. & Scholz, D. L. (1985). Actin in polygonal arrays of microfilaments and sequestered actin bundles (SABs) in lens epithelial cells of rabbits and mice. *Curr. Eye Res.* **4**, 713-718.
- Razin, S. V. (1987). DNA interactions with the nuclear matrix and spatial organization of replication and transcription. *BioEssays* **6**, 19-23.

- Rubin, R. W., Goldstein, L. & Ko, C. (1978). Differences between nucleus and cytoplasm in the degree of actin polymerization. *J. Cell Biol.* **77**, 698-701.
- Rungger, D., Rungger-Brändle, E., Chaponnier, C. & Gabbiani, G. (1979). Intranuclear injection of anti-actin antibodies in *Xenopus* oocytes blocks chromosome condensation. *Nature* **282**, 320-321.
- Ryerse, J. S. (1978). Developmental changes in malpighian tubule fluid transport. *J. Insect Physiol.* **24**, 315-319.
- Saleem, M. & Atkinson, B. G. (1976). Isoelectric points and molecular weights of salt-extractable ribosomal proteins. *Can. J. Biochem.* **54**, 1029-1033.
- Sasaki, S. (1977). Microtubule systems and microtubular crystals in the posterior silk gland cells of *Bombyx mori*. *J. Electron Microsc.* **26**, 121-127.
- Sasaki, S., Nakajima, E., Fujii-Kuriyama, Y. & Tashiro, Y. (1981). Intracellular transport and secretion of fibroin in the posterior silk gland of the silkworm *Bombyx mori*. *J. Cell Sci.* **50**, 19-44.
- Sasaki, S. & Tashiro, Y. (1976). Studies on the posterior silk gland of the silkworm *Bombyx mori* : VI. Distribution of microtubules in the posterior silk gland cells. *J. Cell Biol.* **71**, 565-574.
- Scheer, U., Hinssen, H., Franke, W. W. & Jockusch, B. M. (1984). Microinjection of actin-binding proteins and actin antibodies demonstrates involvement of nuclear actin in transcription of lampbrush chromosomes. *Cell* **39**, 111-122.
- Schindler, M. & Jiang, L.-W. (1986). Nuclear actin and myosin as control elements in nucleocytoplasmic transport. *J. Cell Biol.* **102**, 859-862.
- Scholey, J. M., Neighbors, B., Salmon, E. D. & McIntosh, J. R. (1984). Isolation of microtubules and a dynein-like MgATPase from unfertilized sea urchin eggs. *J. Biol. Chem.* **259**, 6516-6525.
- Schröder, H. C., Trölltsch, D., Wenger, R., Bachmann, M., Diehl-Seifert, B. & Müller, W. E. G. (1987). Cytochalasin B selectively releases ovalbumin mRNA precursors but not the mature ovalbumin mRNA from hen oviduct nuclear matrix. *Eur. J. Biochem.* **167**, 239-245.
- Sears, F. W., Zemansky, M. W. & Young, H. D. (1980). College Physics. Reading, MA.: Addison-Wesley Publishing Co., 880 p.



- Segawa, A. & Yamashina, S. (1989). Roles of microfilaments in exocytosis: a new hypothesis. *Cell Struct. Funct.* **14**, 531-544.
- Sehnal, F. & Akai, H. (1982). Ultrastructure and function of silk glands in *Galleria mellonella*. In *The Ultrastructure and Functioning of Insect Cells*, (ed. H. Akai, R. C. King & S. Morohoshi), pp. 135-138. Sapporo: Society for Insect Cells Japan.
- Simard, R., Bibor-Hardy, V., Dagenais, A., Bernard, M. & Pinard, M.-F. (1986). Role of the nuclear matrix during viral replication. *Meth. Achiev. exp. Pathol.* **12**, 172-199.
- Smith, D. E. & Fisher, P. A. (1989). Interconversion of *Drosophila* nuclear lamin isoforms during oogenesis, early embryogenesis, and upon entry of cultured cells into mitosis. *J. Cell Biol.* **108**, 255-265.
- Smith, D. E., Gruenbaum, Y., Berrios, M. & Fisher, P. (1987). Biosynthesis and interconversion of *Drosophila* nuclear lamin isoforms during normal growth and in response to heat shock. *J. Cell Biol.* **105**, 771-790.
- Smith, H. C., Ochs, R. L., Fernandez, E. A. & Spector, D. L. (1986). Macromolecular domains containing nuclear protein p107 and U-snRNP protein p28: further evidence for an *in situ* nuclear matrix. *Mol. Cell. Biochem.* **70**, 151-168.
- Sontag, J.-M., Aunis, D. & Bader, M.-F. (1988). Peripheral actin filaments control calcium-mediated catecholamine release from streptolysin-O-permeabilized chromaffin cells. *Eur. J. Cell Biol.* **46**, 316-326.
- Spector, D. L. (1989). Higher order nuclear organization: three-dimensional distribution of small nuclear ribonucleoprotein particles. *Proc. Natl. Acad. Sci. USA* **87**, 147-151.
- Staufenbiel, M. & Deppert, W. (1984). Preparation of nuclear matrices from cultured cells: subfractionation of nuclei *in situ*. *J. Cell Biol.* **98**, 1886-1894.
- Stewart, C. & Burke, B. (1987). Teratocarcinoma stem cells and early mouse embryos contain only a single major lamin polypeptide closely resembling lamin B. *Cell* **51**, 383-392.
- Stick, R. & Hausen, P. (1985). Changes in the nuclear lamina composition during early development of *Xenopus laevis*. *Cell* **41**, 191-200.
- Stossel, T. P. (1984). Contribution of actin to the structure of the cytoplasmic matrix. *J. Cell Biol.* **99**, 15s-21s.

- Stossel, T. P., Chaponnier, C., Ezzell, R. M., Hartwig, J. H., Janmey, P. A., Kwiatkowski, D. J., Lind, S. E., Smith, D. B., Southwick, F. S., Yin, H. L. & Zaner, K. S. (1985). Nonmuscle actin-binding proteins. *Ann. Rev. Cell Biol.* **1**, 353-402.
- Tamura, T., Akai, H. & Sakate, S. (1982). Ultrastructure of the silk glands and isolation of the fibroin mRNAs from *Antheraea yamamai* and other non-mulberry silkworms. In *The Ultrastructure and Functioning of Insect Cells*, (ed. H. Akai, R. C. King & S. Morohoshi), pp. 139-142. Sapporo: Society for Insect Cells Japan.
- Tashiro, Y., Matsuura, S. & Hata, K. (1976). Ultrastructural observations on the organogenesis of the posterior silk gland of the silkworm, *Bombyx mori*. *J. Insect Physiol.* **22**, 273-283.
- Tashiro, Y., Matsuura, S. & Sasaki, S. (1982). Roles of the cytoskeletal systems in the biosynthesis, intracellular transport and secretion of fibroin in the posterior silk gland cells of *Bombyx mori*. In *The Ultrastructure and Functioning of Insect Cells*, (ed. H. Akai, R. C. King & S. Morohoshi), pp. 149-152. Sapporo: Society for Insect Cells Japan.
- Tashiro, Y., Morimoto, T., Matsuura, S. & Nagata, S. (1968). Studies on the posterior silk gland of the silkworm, *Bombyx mori*. I. Growth of posterior silk gland cells and biosynthesis of fibroin during the fifth larval instar. *J. Cell Biol.* **38**, 574-588.
- Timoshenko, S. (1936). *Theory of elastic stability*. New York: McGraw-Hill., 518 p.
- Tokuyasu, K. T. (1974). Dynamics of spermiogenesis in *Drosophila melanogaster*. IV. Nuclear transformation. *J. Ultrastruct. Res.* **48**, 284-303.
- Towbin, H., Staehelin, T. & Gordon, J. (1979). Electrophoretic transfer of proteins from polyacrylamide gels to nitrocellulose sheets: procedure and some applications. *Proc. Natl. Acad. Sci. USA* **76**, 4350-4354.
- Ueyama, H., Nakayasu, H. & Ueda, K. (1987). Nuclear actin and transport of RNA. *Cell Biol. Int. Rep.* **11**, 671-677.
- Valkov, N. I., Ivanova, M. I., Uscheva, A. A. & Krachmarov, C. P. (1989). Association of actin with DNA and nuclear matrix from Guerin ascites tumour cells. *Mol. Cell. Biochem.* **87**, 47-56.

- van Dekken, H., Pinkel, D., Mullikin, J., Trask, B., van den Engh, G. & Gray, J. (1989). Three-dimensional analysis of the organization of human chromosome domains in human and human-hamster hybrid interphase nuclei. *J. Cell Sci.* **94**, 299-306.
- Verheijen, R., van Venrooij, W. & Ramaekers, F. (1988). The nuclear matrix: structure and composition. *J. Cell Sci.* **90**, 11-36.
- Vielkind, U. & Vielkind, J. (1970). Nuclear pockets and projections in fish melanoma. *Nature* **226**, 655-656.
- Volkman, L. E. (1988). *Autographa californica* MNPV nucleocapsid assembly: inhibition by cytochalasin D. *Virology* **163**, 547-553.
- Walter, M. F. & Biessmann, H. (1984). Intermediate-sized filaments in *Drosophila* tissue culture cells. *J. Cell Biol.* **99**, 1468-1477.
- Weber, K. & Osborn, M. (1969). The reliability of molecular weight determinations by dodecyl sulfate-polyacrylamide gel electrophoresis. *J. Biol. Chem.* **244**, 4406-4412.
- Weber, K., Plessmann, U. & Ulrich, W. (1989). Cytoplasmic intermediate filament proteins of invertebrates are closer to nuclear lamins than are vertebrate intermediate filament proteins; sequence characterization of two muscle proteins of a nematode. *EMBO J.* **8**, 3221-3227.
- Weeds, A. (1982). Actin-binding proteins: regulators of cell architecture and motility. *Nature* **296**, 811-816.
- Weihing, R. R. (1985). The filaments: properties and functions. *Can. J. Biochem. Cell Biol.* **63**, 397-413.
- Wieland, T. & Govindan, V. M. (1974). Phallotoxins bind to actins. *FEBS Lett.* **46**, 351-353.
- Wieland, T., Miura, T. & Seeliger, A. (1983). Analogs of phalloidin. D-Abu<sup>2</sup>-Lys<sup>7</sup>-phalloin an f-actin binding analog, its rhodamine conjugate (RLP) a novel fluorescent f-actin probe, and D-Ala<sup>2</sup>-Leu<sup>7</sup>-phalloin an inert peptide. *Int. J. Peptide Protein Res.* **21**, 3-10.
- Wiley, M. J. & Lai-Fook, J. (1974). Studies on the silk glands of *Calpodex ethlius* Stoll, (Lepidoptera, Hesperiiidae). *J. Morphol.* **144**, 297-322.
- Wilkinson, R. F., Stanley, H. P. & Bowman, J. T. (1974). Role of microtubules in nuclear shaping of *Drosophila* spermatids. *J. Cell Biol.* **63**, 372a.

- Woodcock, C. L. F. & Woodcock, H. (1986). Nuclear matrix generation during reactivation of avian erythrocyte nuclei: an analysis of the protein traffic in cybrids. *J. Cell Sci.* **84**, 105-127.
- Wunderlich, F. & Herlan, G. (1977). A reversibly contractile nuclear matrix: its isolation, structure, and composition. *J. Cell Biol.* **73**, 271-278.
- Yancheva, N., Markov, D. & Djondjurov, L. (1986). Evidence for the existence in the nuclei of Friend cells of a new type of ribonucleoprotein network. *J. Cell Sci.* **84**, 165-182.
- Yasuzumi, G., Matano, Y., Asai, T., Nagasaka, M. & Yasuzumi, F. (1971). Spermatogenesis in animals as revealed by electron microscopy. XXII. Development of nuclei and cytoplasmic microtubules in the grasshopper spermatids. *Z. Zellforsch* **115**, 543-552.

**Fig. 72. The probable location of the nuclear shell.** The nuclear shell of f-actin most likely corresponds to the randomly oriented microfilaments in the zone of exclusion on the cytoplasmic side of the nuclear envelope. The nuclear lamina corresponds to the electron-dense region which is intimately associated with the inner layer of the nuclear envelope. (Drawing not to scale).